

On a tropicalization of planar polynomial ODEs with a finite number of structurally stable phase portraits

Kristiansen, K. U. and Sarantaris, A. H.

Department of Applied Mathematics and Computer Science,
Technical University of Denmark,
2800 Kgs. Lyngby,
Denmark,
krkri@dtu.dk

February 25, 2025

Abstract

Recently, concepts from the emerging field of tropical geometry have been used to identify different scaling regimes in chemical reaction networks where dimension reduction may take place. In this paper, we try to formalize these ideas further in the context of planar polynomial ODEs. In particular, we develop a theory of a tropical dynamical system, based upon a differential inclusion, that has a set of discontinuities on a subset of the associated tropical curve. We define a phase portrait, a notion of equivalence and characterize structural stability for a tropical dynamical system. Our main result is that there are finitely many equivalence classes of structurally stable phase portraits. We believe that the property of finitely many structurally stable phase portraits underlines the potential of the tropical approach, also in higher dimension, as a method to (systematically) obtain and identify skeleton models in chemical reaction networks in extreme parameter regimes.

Contents

1	Introduction	3
1.1	Summary of the main results	5
1.2	Overview	5
1.3	Tropical Phase Plane	6
2	Tropical geometry	6
3	A tropicalization of planar polynomial ODEs	10
3.1	A set-valued vector-field trop	13
3.2	Tropical sliding and crossing	14

3.3	The set-valued vector-field trop for tropical sliding	16
3.4	The crossing flow	18
3.5	Definition of a tropical dynamical system	19
4	Existence of solutions	20
5	Orbits and phase portraits	23
6	Example: A tropicalized autocatalator	24
7	Equivalence of tropical dynamical systems	30
8	Tropical vertices	33
9	Tropical singularities	35
10	Separatrices and separatrix connections	39
11	Crossing cycles	43
12	The crossing graph	44
12.1	Example: A bifurcating crossing cycle	45
12.2	Example: A structurally stable separatrix connection	49
13	Main results: Structurally stable tropical dynamical systems	51
14	Example: A generalized autocatalator	52
14.1	Case 1^H	53
14.2	Case 1^V	53
14.3	Case 2	54
14.4	Case 3	54
14.5	Case 4^H	58
14.6	Case 4^V	58
14.7	Case 5^H	60
14.8	Case 5^V	60
14.9	Completing the proof of Proposition 14.1	60
15	Discussion	63
15.1	Limit cycles	63
15.2	Tropicalization of the full plane	65
15.3	Extensions to \mathbb{R}^n	66
15.4	The singular perturbation problem defined by $0 < \epsilon \ll 1$	66

1 Introduction

Polynomial systems of ordinary differential equations (ODEs) occur in many different areas of science. Perhaps most notably they occur as models of chemical reaction networks [21] and in compartmental models for pharmacology, epidemiology and ecology [8]. Moreover, (the second part of) Hilbert’s 16th problem [28, 45] – which remains unresolved to this day – is on the existence of an upper bound H_N of the number of limit cycles for planar polynomial ODEs of a fixed degree $N \in \mathbb{N}$, $N \geq 2$:

$$\begin{aligned} x' &= P(x, y), \\ y' &= Q(x, y). \end{aligned} \tag{1}$$

These problems are nonlocal (or simply global). For example, in general chemical reaction network, we are interested in the long term dynamics (stationary points, periodic solutions, or even chaos in dimensions ≥ 3), and although bifurcation theory and numerical computations work well locally and for given parameters, global problems in generality of e.g. (1), are (currently) out of reach.

Tropical geometry is a variant of algebraic geometry based on the semiring where the usual definitions of addition and multiplication of real numbers are replaced by the following operations

$$u \oplus v := \max(u, v), \quad u \star v := u + v, \quad u, v \in \mathbb{R} \cup \{-\infty\}, \tag{2}$$

see [50]. Tropical monomials $F_{i,j}(u, v) = \alpha_{i,j} \star u^{*i} \star v^{*j} = \alpha_{i,j} + iu + jv$ in two variables u and v are therefore affine functions. On the other hand, tropical polynomials are piecewise linear $F_{\max}(u, v) = \max_{i,j} F_{i,j}(u, v)$, much like what one observes when putting the graph of a classical polynomial on a logarithmic paper. This connection between the tropical semi-ring and logarithmic paper can be formalized through:

$$\lim_{\epsilon \rightarrow 0} \epsilon \log \left(e^{u\epsilon^{-1}} + e^{v\epsilon^{-1}} \right) = u \oplus v, \tag{3}$$

see [63], and relates to the Maslov’s dequantization of the real numbers in physics, see [47, 48]. The tropical curve of a tropical polynomial F_{\max} is the set of points (u, v) where the maximum is attained by at least two monomials.

Tropical geometry has in recent years both established itself as an area of its own right – with tropical solutions of polynomial equations forming a kind of skeleton for the classical ones based upon standard arithmetic [62, 63] – but also unveiled deep connections to numerous branches of pure and applied mathematics [6, 29, 50, 57]. Perhaps most noticeably, O. Viro’s *gluing method* in algebraic geometry, which allows algebraic curves to be constructed by a “cut and paste” approach, see [64], has deep connections to (and even inspired the development of) tropical geometry. In [30], the authors developed a modification of Viro’s gluing method to construct polynomial systems (1) of degree N with an order of

$$\approx \frac{N^2 \log N}{2 \log 2}, \tag{4}$$

as $N \rightarrow \infty$, many limit cycles. To the best of our knowledge, this is the best known asymptotic lower bound of H_N , see also [2]. At the same time, Newton polygons have also been used in dynamical systems theory for the local study of singularities, see [7, 19].

Recently, see e.g. [15, 43, 53, 59], tropical geometry has been used to develop computational tools for the analysis and identification of scaling regimes of chemical-reaction networks where dimension reduction may take place. The basis for this approach is related to (3) and the fact that reduction (in a first approximation) takes place where dominating terms of opposite sign balance out. In tropical terms, the balancing occurs along (a subset of) the tropical curve. This reduction approach can be applied successively, eliminating one dimension at a time and can (potentially) be interpreted (and justified) as slow manifolds in multiple time scale systems, see [15, 43]. Consequently, it offers an attractive way to deal with the challenges posed by complex, high-dimensional bio-chemical models that involve numerous parameters varying over different scales, making general dynamical systems analysis (including numerical analysis) difficult. Having manageable skeleton models is highly desirable in such cases, see [53]. While further theoretical development is necessary, we are taking an initial step in this paper by considering *tropicalized* planar polynomial systems. We believe that this serves as a natural starting point for further development of the theory.

Our approach takes as its starting point the setting introduced to the first author by P. Szmolyan, which is partially fleshed out in the Diploma thesis [56] by S. Portisch, wherein (1) is embedded into a certain ϵ -family and where (u, v) is introduced through

$$u = \epsilon \log x, \quad v = \epsilon \log y. \quad (5)$$

Taking the limit $\epsilon \rightarrow 0$, using (3) and a certain reparametrization of time, we obtain a piecewise smooth (PWS) system in the (u, v) -plane, with the tropical curve containing the discontinuities. We believe that the idea of tropicalizing polynomial ODE systems was first introduced in [53]. However, their definition is slightly different from ours (as we for example only work with (u, v)) and was motivated by the Litvinov-Maslov corresponding principle [48] rather than (as in the present case) through a formal limiting process of (1).

PWS systems are important in many different application areas, including mechanics (impact, friction, etc), electronics (switches and diodes, etc.), and control engineering (sliding mode control, etc.), see [17, 31]. At the same time, PWS systems also pose mathematical problems. For one thing, they do not (in general) define a (classical) dynamical system, due to the lack of uniqueness of solutions. During the past decades, there has therefore been an effort to extend the theory of dynamical systems to PWS systems. This includes the work by [9, 61] to extend Peixoto's program of structural stability, see also [26]. Parallel to this effort, there has been an attempt to bound the number of limit cycles in planar PWS linear systems, see [20, 46, 49]. A uniform bound on the number of (crossing) limit cycles for such systems with a line of discontinuities was recently obtained in [11], using the novel characterization of the transition maps in [10].

Finally, recent research has explored how phenomena such as folds, grazing, and boundary singularities in PWS systems can be understood in their smooth version. To achieve this,

researchers have refined methods from Geometric Singular Perturbation Theory (GSPT) and blowup, to resolve the special singular limit of smooth systems approaching PWS ones, see [27, 34, 35, 39, 40, 41]. These methods are also relevant in the present context when connecting the tropical dynamical system back to (1) for $\epsilon > 0$ small enough. In fact, this was the main focus of [56] in the context of the planar Michaelis-Menten model of enzyme reactions. It was found that an attracting one-dimensional manifold exists across a wide range of parameters. In contrast, in the present paper *we will only analyze (and develop) the singular limit ($\epsilon = 0$) case*, and leave this connection to $\epsilon > 0$ to future work.

1.1 Summary of the main results

In order to obtain a well-defined system for $\epsilon = 0$, we first introduce a novel differential inclusion, that extends Filippov's sliding method, see [25], in a meaningful way to our setting. As indicated by (5), we will only consider the first quadrant $(x, y) \in \mathbb{R}_+^2$, $\mathbb{R}_+ := (0, \infty)$. The other quadrants can be handled in a similar way. We then prove existence of solutions of the differential inclusion (see Theorem 2.4) and introduce a new notion of equivalence for our tropical dynamical system that we use to classify the structurally stable systems. In our main result (see Theorem 13.2), we find that for any degree N there are finitely many equivalence classes of structurally stable phase portraits. We do not enumerate or put a bound on these in the present work, but we demonstrate our approach by counting the number (15 in total) of equivalence classes of structurally stable phase portraits for a generalized autocatalator model (see Proposition 14.1). More generally, we believe that our results demonstrate that the global problems offered by (1) become more accessible in their tropical version.

1.2 Overview

The paper is organized as follows: In Section 2, we first review some basic concepts of tropical geometry. Then in Section 3, we introduce the concept of a tropical (polynomial) dynamical system, see Definition 3.17. It is described as a differential inclusion with a discontinuity set of the underlying piecewise smooth system as a subset of the tropical curve. In Section 4, we prove existence of piecewise affine solutions, which in Section 5 lead us to a definition of orbits (as polygonal curves) and a definition of a phase portrait. In Section 6, we illustrate the concepts on the autocatalator model from [37].

Subsequently, in Section 7, we define a (new) notion of equivalence of tropical dynamical systems. In the following sections, see Section 8–Section 11, we then classify structural stability (locally) of tropical vertices, tropical singularities, separatrices and crossing cycles, respectively. Subsequently, in Section 12 we associate a graph (the crossing graph) with a tropical dynamical system. Next, in Section 13, we put everything together (including the crossing graph in Section 12 that will play a crucial role) to state and prove our main results (see Theorem 13.2) on the structural stability of tropical dynamical systems. We demonstrate these results in the context of a generalized autocatalator model in Section 14. We conclude the paper in Section 15 with a discussion section. Here we also state some

perturbation results (delaying proofs to future work) that relate the tropical dynamical system with solutions of the classical version (1) for all $0 < \epsilon \ll 1$ and discuss directions for future work.

1.3 Tropical Phase Plane

To generate the tropical phase portraits, we have used the `Matlab` toolbox `Tropical Phase Plane` developed by the second author in his bachelor thesis, see [58]. The toolbox can be downloaded from

<https://www.mathworks.com/matlabcentral/fileexchange/132058-tropical-dynamics-toolbox/>

2 Tropical geometry

Tropical geometry [50, 51] is a variant of algebraic geometry where addition and multiplication are replaced by \max and addition, respectively, see (2), using $-\infty + u = -\infty$ for every $u \in \mathbb{R} \cup \{-\infty\}$. (2) defines a semi-ring, where $u = -\infty$ is the neutral element of addition and $u = 0$ is the neutral element with respect to multiplication. Notice that there is no additive inverse: Given u and w such that $u > w \geq -\infty$, then the equation $u \oplus v = w$ has no solution v . Moreover, \oplus is idempotent: $u \oplus u = u$ for all $u \in \mathbb{R} \cup \{-\infty\}$.

Remark 2.1. *As usual, $o \subset \mathbb{R} \cup \{-\infty\}$ is open if either (a) o is open in \mathbb{R} or (b) $o = K^c \cup \{-\infty\}$ with K^c the complement of a compact set $K \subset \mathbb{R}$.*

In tropical geometry, classical monomials

$$\alpha_{i,j} u^i v^j, \quad \alpha_{i,j} \in \mathbb{R}, i, j \in \mathbb{N},$$

become affine functions:

$$F_{i,j}(u, v) = \alpha_{i,j} + iu + jv, \quad (u, v) \in \mathbb{R}^2. \quad (6)$$

We will call $\alpha_{i,j} \in \mathbb{R} \cup \{-\infty\}$ the *tropical coefficient* of $F_{i,j}$ and define the degree $\deg F_{i,j}$ of $F_{i,j}$ as the tuple $(i, j) \in \mathbb{N}_0^2$. On the other hand, classical polynomials

$$\sum_{0 \leq i+j \leq N} \alpha_{i,j} u^i v^j,$$

of degree N become piecewise affine functions:

$$F_{\max}(u, v) = \max_{0 \leq i+j \leq N} F_{i,j}(u, v), \quad (u, v) \in \mathbb{R}^2. \quad (7)$$

In tropical geometry, a *tropical curve* \mathcal{T} is then the set of points $(u, v) \in \mathbb{R}^2$ where the maximum in (7) is attained by at least two tropical monomials, i.e.

$$\mathcal{T} := \left\{ (u, v) \in \mathbb{R}^2 : \# \operatorname{argmax}_{(i,j)} F_{i,j}(u, v) \geq 2 \right\},$$

see [50]. Here we use $\#$ for the cardinality of a finite set.

Points (u, v) where

$$\# \operatorname{argmax}_{(i,j)} F_{i,j}(u, v) = 2,$$

lie on line segments (isomorphic to open intervals $]a, b[$) given by

$$\mathcal{E}_{(i_1, j_1), (i_2, j_2)} = \left\{ (u, v) : F_{i_1, j_1}(u, v) = F_{i_2, j_2}(u, v) > F_{i, j}(u, v), \right. \\ \left. \text{for all } (i, j) \neq (i_k, j_k), k = 1, 2 \right\} \quad (8)$$

for some pair $(i_1, j_1), (i_2, j_2)$. We will call such lines *tropical edges*. Notice that $\mathcal{E}_{(i_1, j_1), (i_2, j_2)}$ (if nonempty) is either vertical (if $j_1 = j_2$) or it has rational slope $\frac{i_2 - i_1}{j_1 - j_2}$.

On the other hand, points (u, v) where

$$\# \operatorname{argmax}_{(i,j)} F_{i,j}(u, v) > 2,$$

are called *tropical vertices*. They are in general isolated with

$$\# \operatorname{argmax}_{(i,j)} F_{i,j}(u, v) = 3,$$

see [50], and are in this case given by

$$\mathcal{P}_{(i_1, j_1), (i_2, j_2), (i_3, j_3)} = \left\{ (u, v) : F_{i_1, j_1}(u, v) = F_{i_2, j_2}(u, v) = F_{i_3, j_3}(u, v) > F_{i, j}(u, v), \right. \\ \left. \text{for all } (i, j) \neq (i_k, j_k), k = 1, 2, 3 \right\},$$

for some triplet $(i_1, j_1), (i_2, j_2), (i_3, j_3)$.

Finally, points (u, v) where

$$\# \operatorname{argmax}_{(i,j)} F_{i,j}(u, v) = 1,$$

lie on convex polygonal domains given by

$$\mathcal{R}_{(i_1, j_1)} = \left\{ (u, v) : F_{i_1, j_1}(u, v) > F_{i, j}(u, v), \text{ for all } (i, j) \neq (i_1, j_1) \right\}, \quad (9)$$

for some (i_1, j_1) . We call these sets *tropical regions*. We will frequently drop the subscripts on \mathcal{E} , \mathcal{P} and \mathcal{R} if the indices (specifying the relevant monomials) are not important.

Definition 2.2. Two tropical curves \mathcal{T} and \mathcal{T}' are said to be homotopic if there is a continuous deformation \mathcal{T}_t , $t \in [0, 1]$, with $\mathcal{T}_0 = \mathcal{T}$ and $\mathcal{T}_1 = \mathcal{T}'$, such that (a) the cardinality of the set of tropical vertices of \mathcal{T}_t is constant and (b) only the lengths of the tropical edges of \mathcal{T}_t vary, not their slopes.

The *Newton polygon* of a tropical polynomial (7) is defined as the convex hull of the *point configuration*

$$\left\{ \deg F_{i,j} \in \mathbb{N}_0^2 : \alpha_{i,j} \neq -\infty, 0 \leq i + j \leq N \right\}.$$

Another important concept is that of a *polyhedral subdivision* \mathcal{S} of the Newton polygon. To explain this, consider the points

$$(\deg F_{i,j}, \alpha_{i,j}) \in \mathbb{N}_0^2 \times (\mathbb{R} \cup \{-\infty\}),$$

obtained by assigning the tropical coefficients $\alpha_{i,j}$ of $F_{i,j}$ as a third dimension (a height). Then we take the upper envelope of the resulting set of points. Finally, the subdivision \mathcal{S} is obtained by projecting the edges of the resulting convex polyhedron back to \mathbb{R}^2 , where \mathbb{N}_0^2 is naturally embedded, see [13, 50] and Fig. 1. The different polygons of \mathcal{S} will be called *faces*.

The importance of \mathcal{S} is due to the fact that \mathcal{S} is *dual to the tropical curve* \mathcal{T} in the following sense:

Proposition 2.3. [50, Proposition 3.1.6] *Consider a polyhedral subdivision \mathcal{S} associated with a tropical polynomial. Then each face of the subdivision corresponds to a tropical vertex $(u, v) \in \mathcal{T}$ where*

$$\#\operatorname{argmax}_{(i,j)} F_{i,j}(u, v) > 2, \quad (10)$$

and the edges of \mathcal{S} correspond to the edges (the tropical edges) of \mathcal{T} where

$$\#\operatorname{argmax}_{(i,j)} F_{i,j}(u, v) = 2.$$

In particular, the subdivision \mathcal{S} fixes the tropical curve \mathcal{T} up to homotopy and the dual edges of \mathcal{S} and \mathcal{T} are perpendicular (see Fig. 1(b)).

A subdivision \mathcal{S} where all of its faces are triangles (as in Fig. 1) is called a *triangulation*, and in this case exactly three tropical edges come together at each tropical vertex (so that the left hand side of (10) equals 3).

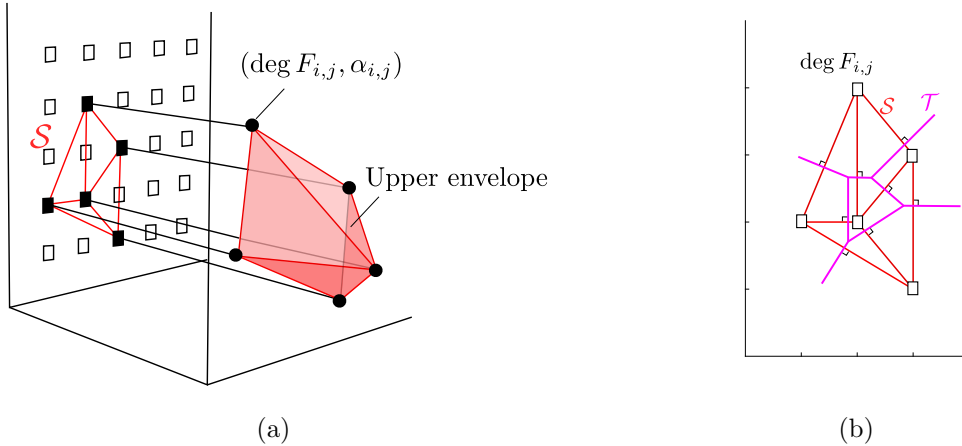


Figure 1: In (a): The upper envelope of the set of points $(\deg F_{i,j}, \alpha_{i,j})$. The subdivision \mathcal{S} of the Newton polygon is the projection of the envelope. In (b): The subdivision \mathcal{S} and the dual tropical curve \mathcal{T} . The subdivision fixes \mathcal{T} up to homotopy and the tropical edges of \mathcal{T} are perpendicular to the edges of \mathcal{S} , see Proposition 2.3.

There are

$$M = M(N) := \frac{1}{2}(N+2)(N+1) \in \mathbb{N}, \quad (11)$$

many coefficients $\{\alpha_{i,j}\}_{0 \leq i+j \leq N}$ of a general (tropical) polynomial of degree N . Let

$$\alpha := (\alpha_{0,0}, \dots, \alpha_{N,0}, \alpha_{0,1}, \dots, \alpha_{N-1,1}, \alpha_{0,2}, \dots, \alpha_{N,0}), \quad (12)$$

and put

$$\mathbf{A}(M) := (\mathbb{R} \cup \{-\infty\})^M. \quad (13)$$

Then $\alpha \in \mathbf{A}(M)$. We use the product topology to obtain a topology on $\mathbf{A}(M)$, recall Remark 2.1.

Now, the subdivisions of the Newton polygon are determined by a set of linear inequalities on the tropical coefficients, see e.g. [13], and each triangulation defines an open convex polytope in the space of coefficients $\mathbf{A}(M)$. This leads to the following simple fact, see [13].

Theorem 2.4. *Fix a degree $N \in \mathbb{N}$. Then the subdivision \mathcal{S} of a tropical polynomial (7) with $\alpha \in \mathbf{A}(M(N))$ is a triangulation on a dense open subset of $\mathbf{A}(M(N))$. This dense subset is the finite union of open convex polytopes.*

In other words, all tropical vertices have $\#\arg\max_{(i,j)} F_{i,j}(u,v) = 3$ on a dense open subset consisting of a finite union of open convex polytopes. Notice that the tropical curves (as well as the subdivisions) are invariant with respect to translations

$$a \mapsto \alpha + a := (\alpha_{0,0} + a, \dots, \alpha_{N,0} + a), \quad a \in \mathbb{R}, \quad (14)$$

of the tropical coefficients. Each of the convex polytopes in Theorem 2.4 are therefore also invariant with respect to such translations. (One could obviously choose to partition $\mathbf{A}(M)$ into equivalence classes, obtained from the action (14), but this will not be important for our purposes, and we will therefore not do so in the present manuscript.)

The actual number of triangulations $T(n)$ for a point configuration of n points is not known, to the best of our knowledge. There are bounds, however, of the form $2^{c_1 n} \leq T(n) \leq 2^{c_2 n}$ for some constants $c_2 \geq c_1 > 0$, see [13, Chapter 3]. Moreover, not every triangulation is *regular*, in the sense that it is realizable as a projection of an upper envelope, see [13].

There are many classical results of algebraic geometry that have counterparts in tropical geometry. One even talks of a (Litvinov-Maslov) *correspondance principle* [48, 53]), in the spirit of the correspondance principle in Quantum Mechanics, between results in classical algebraic geometry and tropical geometry, see [47]. For example, Bézout's theorem also holds in tropical geometry (for details on counting multiplicities, we refer to [50]):

Theorem 2.5. *Consider two tropical curves \mathcal{T} and \mathcal{T}' of degree K and L in \mathbb{R}^2 . Then if they intersect transversally, meaning that each intersection is along the tropical edges of \mathcal{T} and \mathcal{T}' , then they do so KL times (counting multiplicities).*

Moreover, if \mathcal{T} and \mathcal{T}' do not intersect transversally, then

$$\lim_{\epsilon \rightarrow 0} \mathcal{T}_\epsilon \cap \mathcal{T}'_\epsilon,$$

is independent of the choice of perturbations \mathcal{T}_ϵ and \mathcal{T}'_ϵ of \mathcal{T} and \mathcal{T}' , respectively. This is called the *Stable Intersection Principle*, see [50, Theorem 1.3.3].

3 A tropicalization of planar polynomial ODEs

The vector space of real polynomials of degree N in two variables x, y is spanned by the monomials $x^n y^m$, $0 \leq n + m \leq N$. The dimension of this space is $M = M(N)$, recall (11). Now, define

$$\mathcal{U} := \{1, \dots, M\}, \quad \mathcal{V} = \mathcal{U} + M := \{M + 1, \dots, 2M\}. \quad (15)$$

For our purposes, it will then be convenient to write the polynomials P and Q in (1) in the following form

$$P(x, y) = \sum_{k \in \mathcal{U}} a_k x^{n_k} y^{m_k}, \quad Q(x, y) = \sum_{k \in \mathcal{V}} a_k x^{n_{k-M}} y^{m_{k-M}}, \quad (16)$$

using an enumeration of n_k and m_k : The details are not important, but for concreteness, consider

$$q_l := lN - \frac{l(l-3)}{2}, \quad \text{for } l = 0, \dots, N,$$

and $q_{N+1} := M + 1$. Then we define

$$n_k := k - q_l, \quad m_k := l, \quad \text{for } k = q_l, \dots, q_{l+1} - 1, \quad (17)$$

and each $l = 0, \dots, N$. Notice that $q_{l+1} - q_l = N - l + 1$ so that $n_k + m_k = N$ for $k = q_{l+1} - 1$ and all $l = 0, \dots, N$. This enumeration is consistent with (12).

We put

$$\mathcal{I} := \mathcal{U} \cup \mathcal{V} = \{1, \dots, 2M\}.$$

Then $a_k \in \mathbb{R}$ for all $k \in \mathcal{I}$ and $(n_k, m_k) \in \mathbb{N}_0^2$ and $0 \leq n_k + m_k \leq N$ for all $k \in \mathcal{I}$.

We will now introduce a tropical version of (1). We will only consider the first quadrant $(x, y) \in \mathbb{R}_+^2$, $\mathbb{R}_+ := (0, \infty)$; the other quadrants can be handled in a similar way, but we leave the problem of connecting the quadrants to future work (see Section 15 for a further discussion of this aspect).

For any $\epsilon > 0$, consider the transformation:

$$(x, y, \{a_k\}_{k \in \mathcal{I}}) \mapsto (u, v, \{\delta_k\}_{k \in \mathcal{I}}, \{\alpha_k\}_{k \in \mathcal{I}}), \quad (18)$$

of x, y and the coefficients $\{a_k\}_{k \in \mathcal{I}}$, defined by (5) and

$$\delta_k = \text{sign}(a_k) := \begin{cases} 1 & \text{for } a_k \geq 0 \\ -1 & \text{for } a_k < 0 \end{cases}, \quad \alpha_k = \begin{cases} \epsilon \log |a_k| & \text{for } a_k \neq 0 \\ -\infty & \text{for } a_k = 0 \end{cases}, \quad (19)$$

for all $k \in \mathcal{I}$. By introducing the tropical monomials

$$\begin{aligned} F_k(u, v) &:= \alpha_k + (n_k - 1)u + m_k v, \quad k \in \mathcal{U}, \\ F_k(u, v) &:= \alpha_k + n_{k-M}u + (m_{k-M} - 1)v, \quad k \in \mathcal{V}, \end{aligned} \tag{20}$$

for $(u, v) \in \mathbb{R}^2$, an elementary calculation then shows that the application of (18) to (1), with P and Q in the form (16), leads to the following equations:

$$\begin{aligned} u' &= \epsilon \sum_{k \in \mathcal{U}} \delta_k e^{F_k(u, v)\epsilon^{-1}}, \\ v' &= \epsilon \sum_{k \in \mathcal{V}} \delta_k e^{F_k(u, v)\epsilon^{-1}}. \end{aligned} \tag{21}$$

Monomial terms of P and Q in the equations for x and y therefore become exponential terms with the tropical monomials F_k as their arguments. Recall that the tuple (n, m) is the degree $\deg F$ of $F(u, v) = \alpha + nu + mv$. In contrast to Section 2, we can therefore have $\deg F_k = (-1, *)$ and $(*, -1)$. This is not a problem; we can define tropical curves, the Newton polygons and the subdivisions completely analogously. Notice, however, from (20) that

$$\begin{aligned} \deg F_k = (-1, *) &\implies k \in \mathcal{U}, \\ \deg F_k = (*, -1) &\implies k \in \mathcal{V}. \end{aligned} \tag{22}$$

To be able to study the limit $\epsilon \rightarrow 0$ of (21), we “tame” the exponentials (as in [33]) by introducing a new time t defined by

$$\frac{dt}{d\tau} = \epsilon \sum_{k \in \mathcal{I}} e^{F_k(u, v)\epsilon^{-1}} > 0. \tag{23}$$

This produces the equations

$$\begin{aligned} \dot{u} &= \frac{\sum_{k \in \mathcal{U}} \delta_k e^{F_k(u, v)\epsilon^{-1}}}{\sum_{k \in \mathcal{I}} e^{F_k(u, v)\epsilon^{-1}}}, \\ \dot{v} &= \frac{\sum_{k \in \mathcal{V}} \delta_k e^{F_k(u, v)\epsilon^{-1}}}{\sum_{k \in \mathcal{I}} e^{F_k(u, v)\epsilon^{-1}}}, \end{aligned} \tag{24}$$

with $\dot{(\cdot)} = \frac{d}{dt}$. Let $\mathcal{L} = \mathcal{I}, \mathcal{U}$ or \mathcal{V} . We then define

$$F_{\max}^{\mathcal{L}}(u, v) := \max_{k \in \mathcal{L}} F_k(u, v), \quad (u, v) \in \mathbb{R}^2,$$

as the tropical polynomial associated with the monomials F_k , $k \in \mathcal{L}$, and let $\mathcal{T}^{\mathcal{L}}$ denote the associated tropical curve. Similarly, tropical edges, vertices and regions will be denoted by $\mathcal{E}^{\mathcal{L}}$, $\mathcal{P}^{\mathcal{L}}$ and $\mathcal{R}^{\mathcal{L}}$, respectively. Finally, the associated subdivision of the Newton polygon is denoted by $\mathcal{S}^{\mathcal{L}}$. However, we frequently drop the superscript if $\mathcal{L} = \mathcal{I}$ (since this situation will play the most important role). Notice that

$$\begin{aligned} F_{\max}^{\mathcal{U}}(u, v) &:= \max_{k \in \mathcal{U}} F_k(u, v), \quad (u, v) \in \mathbb{R}^2, \\ F_{\max}^{\mathcal{V}}(u, v) &:= \max_{k \in \mathcal{V}} F_k(u, v), \quad (u, v) \in \mathbb{R}^2, \end{aligned}$$

only involve monomials from the u and v -directions, respectively.

Remark 3.1. The point configurations associated with $F_{\max}^{\mathcal{U}}$ and $F_{\max}^{\mathcal{V}}$ each have M points, see (11), whereas the point configuration associated with $F_{\max}^{\mathcal{I}}$ has

$$M + N + 1 = \frac{1}{2}(N + 1)(N + 4), \quad (25)$$

points. This is a simple consequence of (22).

Finally, for any $k \in \mathcal{I}$ we define

$$\mathbf{d}_k = \begin{cases} (\delta_k, 0) & \text{if } k \in \mathcal{U}, \\ (0, \delta_k) & \text{if } k \in \mathcal{V}, \end{cases} \quad (26)$$

as the flow vector associated to the tropical monomial F_k in (20).

Remark 3.2. Notice that in our definition of (20), we can have $\deg F_k = \deg F_j$ but only for $k \in \mathcal{U}$ and $j \in \mathcal{V}$. In particular, the tropical pair $(\mathbf{d}_k, \deg F_k)$ is unique.

Lemma 3.3. The system (1) on $(x, y) \in \mathbb{R}_+^2$ and the system (24) on $(u, v) \in \mathbb{R}^2$ are topologically equivalent for every $\epsilon > 0$ whenever (19) holds.

Moreover, suppose $(u, v) \notin \mathcal{T}$ such that $(u, v) \in \mathcal{R}_l$ with $l = \operatorname{argmax}_{k \in \mathcal{I}} F_k(u, v)$ and fix the lists $\{\delta_k\}_{k \in \mathcal{I}}$ and $\{\alpha_k\}_{k \in \mathcal{I}}$. Then the right hand side of (24) converges as $\epsilon \rightarrow 0$ to the flow vector \mathbf{d}_l , see (26).

Proof. The first part is by construction, with the diffeomorphism $\mathbb{R}_+^2 \ni (x, y) \mapsto (u, v) \in \mathbb{R}^2$ given by (5) and the regular transformation of time given by (23). The second part follows from a straightforward calculation: Given $(u, v) \notin \mathcal{T}$, we have $(u, v) \in \mathcal{R}_l$ with $l = \operatorname{argmax}_{k \in \mathcal{I}} F_k(u, v)$. Hence

$$F_l(u, v) - F_k(u, v) > c > 0 \quad \text{for all } k \neq l,$$

for some $c > 0$ small enough. Suppose that $l \in \mathcal{U}$. Then by (24), we obtain

$$\begin{aligned} \dot{u} &= \frac{\delta_l + \mathcal{O}(e^{-c/\epsilon})}{1 + \mathcal{O}(e^{-c/\epsilon})}, \\ \dot{v} &= \frac{\mathcal{O}(e^{-c/\epsilon})}{1 + \mathcal{O}(e^{-c/\epsilon})}, \end{aligned}$$

and the result follows. The case $l \in \mathcal{V}$ is identical. \square

Remark 3.4. The approach, detailed above, for tropicalizing (1) through (5), (18) and the singular limit $\epsilon \rightarrow 0$, was communicated to the first author by P. Szmolyan in 2019 in a private conversation. It is also partially fleshed out in [56] in the context of the Michaelis-Menten kinetics.

Let

$$|(u, v)|_1 := |u| + |v|, \quad (27)$$

denote the 1-norm on \mathbb{R}^2 , and put $\mathbb{N}_0 := \{0\} \cup \mathbb{N}$ and $\mathbb{N}_{-1} := \{-1\} \cup \mathbb{N}_0$.

Definition 3.5. We define \mathcal{M}^u (\mathcal{M}^v) as the set of all tropical monomials F (i.e. of the form (6)) with degree $\deg F \in \mathbb{N}_{-1} \times \mathbb{N}_0$ ($\deg F \in \mathbb{N}_0 \times \mathbb{N}_{-1}$, respectively) and tropical coefficient $\alpha \in \mathbb{R} \cup \{-\infty\}$.

For each fixed $N \in \mathbb{N}$, we define \mathcal{M}_N^u (\mathcal{M}_N^v) as the subset of \mathcal{M}^u (\mathcal{M}^v , respectively) satisfying

$$\mathcal{M}_N^l = \left\{ F \in \mathcal{M}^l : |\deg F|_1 \leq N + 1 \right\}, \quad l = u, v.$$

3.1 A set-valued vector-field trop

As a consequence of Lemma 3.3, (24) (with $\{\delta_k\}_{k \in \mathcal{I}}$ and $\{\alpha_k\}_{k \in \mathcal{I}}$ fixed) is piecewise smooth (in fact, even piecewise constant) in the limit $\epsilon \rightarrow 0$ and the discontinuity set is a subset of \mathcal{T} . In particular, the limit $\epsilon \rightarrow 0$ is well-defined for $(u, v) \notin \mathcal{T}$ and given by

$$\begin{pmatrix} \dot{u} \\ \dot{v} \end{pmatrix} = \mathbf{d}_{\arg\max_{k \in \mathcal{I}} F_k(u, v)}, \quad (u, v) \notin \mathcal{T}. \quad (28)$$

On the other hand, for $(u, v) \in \mathcal{T}$,

$$\arg\max_{k \in \mathcal{I}} F_k(u, v),$$

contains more than one element by definition.

Let

$$\mathbf{conv}(\mathbf{d}_k, \mathbf{d}_l) = \left\{ q\mathbf{d}_k + (1 - q)\mathbf{d}_l : q \in [0, 1] \right\},$$

denote the convex hull of \mathbf{d}_k and \mathbf{d}_l . If $\mathbf{d}_k \neq \mathbf{d}_l$ then $\mathbf{conv}(\mathbf{d}_k, \mathbf{d}_l)$ is simply the line segment connecting \mathbf{d}_k and \mathbf{d}_l . Otherwise, it is a point.

Remark 3.6. For simplicity, we write $\{(-1, 0), (1, 0)\}$ as $\{(\pm 1, 0)\}$. $\{(0, \pm 1)\}$ is understood in the same way. Moreover, for simplicity of notation, we will throughout assume that it is clear from the context whether tuples should be understood as row or column vectors. As usual, $b \cdot c$ will denote the dot product in \mathbb{R}^n between vectors b and c .

We now define a set-valued vector-field **trop**, which will form the basis for our definition of a tropical dynamical system. For this purpose, we use $2^{\mathbb{R}^2}$ to denote the power set of \mathbb{R}^2 , i.e. the set of all subsets of \mathbb{R}^2 .

Definition 3.7. Consider any $(u, v) \in \mathbb{R}^2$ and write

$$\mathcal{L}^* = \mathcal{L}^*(u, v) := \arg\max_{k \in \mathcal{L}} F_k(u, v) \quad \text{and} \quad \mathbf{d}_{\mathcal{L}^*} := \{\mathbf{d}_k : k \in \mathcal{L}^*\},$$

for $\mathcal{L} = \mathcal{U}, \mathcal{V}$ and \mathcal{I} . We then define the set-valued vector-field

$$(u, v) \mapsto \mathbf{trop}(u, v) \in 2^{\mathbb{R}^2},$$

as follows:

1. If $\mathbf{d}_{\mathcal{I}^*}$ is a singleton, so that $\mathbf{d}_{\mathcal{I}^*} = \{\mathbf{d}\}$ for some flow vector \mathbf{d} , then

$$\mathbf{trop}(u, v) := \{\mathbf{d}\}.$$

2. Otherwise, $\mathbf{d} \in \mathbf{trop}(u, v)$ if and only if either of the following conditions holds true

(a) There exist $\mathbf{t} \in \mathbf{d}_{\mathcal{U}^*}$ and $\mathbf{s} \in \mathbf{d}_{\mathcal{V}^*}$ such that $\mathbf{d} \in \mathbf{conv}(\mathbf{t}, \mathbf{s})$.

(b) $\mathbf{d} = \mathbf{0}$, $\mathbf{d}_{\mathcal{U}^*} = \{(\pm 1, 0)\}$ and $\mathbf{d}_{\mathcal{V}^*} = \{(0, \pm 1)\}$.

Notice that $\mathbf{trop}(u, v) = \{\mathbf{d}_k\}$ for any $(u, v) \in \mathcal{R}_k$, $k \in \mathcal{I}$, (as desired, cf. (28)).

We emphasize that the zero vector $\mathbf{0}$ belongs to $\mathbf{trop}(u, v)$ if and only if $\mathbf{d}_{\mathcal{U}^*} = \{(\pm 1, 0)\}$ and $\mathbf{d}_{\mathcal{V}^*} = \{(0, \pm 1)\}$, cf. 2b. The motivation for this choice should be clear enough, see also Section 6 below. If $\mathbf{0} \in \mathbf{trop}(u, v)$, then (u, v) is called a *tropical singularity*, see Section 9.

The following property of \mathbf{trop} will be important later on.

Lemma 3.8. $\mathbf{trop} : \mathbb{R}^2 \rightarrow 2^{\mathbb{R}^2}$ is upper semi-continuous: For every $(u', v') \in \mathbb{R}^2$ there exists a neighborhood X of (u', v') such that

$$\mathbf{trop}(u, v) \subset \mathbf{trop}(u', v'),$$

for all $(u, v) \in X$.

Proof. The tropical monomials are continuous functions and consequently there is a neighborhood X of (u', v') such that

$$F_l(u, v) < F_i(u, v),$$

for all $i \in \mathcal{L}^*(u', v')$, all $l \notin \mathcal{L}^*(u', v')$, all $(u, v) \in X$ and $\mathcal{L} = \mathcal{U}, \mathcal{V}, \mathcal{I}$. Consequently, $\mathbf{d}_{\mathcal{L}^*(u, v)} \subset \mathbf{d}_{\mathcal{L}^*(u', v')}$ for all $(u, v) \in X$ and every $\mathcal{L} = \mathcal{U}, \mathcal{V}, \mathcal{I}$, and the result then follows from the definition of \mathbf{trop} , see Definition 3.7. \square

In the following Section 3.2, we define the important concepts of tropical sliding and crossing. We then analyze these cases further in Section 3.3 and Section 3.4, where we also compute $\mathbf{trop}(u, v)$.

3.2 Tropical sliding and crossing

Suppose that (u, v) belongs to a tropical edge $\mathcal{E}_{i, j}$, $i, j \in \mathcal{I}$, $i \neq j$, i.e. a line segment defined by the set of points $(u, v) : F_i(u, v) = F_j(u, v) > F_k(u, v)$ for all $k \in \mathcal{I}, k \neq i, j$. This gives

$$(n_j - n_i)u + (m_j - m_i)v + \alpha_j - \alpha_i = 0. \quad (29)$$

Therefore $\mathcal{E}_{i, j}$ is horizontal if $n_i = n_j$ and vertical if $m_i = m_j$. Otherwise, it has rational slope $\frac{n_j - n_i}{m_i - m_j}$. Here we suppose that $\deg F_i \neq \deg F_j$, recall Remark 3.2.

Remark 3.9. Notice that if $\deg F_i = \deg F_j$ then the set defined by $F_i = F_j$ is either the empty set or \mathbb{R}^2 ($\Leftrightarrow \alpha_i = \alpha_j$).

Given (29),

$$\mathbf{n}_{i,j} = \deg F_j - \deg F_i = (n_j - n_i, m_j - m_i), \quad (30)$$

is a normal vector to $\mathcal{E}_{i,j}$.

In the language of PWS dynamical systems theory [16, 25], $\mathcal{E}_{i,j}$ is a switching manifold if $\mathbf{d}_i \neq \mathbf{d}_j$.

Definition 3.10. *Suppose that $\mathcal{E}_{i,j}$ is a switching manifold ($\mathbf{d}_i \neq \mathbf{d}_j$). Then $\mathcal{E}_{i,j}$ is of the following type:*

1. Crossing if \mathbf{d}_i and \mathbf{d}_j point in the same direction relative to $\mathcal{E}_{i,j}$:

$$(\mathbf{d}_i \cdot \mathbf{n}_{i,j})(\mathbf{d}_j \cdot \mathbf{n}_{i,j}) > 0. \quad (31)$$

2. Sliding otherwise:

$$(\mathbf{d}_i \cdot \mathbf{n}_{i,j})(\mathbf{d}_j \cdot \mathbf{n}_{i,j}) \leq 0. \quad (32)$$

More specifically, when (32) holds, then $\mathcal{E}_{i,j}$ is of the following sliding-type:

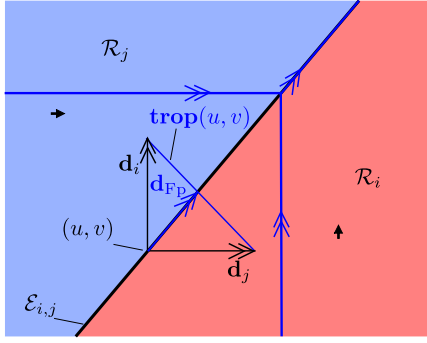
- (a) Transversal (tangential) Filippov if $\mathbf{d}_i \cdot \mathbf{d}_j = 0$ and the left hand side of (32) is nonzero (zero, respectively).
- (b) Transversal (tangential) Nullcline if $\mathbf{d}_i \cdot \mathbf{d}_j = -1$ and the left hand side of (32) is nonzero (zero, respectively).

We will occasionally use a similar terminology of nullcline sliding for the *individual* tropical edges $\mathcal{E}^{\mathcal{L}}$ of $\mathcal{T}^{\mathcal{L}}$, $\mathcal{L} = \mathcal{U}, \mathcal{V}$, see Section 9. Notice that for crossing, then $\mathbf{d}_i \cdot \mathbf{d}_j = 0$ with $i \in \mathcal{U}$ and $j \in \mathcal{V}$ (or vice versa).

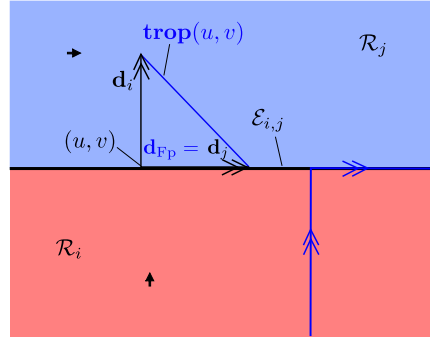
In contrast to general piecewise smooth systems with nonconstant vector-fields [25, 32], we define sliding to hold even when (32) holds with equality. The reason for doing so, is that such tangencies are *robust* with respect to perturbations of α_k in the present case. Indeed, the slope of $\mathcal{E}_{i,j}$ only depends upon the degrees $\deg F_i$ and $\deg F_j$ (which are fixed), not on the tropical coefficients α_i and α_j .

We illustrate the different cases in Fig. 2 and Fig. 3. Fig. 2(a) and (b) illustrate Filippov sliding, whereas (c) and (d) illustrate nullcline sliding.

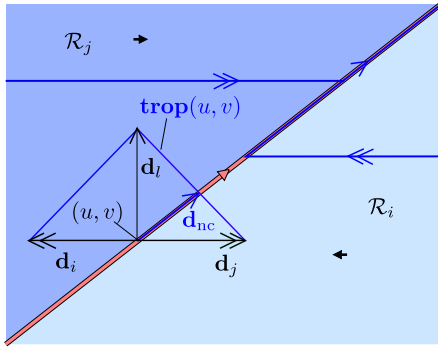
In these figures, we also introduce our convention: Red (brown, see Fig. 5) indicates a vertical flow vector, pointing upwards (downwards, respectively). Blue (light blue), on the other hand, corresponds to a horizontal flow vector, pointing to the right (left, respectively). The little arrow along the switching manifolds in (c) indicate the subdominant direction (\mathbf{d}_l in Fig. 2). It is colored red in the present case because \mathbf{d}_l is pointing upwards. Moreover, full lines indicate switching manifolds of sliding type, whereas dashed lines indicate switching manifolds of crossing type (or later tropical edges $\mathcal{E}_{i,j}$ which are not switching manifolds, i.e. $\mathbf{d}_j = \mathbf{d}_i$).



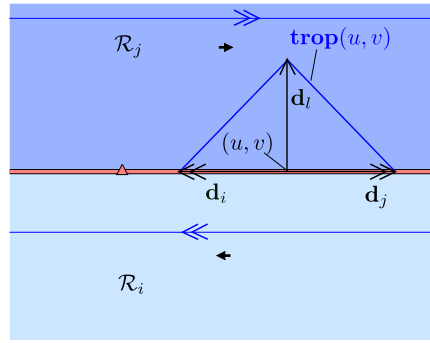
(a) Transversal Filippov sliding



(b) Tangential Filippov sliding



(c) Transversal nullcline sliding



(d) Tangential nullcline sliding

Figure 2: Illustrations of sliding and the set-valued vector-field $\mathbf{trop}(u, v)$, $(u, v) \in \mathcal{E}_{i,j}$. The blue curves show orbits of the differential inclusion $(\dot{u}, \dot{v}) \in \mathbf{trop}(u, v)$. In particular, for Filippov sliding ((a) and (b)), there is a unique vector \mathbf{d}_{FP} , the Filippov sliding-vector, tangent to the switching manifold. For transversal (not tangential) nullcline sliding (c), in a point which is not a tropical singularity, there is also a unique vector \mathbf{d}_{nc} that is tangent to the switching manifold. The direction is also indicated by a little (red) triangle, a convention we will also use in the subsequent figures. In (d) (tangential nullcline sliding), only \mathbf{d}_i and \mathbf{d}_j in $\mathbf{trop}(u, v)$ are tangent to $\mathcal{E}_{i,j}$ at $(u, v) \in \mathcal{E}_{i,j}$.

Filippov sliding (transversal or tangential) as well as transversal nullcline sliding can be stable and unstable, depending on whether vectors point towards or away from $\mathcal{E}_{i,j}$. In Fig. 2 we only illustrate the stable versions.

3.3 The set-valued vector-field \mathbf{trop} for tropical sliding

In this section, we compute $\mathbf{trop}(u, v)$ in the different cases of sliding under the assumption that $\mathbf{0} \notin \mathbf{trop}(u, v)$. The results will be important in our construction of global solutions to $(\dot{u}, \dot{v}) \in \mathbf{trop}(u, v)$ in Theorem 4.1.

Lemma 3.11. *Suppose that $\mathcal{E}_{i,j}$, $i \in \mathcal{U}$, $j \in \mathcal{V}$, is a switching manifold of Filippov sliding*

type (transversal or tangential, see Fig. 2(a) and (b)). Then

$$\mathbf{trop}(u, v) = \mathbf{conv}(\mathbf{d}_i, \mathbf{d}_j), \quad \text{for all } (u, v) \in \mathcal{E}_{i,j}, \quad (33)$$

and there is a unique vector

$$\mathbf{d}_{\text{FP}} = q\mathbf{d}_i + (1 - q)\mathbf{d}_j, \quad q = \frac{\mathbf{n}_{i,j} \cdot \mathbf{d}_j}{\mathbf{n}_{i,j} \cdot \mathbf{d}_j - \mathbf{n}_{i,j} \cdot \mathbf{d}_i}, \quad (34)$$

contained in $\mathbf{trop}(u, v)$, which is tangent to $\mathcal{E}_{i,j}$ at $(u, v) \in \mathcal{E}_{i,j}$.

Proof. By Definition 3.10, $\mathbf{d}_{\mathcal{I}^*} = \{\mathbf{d}_i, \mathbf{d}_j\}$ and $\mathbf{d}_i \cdot \mathbf{d}_j = 0$ with $i \in \mathcal{U}$ and $j \in \mathcal{V}$. We are therefore in situation 2a of Definition 3.7 and (33) follows. Finally, the statement regarding (34) follows from a elementary computation. \square

The vector (34) is the *Filippov sliding vector*, known from the Filippov convention of piecewise smooth systems, see [25]. In our setting, it is constant along a sliding switching manifold $\mathcal{E}_{i,j}$ of Filippov type. Notice that in the tangential case then $q = 0$ ($\mathbf{d}_{\text{FP}} = \mathbf{d}_j$) or $q = 1$ ($\mathbf{d}_{\text{FP}} = \mathbf{d}_i$), whereas in the transversal case $q \in (0, 1)$.

Next, we consider nullcline sliding:

Lemma 3.12. *Suppose that $\mathcal{E}_{i,j}$ is of nullcline sliding type and that $i, j \in \mathcal{U}$, $i \neq j$, (so that u is the dominant direction, see Fig. 2(c) and (d)). Moreover, suppose that $(u, v) \in \mathcal{E}_{i,j} \cap \mathcal{R}_l^\mathcal{V}$ for some $l \in \mathcal{V}$. Then*

$$\mathbf{trop}(u, v) = \left\{ (u', v') \in \mathbb{R}^2 : |(u', v')|_1 = 1 \text{ and } (u', v') \cdot \mathbf{d}_l \geq 0 \right\}, \quad (35)$$

recall (27). Moreover, the following holds:

1. *If $\mathcal{E}_{i,j}$ is of transversal nullcline sliding type, then there exists a unique vector*

$$\mathbf{d}_{\text{nc}} = \frac{\mathbf{d}_l \cdot \mathbf{e}_{i,j}}{|\mathbf{d}_l \cdot \mathbf{e}_{i,j}|} \mathbf{e}_{i,j}, \quad (36)$$

contained in $\mathbf{trop}(u, v)$, which is tangent to $\mathcal{E}_{i,j}$ at $(u, v) \in \mathcal{E}_{i,j} \cap \mathcal{R}_l^\mathcal{V}$. Here $\mathbf{e}_{i,j}$ is a $|\cdot|_1$ -unit vector tangent to $\mathcal{E}_{i,j}$.

2. *If $\mathcal{E}_{i,j}$ is of tangential nullcline sliding type, then \mathbf{d}_i and \mathbf{d}_j are the only vectors contained in $\mathbf{trop}(u, v)$ that are tangent to $\mathcal{E}_{i,j}$.*

Proof. By Definition 3.10, $\mathbf{d}_{\mathcal{I}^*} = \{\mathbf{d}_i, \mathbf{d}_j\}$ with $i, j \in \mathcal{U}$ and $\mathbf{d}_i \neq \mathbf{d}_j$. We are therefore in case 2a of Definition 3.7 (case 2b is not relevant because $\mathbf{d}_{\mathcal{V}^*} = \{\mathbf{d}_l\}$ is a singleton). Hence $\mathbf{d} \in \mathbf{trop}(u, v)$ if only if $\mathbf{d} \in \mathbf{conv}(\mathbf{d}_i, \mathbf{d}_l)$ or $\mathbf{d} \in \mathbf{conv}(\mathbf{d}_j, \mathbf{d}_l)$ and (35) therefore follows. The remaining statements in 1 and 2 are trivial, and further details are therefore left out. \square

The case of Lemma 3.12 where $i, j \in \mathcal{V}$ and $l \in \mathcal{U}$ (so that v is the dominating direction) is similar and the corresponding details are therefore left out for simplicity.

The vector (36) will be called the *nullcline sliding vector*. It is constant on the open subset $\mathcal{E}_{i,j} \cap \mathcal{R}_l^\mathcal{V}$ of $\mathcal{E}_{i,j}$ (of transversal nullcline sliding type).

Remark 3.13. Notice that transversal nullcline sliding is associated with a time scale separation of (24) for $\epsilon \rightarrow 0$. This is due to the fact that the vector \mathbf{d}_l in Fig. 2(c) and (d) corresponds to the flow vector of sub-dominant monomial F_l : $F_l(u, v) < F_i(u, v) = F_j(u, v)$ for $(u, v) \in \mathcal{E}_{i,j} \cap \mathcal{R}_l^\vee$, $\{i, j\} = \operatorname{argmax}_{k \in \mathcal{I}} F_k(u, v)$, and $l = \operatorname{argmax}_{k \in \mathcal{V}} F_k(u, v)$. Consequently, v is slow in comparison with u in (c) and (d) for (24) for $0 < \epsilon \ll 1$. Our figures reflect this fact insofar that we use two types of arrows: Double-headed arrows for fast directions (including \mathbf{d}_{FP}) and single headed arrows for slow directions (along \mathbf{d}_{nc} , see (c)) (a convention frequently used in slow-fast systems).

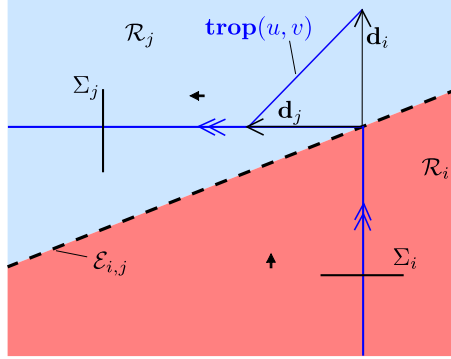


Figure 3: Illustration of crossing.

3.4 The crossing flow

Finally, regarding crossing (see Fig. 3) we notice that a crossing edge $\mathcal{E}_{i,j} \subset \mathcal{T}$ with normal vector $\mathbf{n}_{i,j}$, see (30), is neither horizontal or vertical (i.e. $n_i \neq n_j$ and $m_i \neq m_j$). It follows that the flow of (28) near crossing switching manifolds is well-defined. In fact, as indicated in Fig. 3, it coincides with the usual notion of crossing in PWS systems where orbits are uniquely concatenated across the switching manifold. This process leads to local transition maps that we now describe:

Given that $\mathbf{d}_i \cdot \mathbf{d}_j = 0$, we may suppose that $\mathbf{d}_i = (0, *)$ (otherwise, by the definition of flow vectors in (26), we can shift the role of i and j). We will also suppose that \mathbf{d}_i points towards $\mathcal{E}_{i,j}$; if not, we can reverse the direction of time. We are in the situation illustrated in Fig. 3 (where $\mathbf{d}_i = (0, 1)$), and consider segments $\Sigma_l \subset \mathcal{R}_l$, $l = i, j$, transverse to the flow, defined by fixed $v = \text{const.}$, and $u \in I_i$ for $l = i$, and fixed $u = \text{const.}$, and $v \in J_j$ for $l = j$. Here I_i and J_j are open and nonempty intervals, such that the transition map $P_{i,j} : \Sigma_i \rightarrow \Sigma_j$, induced by the forward flow of (28), is well-defined. Clearly, $P_{i,j}(u)$ satisfies

$$(n_j - n_i)u + (m_j - m_i)P_{i,j}(u) + \alpha_j - \alpha_i = 0, \quad \text{for all } u \in I_i,$$

recall (30). Consequently, we have:

Lemma 3.14.

$$P_{i,j}(u) = \frac{n_j - n_i}{m_i - m_j}u + \frac{\alpha_j - \alpha_i}{m_i - m_j}, \quad \text{for all } u \in I_i. \quad (37)$$

Remark 3.15. *More generally, we can concatenate orbits across consecutive crossing edges of \mathcal{T} and we can describe the dynamics by composing maps of the form (37); this leads to transition maps of the form $u \mapsto cu + b(\alpha)$, with $\alpha \mapsto b(\alpha)$ affine, and where $c \in \mathbb{Q}_+$ only depends on the degrees $\deg F_k$, $k \in \mathcal{I}$. In this sense, (28) (as usual) induces an (incomplete) flow:*

Lemma 3.16. *Let $\mathcal{T}_s \subset \mathcal{T}$ denote the union of all switching manifolds of sliding type. Then the system (28) defines a usual flow (incomplete, in general) on $\mathbb{R}^2 \setminus \mathcal{T}_s$.*

We will often need to refer to this flow and we will do so by using the following reference:

The crossing flow (induced by (28)).

For completeness, we assert that $\mathbf{trop}(u, v) = \mathbf{conv}(\mathbf{d}_i, \mathbf{d}_j)$ on a crossing switching manifold $\mathcal{E}_{i,j}$. Indeed, we are in case 2a of Definition 3.7 with $\mathbf{d}_{\mathcal{I}^*} = \{\mathbf{d}_i, \mathbf{d}_j\}$ and $i \in \mathcal{U}$, $j \in \mathcal{V}$. Most importantly, $\mathbf{0} \notin \mathbf{trop}(u, v)$ in this case. Therefore the flow of the differential inclusion $(\dot{u}, \dot{v}) \in \mathbf{trop}(u, v)$ is well-defined near crossing type switching manifolds and coincides with the crossing flow.

3.5 Definition of a tropical dynamical system

We are now in a position to define our tropical dynamical system. (Recall Definition 3.5.)

Definition 3.17. *Given (a): two nonempty, finite and disjoint index sets $\mathcal{U} \subset \mathbb{N}$ and $\mathcal{V} \subset \mathbb{N}$, (b): $\mathcal{I} := \mathcal{U} \cup \mathcal{V}$ and (c): two sets of tropical pairs:*

1. $(\mathbf{d}_k, F_k) \in \{(\pm 1, 0)\} \times \mathcal{M}^u$ for all $k \in \mathcal{U}$, with all $\deg F_k$, $k \in \mathcal{U}$ distinct,
2. $(\mathbf{d}_k, F_k) \in \{(0, \pm 1)\} \times \mathcal{M}^v$ for all $k \in \mathcal{V}$, with all $\deg F_k$, $k \in \mathcal{V}$ distinct,

we then define a tropical dynamical system (TDS for short) as the differential inclusion:

$$(\dot{u}, \dot{v})(t) \in \mathbf{trop}(u, v)(t), \quad (38)$$

with $(u, v)(t) := (u(t), v(t)) \in \mathbb{R}^2$, $t \in \mathbb{R}$. Finally, we define the degree of the tropical dynamical system as

$$\max_{k \in \mathcal{I}} |\deg F_k|_1 + 1.$$

In this definition, \mathcal{U} and \mathcal{V} are general index sets, not necessarily given by (15). This is convenient in examples (as in the autocatalator below, see Section 6) where only a few monomials are present.

However, in our analysis of general degree N tropical dynamical systems, we will stick to \mathcal{U} and \mathcal{V} and the enumeration of (n_k, m_k) given by (15) and (17), respectively. Specifically, we then define:

Definition 3.18. $\mathcal{TDS}(N, \{\mathbf{d}_k\}_{k \in \mathcal{I}})$ (\mathcal{TDS} for short) is the set of tropical dynamical systems TDS of a fixed degree $N \in \mathbb{N}$ and a fixed list of flow vectors $\{\mathbf{d}_k\}_{k \in \mathcal{I}}$.

Consequently, we have that $TDS \in \mathcal{TDS}$ if and only if $F_k \in \mathcal{M}_N^u$ ($F_k \in \mathcal{M}_N^v$) for all $k \in \mathcal{U}$ ($k \in \mathcal{V}$, respectively), recall (again) Definition 3.5.

Let

$$\alpha := (\alpha_1, \dots, \alpha_{2M}) \in \mathbf{A}(2M),$$

recall (13). We then topologize \mathcal{TDS} in the obvious way:

Definition 3.19. An open neighborhood \mathcal{O} of a tropical dynamical system

$$TDS' \in \mathcal{TDS}(N, \{\mathbf{d}_k\}_{k \in \mathcal{I}}),$$

with tropical coefficients $\alpha' \in \mathbf{A}(2M)$, is the set of tropical dynamical systems TDS with $\alpha \in \mathcal{O}$, $\mathcal{O} \subset \mathbf{A}(2M)$ being an open neighborhood of α' in $\mathbf{A}(2M)$.

In examples, with only a few monomials and a few parameters $(\alpha_1, \dots, \alpha_L) \in (\mathbb{R} \cup \{-\infty\})^L$, as in the autocatalator model below (with $L = 1$, $\alpha_1 = \alpha$), see Section 6, we define a neighborhood completely analogously using open sets $\mathcal{O} \subset (\mathbb{R} \cup \{-\infty\})^L$.

Remark 3.20. In the following, we will use $\mathcal{Y} \subset \mathcal{TDS}$ ($\mathcal{Y} = \mathcal{O}, \mathcal{D}$) to denote open sets in \mathcal{TDS} and denote by $Y \subset \mathbf{A}(2M)$ the associated open subsets of $\mathbf{A}(2M)$. X (as in Lemma 3.8) will denote open sets in \mathbb{R}^2 .

4 Existence of solutions

Our main aim will be to show that there are finitely many distinct structurally stable phase portraits in \mathcal{TDS} . For this purpose, we need to define what we mean by a phase portrait of a $TDS \in \mathcal{TDS}$ and how structural stability can be understood. We start by studying solutions of (38).

As is usual [5, 25], we define solutions of the differential inclusion (38) through (u_0, v_0) to be absolutely continuous functions:

$$(u, v) : \mathbb{R} \rightarrow \mathbb{R}^2,$$

with $(u, v)(0) = (u_0, v_0)$ and for which (38) holds almost everywhere. Given the nature of $\mathbf{trop}(u, v)$, it is natural to restrict attention to piecewise affine solutions, i.e. for every $t_0 \in \mathbb{R}$ there is an $\theta(t_0) > 0$ such that $(u, v)|_I : I \rightarrow \mathbb{R}^2$, $I := (t_0 - \theta, t_0 + \theta)$, satisfies: $(u, v)'|_I(t) = \text{const.}$ for all $t \in I$, $t \neq t_0$. If the const. depends upon the sign of $t - t_0$, then t_0 is said to be a *singular point* of the solution u .

Theorem 4.1. Consider a tropical dynamical system TDS . Then there exists a piecewise affine solution $(u, v) : \mathbb{R} \rightarrow \mathbb{R}^2$ of (38) through every point, whose singular points $\{t_n\}_n$ are enumerable and do not accumulate (if $\{t_n\}_n$ is infinite).

Proof. We first consider the problem of a local piecewise affine solution $(u, v) : I \rightarrow \mathbb{R}^2$, $I = [-\theta, \theta]$, $\theta > 0$, through a point (u_0, v_0) .

If $\mathbf{0} \in \mathbf{trop}(u_0, v_0)$ then we are done. From the results in Section 3.3 and Section 3.4, see also Fig. 2 and Fig. 3, we can also construct local piecewise affine solutions near (u_0, v_0) if

$$1 \leq \# \operatorname{argmax}_{k \in \mathcal{I}} F_k(u_0, v_0) \leq 2. \quad (39)$$

Such solutions can either (a) be extended globally or (b) be extended to points (u_0, v_0) where

$$L := \# \operatorname{argmax}_{k \in \mathcal{I}} F_k(u_0, v_0) \geq 3.$$

We therefore restrict attention to such points (u_0, v_0) . We may here suppose that $\deg F_i$, $i \in \operatorname{argmax}_{k \in \mathcal{I}} F_k(u_0, v_0)$, are mutually distinct, because otherwise we can reduce it to (39). The same is true if $\deg F_i$ were co-linear, since then \mathcal{T} consists of a single tropical edge near (u_0, v_0) .

Consequently, we are left with the case where the point (u_0, v_0) is associated with a L -sided polygon face of the polyhedral subdivision \mathcal{S} , such that L tropical edges of \mathcal{T} come together at (u_0, v_0) . Moreover, $\mathbf{0} \notin \mathbf{trop}(u_0, v_0)$.

There are two cases to consider:

1. $\mathbf{d}_{\mathcal{I}^*} = \mathbf{d}_{\mathcal{L}^*}$, with either $\mathcal{L} = \mathcal{U}$ or \mathcal{V} ,
2. or, $\mathbf{d}_{\mathcal{I}^*} = \mathbf{d}_{\mathcal{U}^*} \cup \mathbf{d}_{\mathcal{V}^*}$.

In case 1, we take $\mathcal{L} = \mathcal{V}$ for simplicity ($\mathcal{L} = \mathcal{U}$ is identical). If $\mathbf{d}_{\mathcal{I}^*}$ only contains one element, then we are done as we can just follow this direction. We therefore suppose that $\mathbf{d}_{\mathcal{I}^*} = \{(0, \pm 1)\}$. We can always follow the positive or negative v -direction in one direction of time. This is consequence of Lemma 3.8; there will be vectors in $\mathbf{trop}(u_0, v)$, $v \in I \setminus \{v_0\}$, with I a neighborhood of v_0 , that are either pointing in the same direction or are in opposition; notice that this also holds if $u = u_0$ contains a tropical edge because vectors within the tropical regions are extended to \mathcal{T} by \mathbf{trop} . Now, if these vectors point in the same direction along $u = u_0$, then we are done. We therefore suppose that these vectors are in opposition and suppose without loss of generality that solutions can be extended backward in time. We will now construct a solution forward in time. For this purpose, we first use that $\mathbf{0} \notin \mathbf{trop}(u_0, v_0)$ to deduce that $\mathbf{d}_{\mathcal{U}^*}$ only contains one element. We suppose it is $(1, 0)$ ($(-1, 0)$ is identical). Then we take an arc going clockwise from the positive v -direction to the negative v -direction of sufficiently small radius. Along this 180° arc, we have to intersect at least one tropical edge (simply due to the fact that the face of \mathcal{S} is an L -sided polygon). By Lemma 3.8, at least one of these tropical edges has to be of nullcline sliding-type. Indeed, if not, then going along the arc each tropical edge would be of crossing type and we arrive at the contradiction that the vectors along $u = u_0$ point in the same direction.

Along the tropical edge of nullcline sliding type, we have a tangent vector, cf. Lemma 3.12, which by Lemma 3.8 belongs to $\mathbf{trop}(u_0, v_0)$. This gives the desired forward solution.

Next, in case 2, only one of $\mathbf{d}_{\mathcal{U}^*}$ and $\mathbf{d}_{\mathcal{V}^*}$ can contain two elements. Otherwise $\mathbf{0} \in \mathbf{trop}(u_0, v_0)$. We suppose $\mathbf{d}_{\mathcal{U}^*} = \{(1, 0)\}$ and that $(0, 1) \in \mathbf{d}_{\mathcal{V}^*}$ without loss of generality.

We now construct a forward solution. The case of a backward solution is similar and therefore left out.

Either we have:

- (a) $(0, 1) \notin \mathbf{trop}(u_0, v)$ and $(1, 0) \notin \mathbf{trop}(u, v_0)$, for all $v > v_0$, $v \sim v_0$ and $u > u_0$, $u \sim u_0$, respectively,
- (b) or we can continue a solution along the positive v -direction or along the positive u -direction.

We are therefore left with the first case. Then by Lemma 3.8, we have $(1, 0) \in \mathbf{trop}(u_0, v)$ and $(0, 1) \in \mathbf{trop}(u, v_0)$, for all $v > v_0$, $v \sim v_0$ and $u > u_0$, $u \sim u_0$. We can then proceed as in case 1 above and take a 90° -arc going clockwise from the positive v -direction to the positive u -direction, which has to intersect at least one tropical edge of Filippov sliding-type. Along this set we have a unique tangent vector $\mathbf{d}_{\text{Fp}} \in \mathbf{trop}(u_0, v_0)$, the Filippov sliding vector, recall Lemma 3.11, which points away from (u_0, v_0) . This completes the proof of existence of a local piecewise affine solution.

Now, we turn to the problem of globalizing the solution. We focus on extending the solution forward in time, since backward in time is identical. For this purpose, we simply apply the same procedure, using $(u_0, v_0) = (u(\theta), v(\theta))$ as initial condition in the first step. This procedure either leads to a global forward solution $(u, v) : [0, \infty) \rightarrow \mathbb{R}^2$, as desired, or there is some $T > 0$ such that the forward solution $(u, v) : [0, T) \rightarrow \mathbb{R}^2$ cannot be continued beyond $T > 0$. From our construction, and the fact that there are finitely many tropical vertices $\mathcal{P} \subset \mathcal{T}$ and finitely many tropical edges $\mathcal{E} \subset \mathcal{T}$, we are left with the only possibility that $(u, v)(t) \rightarrow \infty$ as $t \rightarrow T^-$. But this is impossible in finite time, since all vectors in \mathbf{trop} are bounded in Euclidean norm by 1. Consequently, $T = \infty$. It also follows from these arguments that the singular points $\{t_n\}_n$ of our solution (u, v) do not accumulate, $t_n \not\rightarrow t_*$. \square

Remark 4.2. *Not all solutions are necessarily piecewise affine. Consider for example the case where*

$$F_i(u', v') = F_j(u', v') > F_k(u', v') \quad \text{for all } k \in \mathcal{I}, k \neq i, j, \quad (40)$$

where $\deg F_i = \deg F_j$, $i \in \mathcal{U}$, $j \in \mathcal{V}$, for some (u', v') . In this case, (40) holds on a neighborhood X of (u', v') . Within X , we have $\mathbf{trop}(u, v) = \mathbf{conv}(\mathbf{d}_i, \mathbf{d}_j)$, $\mathbf{d}_i \cdot \mathbf{d}_j = 0$. Consequently, any differentiable curve $s \mapsto (u, v)(s) \in X$, with $\text{sign}(u'(s)\delta_i) = \text{sign}(v'(s)\delta_j)$ can be re-parametrized as a solution $t \mapsto (u, v)(s(t))$ of (38). Having said that, (40) is not stable to perturbations, in the sense that if $\alpha_i \neq \alpha_j$, then (40) holds nowhere, recall Remark 3.9.

Moreover, even if (40) does not hold for any pair $\deg F_i = \deg F_j$, then there may still exist solutions where the singular points $\{t_n\}_n$ of a solution of (38) accumulate, such that $t_n \rightarrow t_*$. These are so called zeno trajectories, and they are covered for classical Filippov systems in [9, Theorem 8.1]. They occur, for example, at so-called elliptic sectors in our

case; an example of this case is a neighborhood of the origin in Fig. 6(b) (compare with [9, Fig. 8]). It is reminiscent of a canard point [44] and here solutions can be continued through the tropical vertex \mathcal{P}_{456} and along the repelling transversal nullcline sliding manifold \mathcal{E}_{46} and then jump back down towards the stable transversal nullcline sliding manifold \mathcal{E}_{45} , arbitrarily close to \mathcal{P}_{456} . In our setting, zeno trajectories also occur along tangential nullcline sliding, see Fig. 2(d) and Remark 9.4.

Having said that, Theorem 2.4 guarantees that there is always a piecewise affine solution of (38) through every point, whose singular points $\{t_n\}_n$ do not accumulate.

5 Orbits and phase portraits

Solutions of a tropical dynamical system are nonunique (as usual for piecewise smooth systems, see [25] and Fig. 2 for an example (due to sliding)), and the tropical system does therefore not define a usual flow. Nevertheless, we can still use the existence of piecewise affine solutions (see Theorem 4.1) to define an orbit (nonunique) through any given point, including a forward orbit and a backward orbit, see also [9, 25]. This also leads to α and ω -limit sets. Moreover, since the solutions of Theorem 4.1 are piecewise affine, we obtain orbits as oriented polygonal curves, i.e. oriented and connected line segments (finitely many or countably infinitely many), and we will restrict attention to such polygonal orbits.

We can write a polygonal orbit γ as the union of a set of edges $E = \{l_i\}_i$ and a set of vertices $V = \{q_i\}_i$ in such a way that (a) l_i is the oriented line segment from q_i to q_{i+1} and (b) l_i and l_{i+1} have different orientations in the sense that the vertices V correspond to the singular points $\{t_i\}_i$ (that do not accumulate) of a solution having $E \cup V$ as its image. Here i runs over:

1. A finite index set, when the orbit is isomorphic to a closed interval or a closed curve.
2. $(-\mathbb{N}) = \{\dots, -2, -1\}$ or \mathbb{N} , when the orbit is isomorphic to $(-\infty, 0]$ (infinitely many line segments in backward time) or $[0, \infty)$ (infinitely line many segments in forward time), respectively.
3. \mathbb{Z} , when the orbit is isomorphic to \mathbb{R} (infinitely many line segments in forward and backward time).

If γ is a point (corresponding to a tropical singularity) then E is the empty set and $V = \{\gamma\}$, whereas if γ is a single straight line then $E = \{\gamma\}$ and V is the empty set.

We then define the *phase portrait of a tropical dynamical system* as the set of polygonal orbits.

For an oriented line segment l_i , we will use “flow orientation” to refer to the orientation of time, whereas we use “line orientation” to refer to the geometric orientation (i.e. the slope) of l_i in \mathbb{R}^2 .

A periodic orbit γ is then a closed polygonal orbit of a piecewise affine periodic solution of (38) and it is a limit cycle if it is the α or ω -limit set of points $p \notin \gamma$. Due to nonuniqueness, we

can (without further assumptions) have two limit cycles γ_1 and γ_2 with nonempty intersection (see Fig. 32 below for an example). Moreover, polygonal orbits in the neighborhood X of a limit cycle γ may (due to sliding) intersect γ in finite forward or backward time. As is usual in piecewise smooth systems, we define:

Definition 5.1. *Suppose that γ is a periodic orbit. Then it is said to be a crossing cycle if it is a periodic orbit of the crossing flow (induced by (28), recall Remark 3.15), with all intersections of the discontinuity subset of \mathcal{T} (where $\mathbf{d}_i \neq \mathbf{d}_j$) belonging to switching manifolds of crossing-type. Otherwise, γ is called a sliding cycle.*

Notice here that a crossing cycle does not pass through tropical vertices of \mathcal{T} . This is convenient for our purposes, see Section 12.2.

Remark 5.2. *The paper [9] establishes generic structural stability (in the usual sense) for Filippov systems on surfaces. Here orbits are not amalgamated (in contrast to the approach by Filippov [25]) along the sliding switching manifolds. Applying this viewpoint to Fig. 2(a), we only have one orbit through any point $\mathcal{E}_{i,j}$ (the set $\mathcal{E}_{i,j}$ itself). In the present paper, when we refer to the crossing flow, then we are only amalgamating orbits across the switching manifolds of crossing type (crossing orbits), “stopping” when these reach sliding segments. However, for our definition of equivalence, see Section 7, it will be important to amalgamate orbits along the switching manifolds of sliding type as in [25]. Consequently, with our convention, we will have infinitely many orbits through any point on $\mathcal{E}_{i,j}$ in Fig. 2(a)).*

6 Example: A tropicalized autocatalator

In this section, we illustrate the concepts further by working on a tropicalized version of the autocatalator model:

$$\begin{aligned}\dot{x} &= \theta(\mu - x - xy^2), \\ \dot{y} &= -y + x + xy^2,\end{aligned}\tag{41}$$

with $0 < \theta \ll 1$ and $\mu > 0$. (41) is referred to as the autocatalator, since it models an autocatalytic chemical process with $(x, y) \in \mathbb{R}_+^2$ being (scaled) concentrations; the autocatalytic nature of the process is modeled by the nonlinear term xy^2 , see [55]. The system was analyzed in [37] using GSPT and has since then become the prime example of a slow-fast polynomial system supporting nonstandard relaxation oscillations (for $\mu > 1$ fixed and all $0 < \theta \ll 1$, see [37, Theorem 2.3]).¹

In further details, [37] shows that there is a Hopf bifurcation at $\mu \approx 1$, which is of canard type [44], in the sense that the Hopf cycles grow (through canard cycles) in amplitude by an $\mathcal{O}(1)$ -amount in a parameter regime of a width of order $\mathcal{O}(e^{-c/\theta})$. But in contrast to e.g. the van der Pol system [44], the canard cycles grow unboundedly for (41) as $\theta \rightarrow 0$.

We illustrate the phase portrait of (41) for $\mu = 2$ and $\theta = 0.001$ in Fig. 4 (computed in `Matlab` using `ODE45` with low tolerances (10^{-12})). Due to the unboundedness of the limit

¹Note that θ is called ϵ in [37]. We adopt this change in notation to avoid confusion with ϵ in (5) and (42) below.

cycle γ_θ (in red) as $\theta \rightarrow 0$ in the (x, y) -coordinates, see Fig. 4(a), we use the zoomed-out coordinates $(x, \theta y)$ in Fig. 4(b). The blue dashed line in Fig. 4(a) is the y -nullcline for (41). It defines a critical manifold for $\theta = 0$, being attracting for $y < 1$ and repelling for $y > 1$. The point $(x, y) = (\frac{1}{2}, 1)$ is a fold point, in particular a canard point for $\mu = 1$ when the x -nullcline (in purple and dashed in Fig. 4) intersects the y -nullcline at the fold of the critical manifold.

For $\mu < 1$ and $0 < \theta \ll 1$, there is a globally attracting stable node; in Fig. 4(a) for $\mu = 2$ (on the other side of the Hopf) it is an unstable node (black dot).

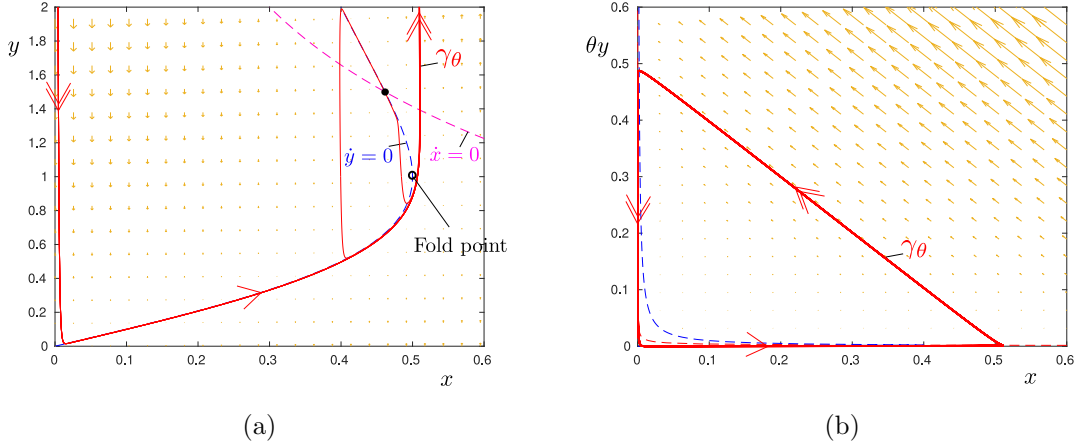


Figure 4: Phase portrait of (41) for $\mu = 2$ and $\theta = 0.001$, using two different scalings: (x, y) in (a) and $(x, \theta y)$ in (b). The limit cycle γ_θ (in red) is unbounded in the (x, y) -coordinates as $\theta \rightarrow 0$ but bounded in $(x, \theta y)$.

We now consider a tropical version of (41) by defining u and v as in (5) and setting

$$\theta = e^{-1/\epsilon}, \quad \mu = e^{\alpha/\epsilon}. \quad (42)$$

Taking the limit $\epsilon \rightarrow 0$ (with α fixed), we are then led to consider the tropical dynamical system (of degree 3) defined by the following tropical pairs:

$$\begin{aligned} F_1(u, v) &:= \alpha - 1 - u, & \mathbf{d}_1 &:= (1, 0), \\ F_2(u, v) &:= -1, & \mathbf{d}_2 &:= (-1, 0), \\ F_3(u, v) &:= -1 + 2v, & \mathbf{d}_3 &:= (-1, 0), \\ F_4(u, v) &:= 0, & \mathbf{d}_4 &:= (0, -1), \\ F_5(u, v) &:= u - v, & \mathbf{d}_5 &:= (0, 1), \\ F_6(u, v) &:= u + v, & \mathbf{d}_6 &:= (0, 1), \end{aligned} \quad (43)$$

and $\mathcal{U} = \{1, 2, 3\}$, $\mathcal{V} = \{4, 5, 6\}$. Notice that α is the single parameter and that it only enters through the tropical coefficient of F_1 . In Fig. 5(a), we show the graph of the associated tropical polynomial

$$F_{\max}(u, v) = \max_{k \in \{1, \dots, 6\}} F_k(u, v),$$

for $\alpha = \frac{1}{4}$. In Fig. 5(b), we illustrate the corresponding subdivision of the Newton polygon. Notice that we label the subdivision according to the associated flow vector in the tropical pair, see (43). The purple edges then indicate where we have crossing (see (31)); this colouring relates to the concept of a crossing graph introduced in Section 12 below. In Fig. 5(c), we show the resulting tropical phase portrait for the same value of α . The numbers 1, 3, 4, 5, 6 in Fig. 5 correspond to the number of the dominating monomial, see (43). Notice that 2 is missing. This is due to the fact that the set \mathcal{R}_2 is the empty set in the present case: $F_2(u, v) = -1 < F_4(u, v) = 0 \leq F_{\max}(u, v)$ for all $(u, v) \in \mathbb{R}^2$ and all $\alpha \in \mathbb{R} \cup \{-\infty\}$. The corresponding flow vectors are indicated as black arrows in Fig. 5(c).

We notice the following in Fig. 5(c). Firstly, there is a point $\mathcal{Q}_{1346} = (\frac{1}{4}, \frac{1}{4})$ where $\mathbf{0} \in \mathbf{trop}(u, v)$ (white disc with black boundary). This is due to the intersection of the transversal nullcline sliding switching manifolds $\mathcal{E}_{13}^{\mathcal{U}}$ and $\mathcal{E}_{46}^{\mathcal{V}}$. They are both of unstable type and \mathcal{Q}_{1346} , which we call a tropical singularity, acts like an unstable node (or source); see further details in Section 9. Secondly, there is also an attracting sliding limit cycle (in red). Notice that it slides along \mathcal{E}_{14} (tangential Filippov) and along $\mathcal{E}_{13}^{\mathcal{U}}$ and $\mathcal{E}_{45}^{\mathcal{V}}$ (both stable transversal nullcline). The tropical vertex \mathcal{P}_{456} is reminiscent of a classical fold point (see Fig. 4(a)) of a slow-fast system, insofar that \mathcal{P}_{456} also separates an attracting nullcline from a repelling one.

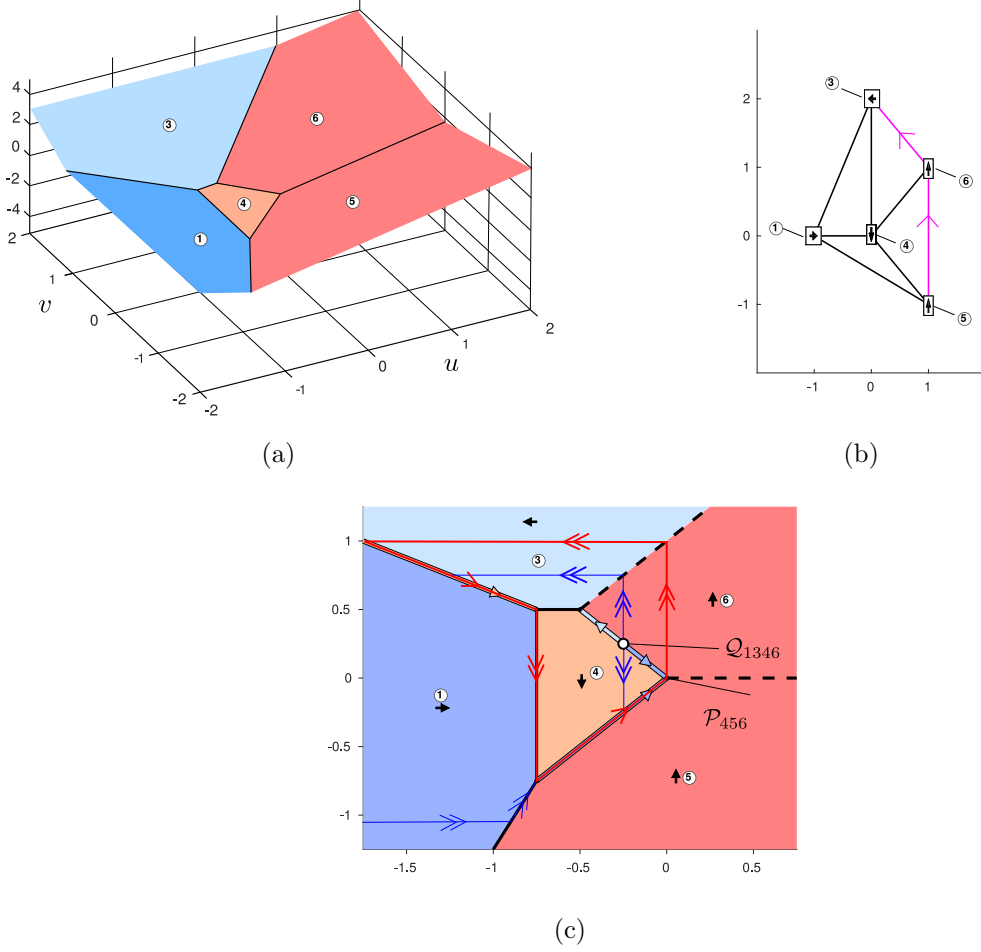


Figure 5: In (a): The graph of the tropical polynomial F_{\max} associated with the tropical monomials in (43). In (b): The (labelled) subdivision associated with monomial in (43). In all figures, $\alpha = \frac{1}{4}$. Finally, in (c): The tropical phase portrait with a source Q_{1346} and a sliding limit cycle (in red).

In Fig. 4, we used $\mu = 2$. This corresponds to $\alpha = \epsilon \log 2 \rightarrow 0$ as $\epsilon \rightarrow 0$ (or equivalently $\theta \rightarrow 0$) upon using (42). We therefore illustrate the case $\alpha = 0$ in Fig. 6, see (b), together with three other values of α : $\alpha = -\frac{1}{4}$ in (a), $\alpha = \frac{1}{2}$ in (c) and $\alpha = \frac{3}{4}$ in (d). We notice the following: For $\alpha = 0$, the tropical singularity Q_{1346} has moved onto the tropical vertex P_{456} . Just like in the canard situation of (41), this value of α also marks the onset of limit cycles; compare Fig. 5(c) for $\alpha = \frac{1}{4}$ with Fig. 6(a) for $\alpha = -\frac{1}{4}$. In the former case, we have a stable limit cycle, whereas in the latter case, we have a sink Q_{1345} on \mathcal{E}_{45}^V , which attracts all points. Essentially, the phase portraits for any $\alpha < 0$ and any $\alpha \in (0, \frac{1}{2})$ are qualitatively similar to those in Fig. 6(a) and Fig. 5(c), respectively. (We will make this more precise below in Section 7). In the case $\alpha = 0$, we see (as in the classical canard explosion) cycles (in red) of different amplitudes co-existing. The compelling thing about the tropical phase portrait is that all scales (on the logarithmic scale induced by (5)) are visible all at once. The blowup method offers a similar “compactification”, see [37, Fig. 7]. In comparison, we had to use

two separate scales in Fig. 4 to visualize the dynamics.

The limit cycle we see in Fig. 5(c) for $\alpha = \frac{1}{4}$ is not covered by the analysis of [37] (in a singular limit). Indeed, in [37] the authors keep $\mu = \mathcal{O}(1)$ as $\theta \rightarrow 0$. Based on the findings of the tropical dynamical system, see also Conjecture 15.1 below, we find that the limit cycles of [37] can be continued for μ -values growing unboundedly (at a rate $\mu = e^{\alpha/\epsilon} \rightarrow \infty$ as $\epsilon \rightarrow 0$ with $\alpha \in (0, \frac{1}{2})$). (Formally this requires a separate GSPT analysis, which we will leave to future work.) Within this context, it is interesting to note that there is another bifurcation at $\alpha = \frac{1}{2}$ (see Fig. 6(c)), where the source \mathcal{Q}_{1346} has moved on top of a different tropical vertex, \mathcal{P}_{1346} , so that $\mathbf{0} \in \mathbf{trop}(\mathcal{P}_{1346})$. This tropical vertex (as indicated by the subscripts 1346) is degenerate in the sense that the four monomials F_1, F_3, F_4 and F_6 attain the same value at this point. In Fig. 7, we show the subdivision associated with this case. In agreement with Fig. 6(c), the subdivision is not a triangulation (in contrast to Fig. 5(b)).

The value $\alpha = \frac{1}{2}$ marks the termination of oscillations. In particular, as indicated in Fig. 6(d), we have a sink \mathcal{Q}_{1346} on $\mathcal{E}_{13}^{\mathcal{U}}$ for any $\alpha \in (\frac{1}{2}, 1)$. In future work, it would be interesting to study the bifurcation at $\alpha = \frac{1}{2}$ further as a singular bifurcation for $\theta \rightarrow 0$. We expect that the techniques, developed in [35, 34, 42] for the analysis of bifurcations of smooth systems approaching nonsmooth ones, as well as those in [38] for dealing with exponential nonlinearities, will all be useful in this regard.

Notice that although the situation near $\alpha = \frac{1}{2}$ again bears some similarities with the canard explosion, it is clearly different, as it involves a mixture of fast directions. Indeed, along \mathcal{E}_{46} the v -direction is fast/dominating, whereas along \mathcal{E}_{13} the u -direction is fast/dominating. We notice that $\alpha = \frac{1}{2}$ corresponds to

$$\mu = \theta^{-\frac{1}{2}},$$

by (42). The following result demonstrates the effectiveness of the tropical approach in identifying significant scalings.

Lemma 6.1. *The system (41) has two Hopf bifurcations at*

$$\begin{aligned} \mu &= \theta^{-\frac{1}{2}} \sqrt{\frac{1 - 2\theta + \sqrt{1 - 8\theta}}{2}} = \theta^{-\frac{1}{2}} \left(1 - \frac{3}{2}\theta + \mathcal{O}(\theta^2) \right), \\ \mu &= \theta^{-\frac{1}{2}} \sqrt{\frac{1 - 2\theta - \sqrt{1 - 8\theta}}{2}} = 1 + 2\theta + \mathcal{O}(\theta^2), \end{aligned}$$

for all $0 < \theta \ll 1$.

Proof. Follows from a direct calculation: The unique singularity is at

$$(x, y) = \left(\frac{\mu}{\mu^2 + 1}, \mu \right),$$

and the determinant and trace of the linearization are given by

$$\theta(1 + \mu^2), \quad \frac{\mu^2 - 1}{\mu^2 + 1} - \theta(\mu^2 + 1),$$

respectively. With the determinant being positive, we obtain the result, specifically the expressions for μ by setting the trace equal zero. \square

Finally, regarding Fig. 6(d) for the value $\alpha = \frac{3}{4}$, we notice that the purple orbit (reminiscent of a strong stable manifold of \mathcal{Q}_{1346}) goes through the tropical vertex \mathcal{P}_{146} . At first sight, this might seem special. One would perhaps expect that if we vary α then this connection would break up. To see that this is not the case, we can either note that the line \mathcal{E}_{36} is the bisector of the line $(\mathcal{P}_{146}, \mathcal{Q}_{1346})$ or proceed by the direct calculation:

\mathcal{Q}_{1346} has coordinates (α, α) and it lies on \mathcal{E}_{13}'' for $\alpha > \frac{1}{2}$. The purple orbit, obtained by following the flow vector \mathbf{d}_3 backwards from \mathcal{Q}_{1346} then intersects the crossing switching manifold \mathcal{E}_{36} , given by $v = u + 1$, at a point

$$(-1 + \alpha, \alpha). \quad (44)$$

At the same time, the tropical vertex \mathcal{P}_{146} , obtained by setting $F_1(u, v) = F_4(u, v) = F_6(u, v)$, has coordinates

$$(-1 + \alpha, 1 - \alpha). \quad (45)$$

The u -components of (44) and (45) coincide and the situation illustrated in Fig. 6(d) is therefore not special, but *persistent*.

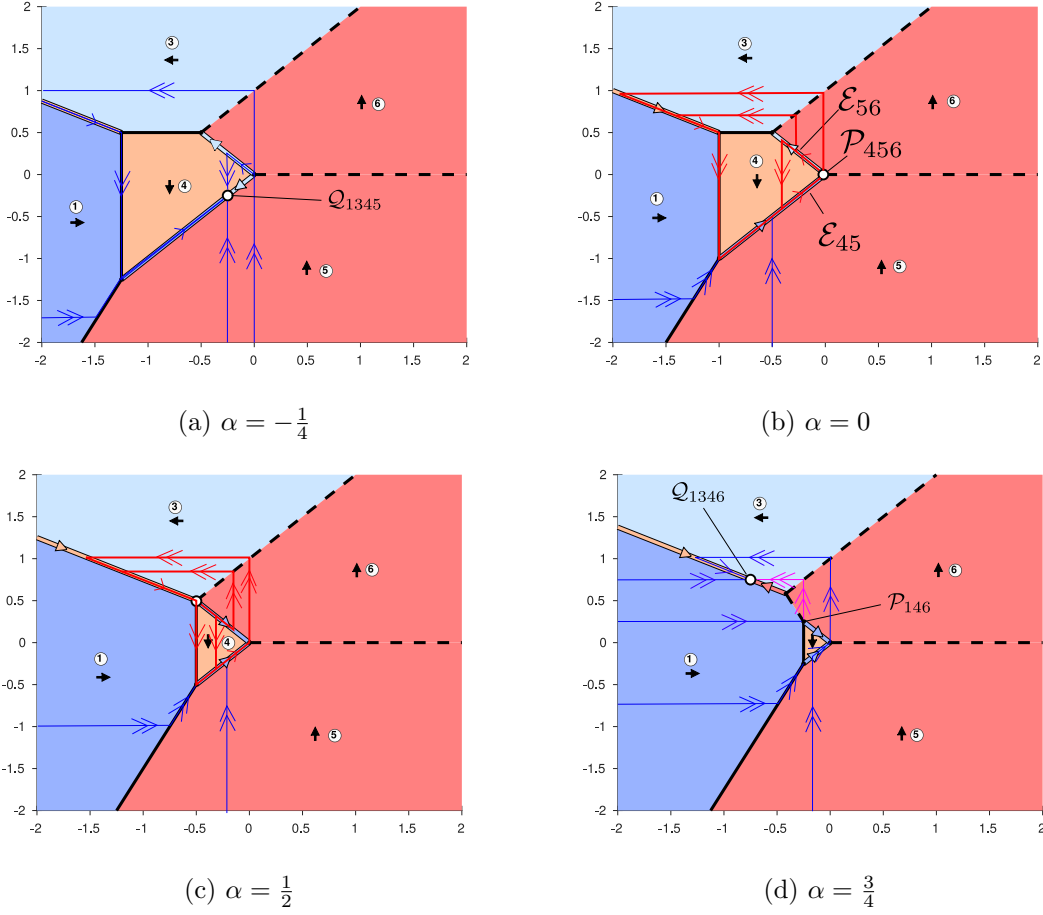


Figure 6: The phase portraits of the tropicalized autocatalator given by the tropical pairs (43) for four different values of α (see sub-captions). $\alpha = 0$ (b) and $\alpha = \frac{1}{2}$ (c) are bifurcation points, reminiscent of canard points in slow-fast systems, where the stability of the tropical singularity (white circle) changes from a source to a sink (and vice versa) and where limit cycles are created/destroyed, respectively, in a dramatic (or explosive) fashion. See also Fig. 5(c).

7 Equivalence of tropical dynamical systems

In smooth dynamical systems theory, we say that two planar systems are topologically equivalent if there is a(n) (orientation preserving) homeomorphism $h : \mathbb{R}^2 \rightarrow \mathbb{R}^2$ that maps orbits to orbits (often on invariant compact submanifolds such as the (Poincaré) sphere, i.e. $h : S^2 \rightarrow S^2$, leaving the equator invariant in the case of the Poincaré sphere) and preserve the direction of time, see [54]. For equivalence in PWS systems, (a) the discontinuity set is either assumed to be fixed (and smooth) or (b) h is also assumed to be a homeomorphism on the discontinuity sets, see [9, 25]. This is called Σ -equivalence in [26]. [26] also defines topological equivalence as equivalence in the usual sense, without the requirement of neither (a) not (b). However, [26, Proposition 2.17] and [26, Remark 2.19] show that only diffeo-

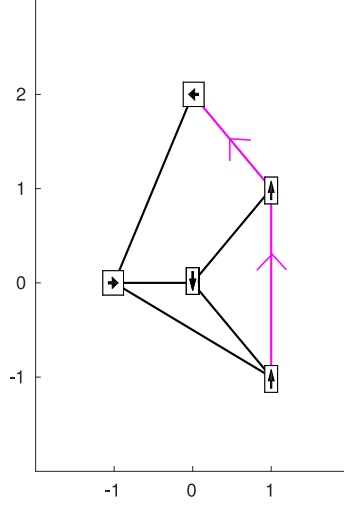


Figure 7: The (labelled) subdivision associated with the tropical monomials (43) for $\alpha = \frac{1}{2}$, see Fig. 6(c). In contrast to the subdivision in Fig. 5(b), the subdivision is not a triangulation.

morphisms preserve Filippov in general and therefore demonstrate the subtleties with these notions of equivalence.

In any case, we believe that these definitions of equivalence based on homeomorphisms are too restrictive, if not just simply too difficult to work with, for tropical dynamical systems. This belief is based on the fact that h has to preserve lines, including horizontal and vertical ones; after all, every orbit of (28) is a polygonal curve with horizontal and vertical segments in the tropical regions and (possibly) inclined segments along tropical edges of sliding type. Instead, we suggest the following definition of equivalence (which is also more in tune with Definition 2.2 and tropical geometry in general):

Consider a polygonal orbit γ and let $E = \{l_i\}_i$ denote the edges of γ and $V = \{q_i\}_i$ its vertices. As before, (a) i runs over a finite index set, $\pm\mathbb{N}$ or \mathbb{Z} , (b) l_i is the line segment connecting q_i with q_{i+1} , and (c) l_i and l_{i+1} have different orientations (either flow or line orientations). Finally, if γ is a point, corresponding to a tropical singularity, then E is the empty set and $V = \{\gamma\}$, whereas if γ is a single straight line then $E = \{\gamma\}$ and V is the empty set.

Definition 7.1. *An oriented polygonal curve γ' , having $E' = \{l'_i\}_i$ as its edges and $V' = \{q'_i\}_i$ as its vertices, is said to be homotopic to an oriented polygonal curve γ , having $E = \{l_i\}_i$ as its edges and $V = \{q_i\}_i$ as its vertices, if there are continuous functions $f_i : [0, 1] \rightarrow \mathbb{R}^2$, such that $V = \{f_i(0)\}_i$, $V' = \{f_i(1)\}_i$ and $V(t) = \{f_i(t)\}_i$ for each $t \in [0, 1]$ are vertices of an oriented polygonal curve, where only the lengths and positions of the associated edges $E(t)$ change, not their flow and line orientations, and such that $f_i(t) \neq f_j(t)$ for all $i \neq j$ and all $t \in [0, 1]$.*

If γ' is a single straight line, so that $V' = \emptyset$, then γ' is homotopic to γ if γ is also a straight line having the same flow and line orientations (i.e. γ and γ' are translations of

each other with the same flow orientation).

Since continuous mappings can be composed, we obtain *equivalence classes of orbits that are oriented polygonal curves*. Consider a tropical dynamical system TDS and all of its orbits that are oriented polygonal curves. We then group homotopic (polygonal) orbits into equivalence classes and define equivalence of tropical dynamical systems as follows.

Definition 7.2. *Two tropical dynamical systems TDS and TDS' are equivalent, if they have the same polygonal orbit equivalence classes.*

We will define local equivalence analogously, saying that TDS and TDS' are locally equivalent if they have the same *local* polygonal orbit equivalence classes on an open set X of \mathbb{R}^2 . (Here a local polygonal orbit is just the intersection of a polygonal orbit with an open set X .)

Remark 7.3. *Notice that the line segments of two homotopic polygonal curves have the same slopes. Consequently, in our definition of equivalence, two equivalent tropical dynamical systems have sliding switching manifolds with the same slope (line orientation). One could argue that this leads to too many structurally stable tropical dynamical systems. But we believe the definition is a natural one, since the line segments of the polygonal orbits only have rational slope. In particular, horizontal and vertical lines are intrinsic for the tropical dynamical systems. If we were to allow the slopes to vary, then we obtain lines with irrational slopes under homotopy. Finally, the definition is in line with Definition 2.2.*

Definition 7.4. *Fix $N \in \mathbb{N}$ and a list of flow vectors $\{\mathbf{d}_k\}_{k \in \mathcal{I}}$. A tropical dynamical system*

$$TDS' \in \mathcal{TDS}(N, \{\mathbf{d}_k\}_{k \in \mathcal{I}}),$$

is structurally stable if there is a neighborhood \mathcal{O} of TDS' in \mathcal{TDS} such that TDS and TDS' are equivalent for all $TDS \in \mathcal{O}$. Otherwise, TDS' is said to be structurally unstable.

We will define local structural stability completely analogously when it holds on an open neighborhood X of (u, v) in \mathbb{R}^2 .

Lemma 7.5. *Suppose that a tropical dynamical system $TDS' \in \mathcal{TDS}$ is structurally stable and let \mathcal{O} be any neighborhood of TDS' in \mathcal{TDS} . Then there is a $TDS \in \mathcal{O}$ for which the following holds:*

1. *The polyhedral subdivisions $\mathcal{S}^{\mathcal{L}}$ of the Newton polygons associated to the tropical polynomials $F_{\max}^{\mathcal{L}}$ are triangulations for $\mathcal{L} = \mathcal{U}, \mathcal{V}$ and \mathcal{I} .*
2. *$\deg F_i = \deg F_j, i \neq j \implies \alpha_i \neq \alpha_j$.*
3. *$\mathcal{T}^{\mathcal{U}}$ and $\mathcal{T}^{\mathcal{V}}$ intersect transversally (i.e. all intersections of $\mathcal{T}^{\mathcal{U}}$ and $\mathcal{T}^{\mathcal{V}}$ occur along their tropical edges).*

Proof. This should be clear enough, see also [13]. □

This means that for structurally stable systems, we may assume that (or more accurately, consider a representative of the structural stable system for which) the tropical curves $\mathcal{T}^{\mathcal{U}}$, $\mathcal{T}^{\mathcal{V}}$ and $\mathcal{T}^{\mathcal{I}}$ consist of tropical edges and tropical vertices where precisely three tropical edges come together. Also, for structurally stable systems, we may assume (in the same sense as before) that tropical singularities (u', v') , where $\mathbf{0} \in \mathbf{trop}(u', v')$, lie on the tropical edges of \mathcal{T} . This is a consequence of item 3 of Lemma 7.5, see also Lemma 8.1 below.

Definition 7.6. *We say that $(\mathcal{T}, \mathcal{T}^{\mathcal{U}}, \mathcal{T}^{\mathcal{V}})$ (of a tropical dynamical system TDS) is in general position, if items 1–3 of Lemma 7.5 hold.*

Lemma 7.7. *Consider a tropical dynamical system $TDS' \in \mathcal{TDS}(N, \{\mathbf{d}_k\}_{k \in \mathcal{I}})$ and suppose that TDS' is structurally stable in the following (strong) sense of homeomorphisms (by Σ -equivalence, see e.g. [26, definition 2.15]): For every $\theta > 0$, there is a sufficiently small neighborhood \mathcal{O} of TDS' such that for any $TDS \in \mathcal{O}$ there is a homeomorphism $h : \mathbb{R}^2 \rightarrow \mathbb{R}^2$, satisfying:*

1. *h maps orbits of TDS' to orbits of TDS , preserving the direction of time.*
2. *h maps \mathcal{T}' homeomorphically onto \mathcal{T} , including tropical vertices of \mathcal{T}' to tropical vertices of \mathcal{T} ,*
3. *h is near-identity: $|h(u, v) - (u, v)| < \theta$ for all $(u, v) \in \mathbb{R}^2$.*

Then TDS' is also structural stable in the sense of Definition 7.4.

Proof. Let γ' be any polygonal orbit of TDS' . Then $\gamma = h(\gamma')$ is a polygonal orbit of $TDS \in \mathcal{O}$ by property 1, and as a consequence of property 2, h maps the vertices and edges of γ' homeomorphically onto the edges and vertices of γ . Moreover, by taking $\theta > 0$ small enough in property 3, we conclude that the corresponding edges of γ' and γ have to have the same slope; recall here that the slopes are rational and that there are only (with $N \in \mathbb{N}$ fixed) finitely many possibilities in \mathcal{TDS} . Hence γ' and γ are homotopic. In turn, we conclude that TDS' is structural stable in the sense of Definition 7.4. \square

We leave the details of going the other way in Lemma 7.7 to future work. In the following, we study local phenomena (tropical vertices and tropical singularities) and characterize the structurally stable situations (locally). For these local phenomena, we will construct the local equivalence in terms of a translation, mapping orbits to orbits locally.

Definition 7.8. *We will say that a transformation $T_\alpha : (u, v) \mapsto (u, v) + b(\alpha)$, with $\alpha \mapsto b(\alpha) \in \mathbb{R}^2$ affine, is an affine translation with respect to α .*

8 Tropical vertices

We define tropical vertices as points $\mathcal{P} : (u, v)$ where $\# \operatorname{argmax}_{k \in \mathcal{I}} F_k(u, v) \geq 3$.

Lemma 8.1. *Consider a tropical dynamical system TDS' with $(\mathcal{T}', \mathcal{T}^{\mathcal{U}}, \mathcal{T}^{\mathcal{V}})$ in general position and suppose that $\mathcal{P}' : (u', v')$ is a tropical vertex. Then*

1. $\operatorname{argmax}_{k \in \mathcal{I}} F_k(u', v') = \{i, j, l\}$ for some distinct $i, j, l \in \mathcal{I}$.
2. \mathcal{P}' is isolated, i.e. there is a neighborhood X of (u', v') where \mathcal{P}' is the only tropical vertex.
3. The degrees $\deg F_k$, $k = i, j, l$ are distinct.
4. $\mathbf{0} \notin \mathbf{trop}(u', v')$.

Proof. The statements 1–3 directly follow from the definition of $(\mathcal{T}', \mathcal{T}'^{\mathcal{U}}, \mathcal{T}'^{\mathcal{V}})$ being in general position, see Definition 7.6. Now regarding item 4, we use item 1 and the definition of \mathbf{trop} to conclude that $\mathbf{0} \in \mathbf{trop}(u', v') \Rightarrow \mathcal{P}' = \mathcal{P}'^{\mathcal{L}}$ for either $\mathcal{L} = \mathcal{U}$ or $\mathcal{L} = \mathcal{V}$. But then \mathcal{P}' is the intersection point of $\mathcal{T}'^{\mathcal{U}}$ and $\mathcal{T}'^{\mathcal{V}}$, and this contradicts $(\mathcal{T}', \mathcal{T}'^{\mathcal{U}}, \mathcal{T}'^{\mathcal{V}})$ being in general position, see item 3 of Definition 7.6. \square

Lemma 8.2. *Suppose that the assumptions of Lemma 8.1 hold and that*

$$TDS' \in \mathcal{TDS}(N, \{\mathbf{d}_k\}_{k \in \mathcal{I}}).$$

Then there is a neighborhood \mathcal{O} of TDS' and a neighborhood X of (u', v') , such that there is a unique tropical vertex $\mathcal{P}(\alpha) \in X$ of $TDS \in \mathcal{O}$, having coordinates $(u(\alpha), v(\alpha))$ with $(u(\alpha'), v(\alpha')) = (u', v')$, of the following form:

$$w(\alpha) = w' + b_w \cdot (\alpha_i - \alpha'_i, \alpha_j - \alpha'_j, \alpha_l - \alpha'_l), \quad w = u, v, \quad (46)$$

with $b_w := (b_{w,i}, b_{w,j}, b_{w,l}) \neq (0, 0, 0)$, $b_{w,i} + b_{w,j} + b_{w,l} = 0$ and $\operatorname{argmax}_{k \in \mathcal{I}} F_k(u', v') = \{i, j, l\}$.

Proof. Given item 1 of Lemma 8.1, we obtain two equations for the coordinates of (u, v) (see e.g. (29)):

$$\begin{pmatrix} \deg F_i - \deg F_j \\ \deg F_i - \deg F_l \end{pmatrix} \begin{pmatrix} u \\ v \end{pmatrix} + \begin{pmatrix} \alpha_i - \alpha_j \\ \alpha_i - \alpha_l \end{pmatrix} = 0.$$

But then by item 2 of Lemma 8.1 and the fact that \mathcal{P}' is isolated, we conclude that the coefficient matrix is regular. The fact, that the sum of the components of b_w is zero, is the consequence of the invariance of the tropical system to translations of the tropical coefficients, see (14). \square

The tropical edges emanating (locally) from $\mathcal{P}(\alpha)$ are clearly affine translations of those of \mathcal{P}' . In particular, the slopes of the tropical edges do not depend on α (but only on the degrees $\deg F_k$, $k = i, j, l$.)

Lemma 8.3. *Consider a tropical dynamical system*

$$TDS' \in \mathcal{TDS}(N, \{\mathbf{d}_k\}_{k \in \mathcal{I}}),$$

with $(\mathcal{T}', \mathcal{T}'^{\mathcal{U}}, \mathcal{T}'^{\mathcal{V}})$ in general position and suppose that \mathcal{P}' with coordinates (u', v') is a tropical vertex of \mathcal{T}' . Then the TDS' is locally structurally stable in a neighborhood X of (u', v') .

Proof. We first use Lemma 8.2 and define the affine translation T_α with respect to α by

$$T_\alpha(u, v) = (u, v) + (u(\alpha) - u', v(\alpha) - v'),$$

with $w(\alpha)$, $w = u, v$, given by (46). Clearly, T_α maps $\mathcal{T}' \cap X$ to $\mathcal{T} \cap X$ and since $\mathbf{0} \notin \mathbf{trop}(u', v')$ it follows that $\mathbf{trop}(\mathcal{P}') = \mathbf{trop}(\mathcal{P}(\alpha))$ and that T_α locally map orbits of TDS' to orbits of $TDS \in \mathcal{O}$, with \mathcal{O} being a neighborhood of TDS' . Consequently, TDS' is locally structurally stable. \square

Definition 8.4. *We say that a tropical vertex $\mathcal{P}' : (u', v')$ of a tropical dynamical system TDS' is in general position if items 1–4 of Lemma 8.1 all hold true.*

For a given degree N , there are finitely many equivalence classes of locally structurally stable tropical vertices \mathcal{P} . We will not worry about the exact number, but these different systems are given by different slopes (line orientations) of the tropical edges meeting at \mathcal{P} and the different relevant flow vectors \mathbf{d}_k , $k = i, j, l$. This follows from Lemma 8.1 and Lemma 8.3.

In Fig. 8, we sketch different local phase portraits in a table. The rows of Fig. 8 correspond to different conditions on how orbits approach the tropical vertices, whereas the columns correspond to different conditions on how orbits leave. The examples are not unique, the list is not exhaustive (in fact, we have left some out on purpose) and some cases appear more than once (e.g. upon applying certain symmetries). Moreover, each example do come in different equivalence classes since different slopes of the tropical edges lead to distinct phase portraits, according to our definition Definition 7.2, see also Remark 7.3. The main point of Fig. 8 is to demonstrate the variety of possibilities. Examples for each of the cases can easily be constructed using the subdivision of the Newton polygon. Empty entries reflect cases that are (probably!) not possible. We leave a more thorough classification of the tropical vertices to future work.

9 Tropical singularities

A point (u, v) is a tropical singularity (or just singularity for short) of a tropical dynamical system TDS if $\mathbf{0} \in \mathbf{trop}(u, v)$. We now classify the structurally stable ones, and therefore suppose that $(\mathcal{T}, \mathcal{T}^\mathcal{U}, \mathcal{T}^\mathcal{V})$ is in general position, recall Definition 7.6. By Lemma 8.1, (u, v) is not a tropical vertex. Consequently, by the definition of \mathbf{trop} , see Definition 3.7, a tropical singularity (u, v) is the intersection of $\mathcal{E}_{i,j}^\mathcal{U} \subset \mathcal{T}^\mathcal{U}$ and $\mathcal{E}_{l,p}^\mathcal{V} \subset \mathcal{T}^\mathcal{V}$ with both sets being switching manifolds of nullcline sliding-type (either transversal or tangential). With $(\mathcal{T}, \mathcal{T}^\mathcal{U}, \mathcal{T}^\mathcal{V})$ being in general position, the intersection is transverse at (u, v) , see item 3 of Definition 7.6, such that

$$\det \begin{pmatrix} \deg F_i - \deg F_j \\ \deg F_l - \deg F_p \end{pmatrix} \neq 0. \quad (47)$$

Moreover, $\mathcal{E}_{i,j}^\mathcal{U}$ or $\mathcal{E}_{l,p}^\mathcal{V}$ is a tropical edge of \mathcal{T} but not both (since then (u, v) would be a tropical vertex of $\mathcal{T}^\mathcal{I}$ with $\#\arg\max_{k \in \mathcal{I}} F_k(u, v) = 4$, in contradiction with $(\mathcal{T}, \mathcal{T}^\mathcal{U}, \mathcal{T}^\mathcal{V})$

Exit Enter	Stable transversal Filippov	Unstable transversal Filippov	Stable transversal nullcline	Unstable transversal nullcline	Stable tangential Filippov	Unstable tangential Filippov	Tangential nullcline	Crossing
Stable transversal Filippov								
Unstable transversal Filippov								
Stable transversal nullcline								
Unstable transversal nullcline								
Stable tangential Filippov								
Unstable tangential Filippov								
Tangential nullcline								

Figure 8: A table with different local dynamics near a tropical vertex \mathcal{P} with $(\mathcal{T}, \mathcal{T}^u, \mathcal{T}^v)$ in general position (e.g. $\mathbf{0} \notin \mathbf{trop}(\mathcal{P})$). The table is organized around different types of entrance (the rows) and different types of exits (the columns). Empty entries reflect cases that are (probably!) not possible. The list is not exhaustive and the cases shown are examples; they are not unique. In fact, according to our notion of topological equivalence, different slopes lead to different equivalence classes, see Remark 7.3.

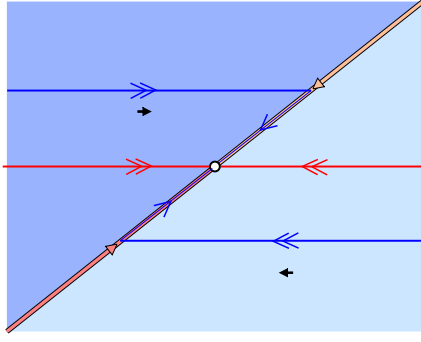
being in general position). Suppose the former. (The latter is identical). Then in the case of transversal nullcline sliding, the nullcline sliding vector \mathbf{d}_{nc} , recall Lemma 3.12, is well-defined on either side of (u, v) on $\mathcal{E}_{i,j}^{\mathcal{U}}$ and it is discontinuous at (u, v) .

Definition 9.1. *Under the assumptions stated above, we say that (u, v) is a*

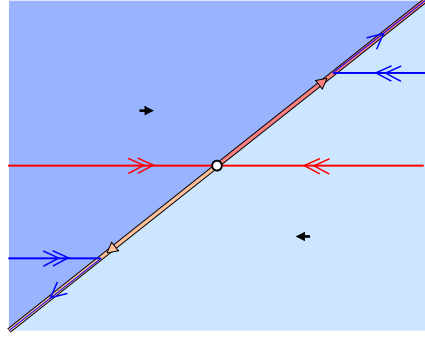
1. A sink if $\mathcal{E}_{i,j}^{\mathcal{U}}$ is a stable transversal nullcline sliding switching manifold, and \mathbf{d}_{nc} on either side of (u, v) points towards (u, v) .
2. A source if $\mathcal{E}_{i,j}^{\mathcal{U}}$ is an unstable transversal nullcline sliding switching manifold, and \mathbf{d}_{nc} on either side of (u, v) points away from (u, v) .
3. A strong-stable saddle if $\mathcal{E}_{i,j}^{\mathcal{U}}$ is a stable transversal nullcline sliding switching manifold, and \mathbf{d}_{nc} on either side of (u, v) points away from (u, v) .
4. A strong-unstable saddle if $\mathcal{E}_{i,j}^{\mathcal{U}}$ is an unstable transversal nullcline sliding switching manifold, and \mathbf{d}_{nc} on either side of (u, v) points towards (u, v) .
5. A hybrid point if $\mathcal{E}_{i,j}^{\mathcal{U}}$ is a tangential nullcline sliding switching manifold.

In the situations where reference to whether the dominating directions are stable or unstable is not important, we just write either a strong-stable saddle or a strong-unstable saddle as a saddle.

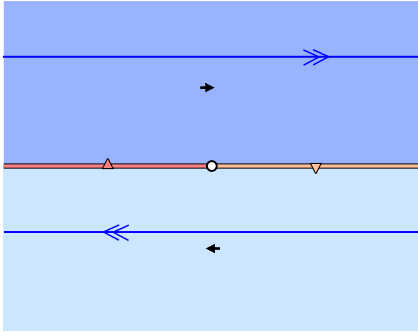
We illustrate the different tropical singularities in Fig. 9. In particular, Fig. 9(a) is a sink whereas Fig. 9(b) is a strong-stable saddle. The source and the strong-unstable saddle are identical upon time reversal. Finally, Fig. 9(c)–(d) are hybrid points; notice that the hybrid points come in two types: One where the dominant and sub-dominate vectors have a well-defined direction of rotation, see (c), (like a center) and one where there is no direction of rotation (like a saddle), see (d). Due to our definition of equivalence, see Remark 7.3, for two tropical singularities of sink, source, or saddle-type to be equivalent, the transversal sliding switching manifolds have to have the same slopes. However, for a fixed degree N , there are finitely many possible slopes (the actual number is not important for us, but it can be expressed in terms of Euler's totient number) and therefore finitely many equivalence classes of locally structurally stable tropical singularities.



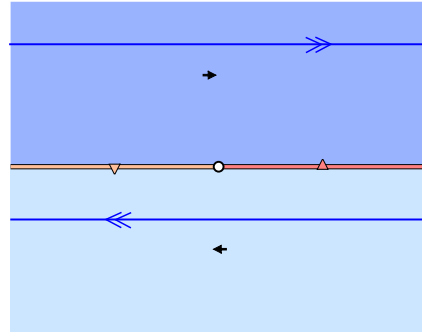
(a) Sink



(b) Saddle



(c) Hybrid point (center-type)



(d) Hybrid point (saddle-type)

Figure 9: Illustration of the different tropical singularities, see sub-caption. In the case of the sink and saddle we indicate the arrival separatrices in red, see Section 10. The triangles along the sliding manifolds indicate the direction of \mathbf{d}_{nc} in (a) and (b) and the direction of the flow vector of the subdominant direction (v in this case) in (c) and (d).

Lemma 9.2. *Consider a tropical dynamical system*

$$TDS' \in \mathcal{TDS}(N, \{\mathbf{d}_k\}_{k \in \mathcal{I}}),$$

with $(\mathcal{T}', \mathcal{T}'^u, \mathcal{T}'^v)$ in general position and suppose that \mathcal{P}' is a tropical singularity. Then \mathcal{P}' is a sink, source, saddle or a hybrid point and it is locally structurally stable on a neighborhood X of \mathcal{P}' .

Moreover, for any $TDS \in \mathcal{O}$, with \mathcal{O} a sufficiently small neighborhood of TDS' , there is a unique tropical singularity $\mathcal{P}(\alpha)$, of the same type (sink/source/saddle/hybrid point) as \mathcal{P}' , and whose coordinates $(u(\alpha), v(\alpha))$ are affine functions of $\alpha \in \mathcal{O}$ (and invariant with respect to (14)).

Proof. We first obtain $\mathcal{P}(\alpha)$ with the coordinates $(u(\alpha), v(\alpha))$ by proceeding as in Lemma 8.2. Then we define an affine translation T_α with respect to $\alpha \in \mathcal{O}$ by

$$T_\alpha(u, v) = (u, v) + (u(\alpha) - u', v(\alpha) - v').$$

Clearly, T_α sends \mathcal{T}' to $\mathcal{T}(\alpha)$ and locally orbits of TDS' to orbits of $TDS \in \mathcal{O}$, since $\mathbf{trop}(\mathcal{P}') = \mathbf{trop}(\mathcal{P}(\alpha))$ for all $\alpha \in O$. \square

Definition 9.3. *We say that a tropical singularity is in general position if it is a sink, source, saddle or a hybrid point.*

Remark 9.4. *Notice that a sink, a source and saddle each have nine local orbits up to equivalence (one point, two separatrices, two along the switching manifolds and then four with fast and slow segments; only five (including the singularity itself) are shown in Fig. 9(a) and (b) in the cases of a sink and saddle). Notice also that solutions are nonunique at a tropical singularity.*

On the other hand, with our definition of an orbit, a hybrid point has infinitely many polygonal orbits, as we can slide back and forth any finite number of times before either leaving the neighborhood or ending at the singularity. In the present manuscript, it will not be important, but in future work one might consider restricting the set of orbits further and rule out pathological examples.

10 Separatrices and separatrix connections

In Section 8 and Section 9, we focused on local phenomena. We now turn our attention to global ones. For this purpose, tropical vertices and tropical singularities play an important role. Indeed if there is an orbit connecting two such points by crossing only, then this situation *may be* structurally unstable, see the example in Fig. 10 and the figure caption for further details.

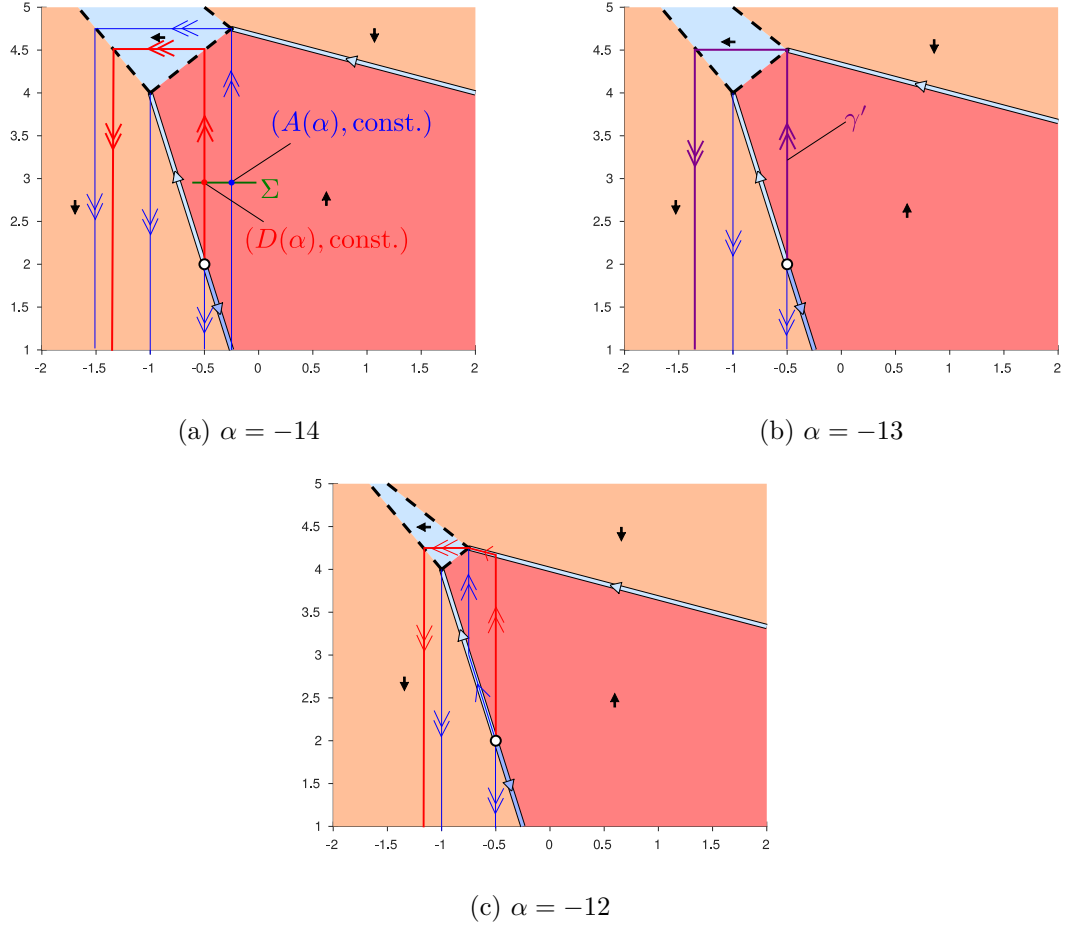


Figure 10: Example of an unfolding of a separatrix connection. The system is given by (51) below. For $\alpha = -13$, see (b), there is a separatrix connection (in purple) between the tropical source at $(-0.5, 2)$ and the tropical vertex at $(-0.5, 4.5)$. This gives rise to two non-equivalent phase portraits upon perturbation, see (a) and (c) for $\alpha = -14$ and $\alpha = -12$, respectively. In particular, the red orbits in (a) and (c) are not homotopic to any orbits in (c) and (a), respectively, cf. Definition 7.1.

We now introduce the notion of arrival and departure separatrices ([9] uses similar concepts).

Definition 10.1. *Consider a point \mathcal{P} , which is either a tropical vertex or a tropical singularity of a tropical dynamical system. Then a departure (an arrival) separatrix is a forward (backward, respectively) orbit of the crossing flow with initial condition at \mathcal{P} .*

A departure separatrix of \mathcal{P} either corresponds to a global forward solution $(u, v) : [0, \infty) \rightarrow \mathbb{R}^2$, $(u, v)(0) = \mathcal{P}$, of the crossing flow (being either unbounded as $t \rightarrow \infty$ or having a crossing limit cycle (see Section 11) as the ω -limit set) or it intersects a sliding switching manifold $\mathcal{E} \subset \mathcal{T}$ (transversal nullcline type) or a tropical vertex \mathcal{Q} in a (smallest) finite time $T > 0$: $(u, v)(T) \in \mathcal{E}$, $(u, v)(T) = \mathcal{Q}$, respectively. The same holds for an arrival separatrix in backward time.

Sinks and strong-stable saddles have two arrival separatrices, see Fig. 9(a) and (b) (red curves), whereas sources and strong-unstable saddles each have two departure separatrices.

Notice that a hybrid point does *not* have a separatrix (since this would necessarily be along the tropical edge and it is therefore not given by crossing, see Fig. 9(c) and (d)). This is our definition and it is motivated by the fact that connections along sliding segments are not (in themselves) associated with bifurcations.

By Lemma 8.1 and Lemma 9.2, we directly obtain the following.

Lemma 10.2. *Consider a tropical dynamical system*

$$TDS' \in \mathcal{TDS}(N, \{\mathbf{d}_k\}_{k \in \mathcal{I}}),$$

and a point $\mathcal{P}' : (u', v')$, which is either (a) a tropical vertex in general position or (b) a tropical sink, source or saddle, recall Definition 8.4 and Definition 9.1, respectively. (We will refer to this as the type of \mathcal{P}' .) Then there is a neighborhood X of \mathcal{P}' such that the separatrices of the point $\mathcal{P}(\alpha)$ of $TDS \in \mathcal{O}$, which is of the same type as \mathcal{P}' , are affine translations with respect to $\alpha \in \mathcal{O}$ in X .

Definition 10.3. We say that an orbit γ of the crossing flow is a separatrix connection if it is both a departure separatrix and an arrival separatrix of points \mathcal{P} and \mathcal{Q} , respectively. In the affirmative case, we will say that γ departs from \mathcal{P} and arrives at \mathcal{Q} . If $\mathcal{P} = \mathcal{Q}$ then it is a homoclinic separatrix connection; otherwise, it is said to be a heteroclinic separatrix connection.

Lemma 10.4. *Consider a tropical dynamical system*

$$TDS' \in \mathcal{TDS}(N, \{\mathbf{d}_k\}_{k \in \mathcal{I}}),$$

with $(\mathcal{T}', \mathcal{T}'^u, \mathcal{T}'^v)$ in general position and tropical coefficients α' . Suppose that γ' is a separatrix connection, departing from \mathcal{P}' and arriving at \mathcal{Q}' . Here each \mathcal{P}' and \mathcal{Q}' is either a tropical vertex in general position or a tropical sink, source or saddle.

Then there is a neighborhood \mathcal{O} of TDS' such that for each $TDS \in \mathcal{O}$ there are points $\mathcal{P}(\alpha)$ and $\mathcal{Q}(\alpha)$ of the same type as \mathcal{P}' and \mathcal{Q}' , respectively. Moreover, there is a section Σ transverse to γ' , see Fig. 10(a) and (b), defined by either (i) $v = \text{const.}$, $u \in I$, or (ii) $u = \text{const.}$, $v \in I$, where I is an open interval, such that the departure separatrix of $\mathcal{P}(\alpha)$ and the arrival separatrix of $\mathcal{Q}(\alpha)$ intersect Σ for all $\alpha \in \mathcal{O}$ in the following points:

(i) $(D(\alpha), \text{const.})$ and $(A(\alpha), \text{const.})$.

(ii) $(\text{const.}, D(\alpha))$ and $(\text{const.}, A(\alpha))$,

in cases (i) and (ii), respectively. In particular,

$$\Delta(\alpha) := D(\alpha) - A(\alpha) = b \cdot (\alpha - \alpha'), \quad \alpha \in \mathcal{O},$$

for some

$$b = (b_1, \dots, b_{2M}) \in \mathbb{Q}^{2M}, \tag{48}$$

is an affine function of α . Moreover, it is invariant with respect to the action (14) (i.e. $\sum_{k=1}^{2M} b_k = 0$) and roots of Δ correspond to separatrix connections of \mathcal{P} and \mathcal{Q} .

Proof. This should be clear enough, recall Lemma 10.2. In particular, the expression for Δ is a consequence of Lemma 3.14 and Lemma 8.1. \square

Remark 10.5. Δ only depends on the α_i 's with $i \in \alpha_{\arg\max_{k \in \mathcal{I}} F_k(u,v)}$ for some $(u, v) \in \gamma$ (like the quantities in Lemma 3.14 and Lemma 8.1), but this will not be important.

The vector b (48) will be called a *splitting constant* associated with γ' . Clearly, the splitting constant depends upon the section Σ , but at the same time:

Lemma 10.6. *If b and b' are two splitting constants then $b = cb'$ for some $c \in \mathbb{Q}$, $c \neq 0$.*

Proof. Let $\Delta(\alpha) = b \cdot (\alpha - \alpha')$ and $\Delta'(\alpha) = b' \cdot (\alpha - \alpha')$ be two different distance functions. They are defined along different sections Σ and Σ' , respectively. Consequently, we can conjugate Δ and Δ' through the transition map from Σ to Σ' . This map is affine and invertible, since it is a composition of maps of the form Lemma 3.14. The result therefore follows. \square

Most importantly, $b = 0 \Leftrightarrow b' = 0$, since b can vanish; for a simple example, recall Fig. 6(d) (purple orbit).

Lemma 10.7. *Suppose that the assumptions of Lemma 10.4 hold true and let b' denote a splitting constant associated to the separatrix connection γ' . Then the tropical dynamical system TDS' is locally structurally stable on a neighborhood X of γ' if $b' = 0$.*

Proof. If $b' = 0$ then $\Delta(\alpha) \equiv 0$ and there is a separatrix connection $\gamma(\alpha)$, with $\gamma(\alpha') = \gamma'$, for all $\alpha \in O$. The system is locally structurally stable, as no equivalence classes are produced or destroyed by perturbations. \square

Remark 10.8. *On the other hand, if the splitting constant b' is nonzero for a separatrix connection γ' , then for any neighborhood O of α' , there is an $\alpha \in O$ such that TDS does not have separatrix connection near γ . This may not lead to structural instability; \mathcal{P}' not being a discontinuity point is an obvious example, but see also Fig. 16 below for a (more) nontrivial example. In any case, for a structurally stable system TDS' , we may assume that (or more accurately, consider a representative of the structural stable system for which) all separatrix connections γ' of TDS' have a vanishing splitting constant, i.e. $b' = 0$.*

Definition 10.9. *We say that a separatrix connection γ is in general position if its splitting constant $b \in \mathbb{Q}^{2M}$ vanish: $b = 0$.*

This definition is independent of the section Σ , cf. Lemma 10.6.

11 Crossing cycles

The dynamical system defined by the crossing flow (induced by (28), recall Remark 3.15) can have closed orbits. We call these crossing cycles, when they only intersect the discontinuity set of \mathcal{T} along switching manifolds of crossing type, recall also Definition 5.1. We describe these, as in classical dynamical systems theory, using a return map.

Lemma 11.1. *Consider a tropical dynamical system $TDS' \in \mathcal{TDS}$ with tropical coefficients α' . Suppose that $(\mathcal{T}', \mathcal{T}'^u, \mathcal{T}'^v)$ is in general position and that there is a crossing cycle γ' of the crossing flow, i.e. a closed polygonal orbit that does not go through the tropical vertices of \mathcal{T}' , see Definition 11.3. Then there is a neighborhood O of α' in $\mathbf{A}(2M)$ and a section Σ defined by $v = \text{const.}, u \in I$, transverse to γ' with $\gamma' \cap \Sigma = (u', \text{const.})$ and I an open interval, such that for all $TDS \in \mathcal{O}$, we have a well-defined return map $P(\cdot, \alpha) : \Sigma \rightarrow \Sigma$ of the following form:*

$$P(u, \alpha) = u' + c(u - u') + b \cdot (\alpha - \alpha'), \quad u \in \Sigma, \alpha \in O, \quad (49)$$

satisfying $P(u', \alpha') = u'$, with $c \in \mathbb{Q}_+$, and $b = (b_1, \dots, b_{2M}) \in \mathbb{Q}^{2M}$ with $\sum_{k=1}^{2M} b_k = 0$.

Proof. We simply compose the transition maps in Lemma 3.14. \square

The value $c > 0$ is independent of the section Σ and it is called *the multiplier* of γ' . This is standard, see [54]. The vector $b \in \mathbb{Q}^{2M}$ will be called a *splitting constant* associated to γ' .

As usual, if $c = 1$ then the fixed point $u = u'$ of $P(\cdot, \alpha')$ is non-hyperbolic, whereas if $c \neq 1$ then it is hyperbolic, being attracting for $c \in (0, 1)$ and repelling for $c > 1$. This is standard, see [54]. Since $P(\cdot, \alpha')$ is affine, γ' is only a limit cycle in the hyperbolic case. In particular, γ' is not isolated when $c = 1$, but surrounded by closed orbits (since I is open).

Lemma 11.2. *Suppose that the assumptions of Lemma 11.1 hold true and let c denote the multiplier of γ' and let b be an associated splitting constant, see (49). Then TDS' is locally structurally stable in a neighborhood X of γ' if and only if either of the following statements hold true:*

- (a) γ' is hyperbolic ($c \neq 1$).
- (b) γ' is nonhyperbolic ($c = 1$) and $b = 0$.

Proof. Suppose first that neither (a) nor (b) holds. Then γ' is nonhyperbolic with $c = 1$ and $b \neq 0$. But then there is an $\alpha \in O$ such that the Poincaré map does not have a fixed-point. This shows the only if part.

Next, for the if part. Suppose first that (a) holds. Then for all $\alpha \in O$ there is a limit cycle $\gamma(\alpha)$, satisfying $\gamma(\alpha') = \gamma'$, with the same stability as γ' . In particular, $\gamma(\alpha)$ intersects the section Σ in the unique fixed-point of $P(\cdot, \alpha)$. This proves the locally structural stability in this case. Finally, suppose (b). Then $P(\cdot, \alpha') = P(\cdot, \alpha) = \text{id}$ for all $\alpha \in O$. Since all crossing switching manifolds are translated in an affine way with respect to α , the result follows. \square

Definition 11.3. *We say that a crossing cycle γ , with multiplier c and a splitting constant b , is in general position if either (a) or (b) of Lemma 11.2 hold true.*

12 The crossing graph

Consider a tropical dynamical system TDS with a polyhedral subdivision \mathcal{S} of the Newton polygon associated with F_{\max} . For simplicity, we suppose that $(\mathcal{T}, \mathcal{T}^u, \mathcal{T}^v)$ is in general position. Then for each vertex $\deg F_k$ of the subdivision, we assign the flow vector \mathbf{d}_k as a label to $\deg F_k$, as we did in Section 6. This leads to our *labelled subdivision*. From the subdivision, we obtain \mathcal{T} (up to homotopy, see Proposition 2.3). Each labelled $\deg F_k$ corresponds to a tropical region \mathcal{R}_k with flow vector \mathbf{d}_k .

Definition 12.1. *The labelled subdivision \mathcal{S} defines a directed graph \mathcal{G} (the crossing graph) in the following way: The labelled degrees $\deg F_k$ of \mathcal{S} are vertices of \mathcal{G} and there is a directed edge from $\deg F_i$ to $\deg F_j$, $i \neq j$, if the edge $(\deg F_i, \deg F_j)$ is a subset of \mathcal{S} and*

$$(\mathbf{d}_j \cdot (\deg F_j - \deg F_i))(\mathbf{d}_i \cdot (\deg F_j - \deg F_i)) > 0. \quad (50)$$

By construction, the crossing graph \mathcal{G} is a planar graph. Notice the following:

Lemma 12.2. *Suppose that there is directed edge of the crossing graph \mathcal{G} between $\deg F_i$ and $\deg F_j$. Then either (a) $\mathbf{d}_j = \mathbf{d}_i$ or (b) $\mathbf{d}_j \cdot \mathbf{d}_i = 0$ and there is crossing along the associated tropical edge $\mathcal{E}_{i,j}$.*

Proof. The statement follows from the definition of crossing, see (31), and the fact that the tropical edges $\mathcal{E}_{i,j}$ are perpendicular to edges of the subdivision, see Proposition 2.3. \square

Notice that there is specifically a directed edge of \mathcal{G} between $\deg F_i$ and $\deg F_j$ if $\mathcal{E}_{i,j} \subset \mathcal{T}$ with $\mathbf{d}_i = \mathbf{d}_j$ (so that $\mathcal{E}_{i,j}$ is not a switching manifold).

Lemma 12.3. *Suppose that a tropical dynamical system TDS has a crossing cycle that passes through n tropical regions: $\mathcal{R}_{k_1}, \dots, \mathcal{R}_{k_n}$, with $k_1, \dots, k_n \in \mathcal{I}$ distinct and $n \in \mathbb{N}, n \geq 4$. Then the crossing graph \mathcal{G} has a cycle through the associated vertices $\deg F_{k_1}, \dots, \deg F_{k_n}$.*

Proof. This should be clear enough. \square

The graph also encodes the multiplier c because this quantity is determined as a product of the slopes, see Lemma 11.1 and (37), of the crossing switching manifolds.

We cannot go the other way in Lemma 12.3, because the edges of the crossing graph \mathcal{G} only relate to existence of one single orbit segment going from one tropical region to another. So a cycle of the crossing graph \mathcal{G} does not imply that there is a closed orbit passing through each of the corresponding tropical regions; this depends upon the degrees and the position of the separatrices of the tropical vertices, see the examples below in Section 12.1 and Section 12.2. In other words, the number of cycles in the crossing graph \mathcal{G} is (only) an upper bound for the number of crossing cycles. We refer to [1] for optimal bounds on cycles of planar graphs, see also Section 15 below.

For our purposes, the crossing graph \mathcal{G} will be useful to understand the possible separatrix connections. To explain this, consider a tropical singularity \mathcal{Q} . If we are in general position, then it belongs to a tropical edge $\mathcal{E}_{i,j}$ at an interface between \mathcal{R}_i and \mathcal{R}_j , i.e. $\mathcal{E}_{i,j} \subset \overline{\mathcal{R}_i} \cap \overline{\mathcal{R}_j}$.

To study the departure separatrices of \mathcal{Q} , we therefore follow the paths in the directed graph from the corresponding vertices $\deg F_i$ and $\deg F_j$. To study the arrival separatrices, we have to reverse the directions of the edges of the graph.

Similarly, for a tropical vertex \mathcal{P} in general position, we have three adjacent tropical regions \mathcal{R}_i , \mathcal{R}_j and \mathcal{R}_l , $i, j, l \in \mathcal{I}$ distinct, i.e. $\mathcal{P} = \overline{\mathcal{R}}_i \cap \overline{\mathcal{R}}_j \cap \overline{\mathcal{R}}_l$, and we can follow the departure separatrices of \mathcal{P} by following the paths in the directed graph from the corresponding vertices $\deg F_i$, $\deg F_j$ and $\deg F_l$. Arrival separatrices are studied in a similar way by reversing the directions of the edges.

In other words, each tropical singularity of sink, source or saddle-type is associated with two vertices of the crossing graph \mathcal{G} , whereas each tropical vertex in general position is associated with three vertices of \mathcal{G} . We conclude the following.

Lemma 12.4. *Consider a tropical dynamical system with $(\mathcal{T}, \mathcal{T}^{\mathcal{U}}, \mathcal{T}^{\mathcal{V}})$ in general position and suppose that there is a separatrix connection, departing from \mathcal{P} and arriving at \mathcal{Q} . Then there is a path in the crossing graph \mathcal{G} between the vertices associated with \mathcal{P} and the vertices associated with \mathcal{Q} .*

Remark 12.5. *The labelled subdivision $\mathcal{S} = \mathcal{S}^{\mathcal{I}}$ (and the crossing graph \mathcal{G}) describe the flow on all tropical edges, except on edges with nullcline sliding. The flow on these are essentially determined by the intersection of the tropical curves $\mathcal{T}^{\mathcal{U}}$ and $\mathcal{T}^{\mathcal{V}}$ of the u - and v -polynomials, $F_{\max}^{\mathcal{U}}$ and $F_{\max}^{\mathcal{V}}$, respectively. These intersections can be encoded in the Minkowski sum of $\mathcal{S}^{\mathcal{U}}$ and $\mathcal{S}^{\mathcal{V}}$, see [13] for details.*

12.1 Example: A bifurcating crossing cycle

In this section, we consider a simple one-parameter-family of tropical dynamical systems, defined by the following tropical pairs:

$$\begin{aligned} F_1(u, v) &:= u, & \mathbf{d}_1 &:= (1, 0), \\ F_2(u, v) &:= -5 + 3u + 3v, & \mathbf{d}_2 &:= (-1, 0), \\ F_3(u, v) &:= v, & \mathbf{d}_3 &:= (0, -1), \\ F_4(u, v) &:= 4u + 2v, & \mathbf{d}_4 &:= (0, 1), \\ F_5(u, v) &:= \alpha + 5u + 5v, & \mathbf{d}_5 &:= (0, -1), \end{aligned} \tag{51}$$

with $\mathcal{U} = \{1, 2\}$, $\mathcal{V} = \{3, 4, 5\}$, that (among other things) supports a bifurcating crossing cycle. A simple calculation shows that for all $\alpha < -11$, we obtain the labelled subdivision \mathcal{S} in Fig. 11(a). We restrict attention to this set of α -values.

We have also illustrated the associated crossing graph \mathcal{G} in Fig. 11(a) (purple edges). There is a single cycle of the graph given by

$$(1, 0) \rightarrow (4, 2) \rightarrow (3, 3) \rightarrow (0, 1) \rightarrow (1, 0). \tag{52}$$

There are three important tropical vertices associated with the tropical polynomial $F_{\max}(u, v) = \max_{k \in \{1, \dots, 5\}} F_k(u, v)$:

$$\mathcal{P}_{134} = (0, 0), \quad \mathcal{P}_{234} = (-1, 4),$$

and

$$\mathcal{P}_{245} = \left(-\frac{15}{4} - \frac{\alpha}{4}, \frac{5}{4} - \frac{\alpha}{4} \right), \quad (53)$$

for $\alpha < -11$. There is also a unique tropical singularity \mathcal{Q}_{1234} at

$$\left(-\frac{1}{2}, 2 \right),$$

due to the intersection of $\mathcal{E}_{12}^{\mathcal{U}}$ and $\mathcal{E}_{34}^{\mathcal{V}}$.

In Fig. 11(b), we illustrate the phase portrait of the tropical system for $\alpha = -25$. Here we see a stable crossing limit cycle (in red) intersecting Σ (in green) defined by $v = 0$ in the point $u = 2$. In agreement with the cycle (52), it goes from \mathcal{R}_1 (blue) to \mathcal{R}_4 (red) and then to \mathcal{R}_2 (light blue) and finally to \mathcal{R}_3 (brown), before it repeats itself. It is easy to show that the return map $P(\cdot, \alpha) : \Sigma \rightarrow \Sigma$ satisfies:

$$P(u, \alpha) = \frac{4}{9}u + \frac{10}{9}.$$

We see that $u = 2$ is a stable fixed point ($P(2, \alpha) = 2$, $c := P'_u(2, \alpha) = \frac{4}{9} \in (0, 1)$) and that P is independent of α , see Lemma 11.1. However, this expression is only valid if

$$2 < -\frac{15}{4} - \frac{\alpha}{4},$$

where the right hand side is the u -component of \mathcal{P}_{245} , see (53). This gives

$$\alpha < -23.$$

At $\alpha = -23$ there is a structurally unstable homoclinic separatrix connection, arriving and departing from \mathcal{P}_{245} , see Fig. 12(a). There are also structurally unstable separatrix connections at the following values of $\alpha \in (-11, -23)$.

1. For $\alpha = -\frac{167}{9}$, there is a separatrix connection, departing from \mathcal{Q}_{1234} (moving upwards) and arriving at \mathcal{P}_{245} , see Fig. 12(b).
2. For $\alpha = -\frac{53}{3}$, there is a separatrix connection, departing from \mathcal{P}_{234} and arriving at \mathcal{P}_{245} , see Fig. 12(c).
3. For $\alpha = -\frac{49}{3}$, there is a separatrix connection, departing from \mathcal{Q}_{1234} (moving downwards) and arriving at \mathcal{P}_{245} , see Fig. 12(d).
4. For $\alpha = -15$, there is a separatrix connection, departing from \mathcal{P}_{134} and arriving at \mathcal{P}_{245} , see Fig. 12(e).
5. For $\alpha = -13$, there is another separatrix connection, departing from \mathcal{Q}_{1234} and arriving at \mathcal{P}_{245} . See Fig. 10(b).

For $\alpha = -11$, we have $\mathcal{P}_{234} = \mathcal{P}_{245} := \mathcal{P}_{2345}$ (not shown). There are no crossing cycles for $\alpha \in [-23, -11)$, cf. Definition 5.1, but as is clear from Fig. 12, there is a (unique) stable sliding cycle for every $\alpha \in [-23, -11)$. However, the α -parameter family defined by (51) is only structurally stable within $\alpha < -11$ for $\alpha \notin \{-23, -\frac{167}{9}, -\frac{53}{3}, -\frac{49}{3}, -15, -13\}$.

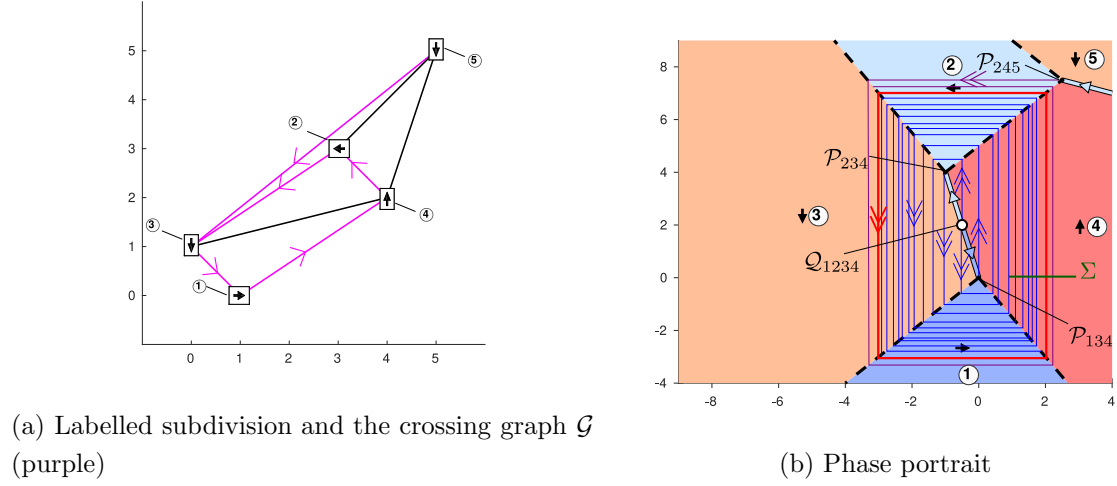
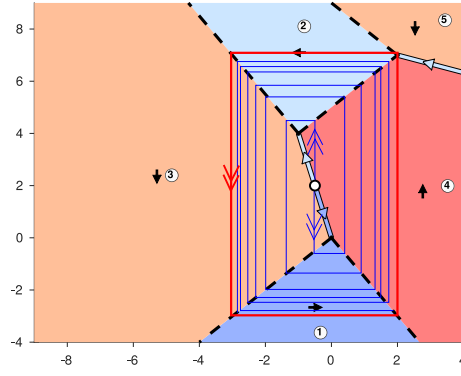
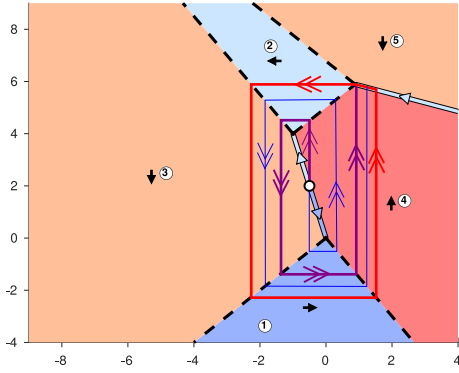


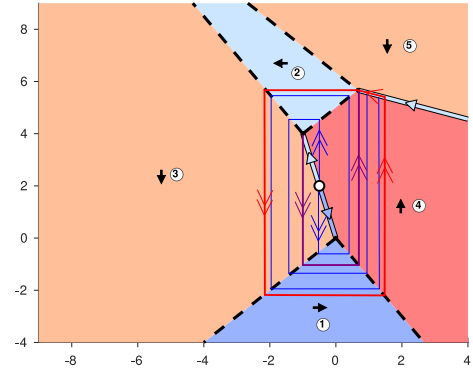
Figure 11: In (a): The labelled subdivision and the crossing graph \mathcal{G} (purple) for the tropical dynamical system defined by (51) for $\alpha < -11$. There is a single cycle of the graph, see (52). In (b): The associated phase portrait for $\alpha = -25$. There is a crossing limit cycle in red. The system is structurally stable (within the one-parameter family defined by (51)).



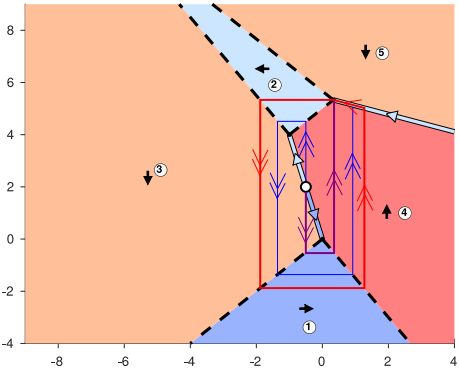
(a) $\alpha = -23$



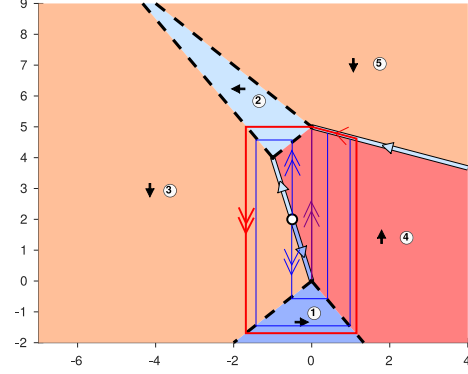
(b) $\alpha = -\frac{167}{9}$



(c) $\alpha = -\frac{53}{3}$



(d) $\alpha = -\frac{49}{3}$



(e) $\alpha = -15$

Figure 12: Bifurcations of the tropical dynamical system defined by (51) due to separatrix connections. In (a), where $\alpha = -23$, the crossing limit cycles goes through the point \mathcal{P}_{245} giving rise to a homoclinic separatrix connection. In (b), where $\alpha = -\frac{167}{9}$, there is a separatrix connection, departing from \mathcal{Q}_{1234} and arriving at \mathcal{P}_{245} . In (c), where $\alpha = -\frac{53}{3}$, there is a separatrix connection, departing from \mathcal{P}_{234} and arriving at \mathcal{P}_{245} (see Fig. 11). In (d), where $\alpha = -\frac{49}{3}$, there is a separatrix connection, departing from the tropical source \mathcal{Q}_{1234} and arriving at \mathcal{P}_{245} . Finally, in (e), where $\alpha = -15$, there is a separatrix connection departing from \mathcal{P}_{134} and arriving at \mathcal{P}_{245} .

12.2 Example: A structurally stable separatrix connection

Now, consider instead the following one-parameter-family of tropical dynamical systems, defined by the following tropical pairs:

$$\begin{aligned}
F_1(u, v) &:= 2u, & \mathbf{d}_1 &:= (1, 0), \\
F_2(u, v) &:= -2 + 2u + 3v, & \mathbf{d}_2 &:= (-1, 0), \\
F_3(u, v) &:= v, & \mathbf{d}_3 &:= (0, -1), \\
F_4(u, v) &:= 4u + v, & \mathbf{d}_4 &:= (0, 1), \\
F_5(u, v) &:= \alpha + 5u + 4v, & \mathbf{d}_5 &:= (0, -1),
\end{aligned} \tag{54}$$

with $\mathcal{U} = \{1, 2\}$, $\mathcal{V} = \{3, 4, 5\}$. It is easy to show that for all $\alpha < -3$, we obtain the labelled subdivision \mathcal{S} in Fig. 13(a). We restrict attention to this set of α -values. There is a single cycle of the crossing graph \mathcal{G} given by

$$(2, 0) \rightarrow (4, 1) \rightarrow (2, 3) \rightarrow (0, 1) \rightarrow (2, 0). \tag{55}$$

There are as before three important tropical vertices of the tropical polynomial $F_{\max}(u, v) = \max_{k \in \{1, \dots, 5\}} F_k(u, v)$:

$$\mathcal{P}_{134} = (0, 0), \quad \mathcal{P}_{234} = (0, 1),$$

and

$$\mathcal{P}_{245} = \left(-\frac{3}{4} - \frac{\alpha}{4}, \frac{1}{4} - \frac{\alpha}{4} \right),$$

for $\alpha < -3$. However, there are now two tropical singularities: \mathcal{Q}_{1234} at

$$\left(0, \frac{2}{3} \right),$$

due to the intersection of $\mathcal{E}_{12}^{\mathcal{U}}$ and $\mathcal{E}_{34}^{\mathcal{V}}$, and \mathcal{Q}_{1245} at

$$\left(-\alpha - 2, \frac{2}{3} \right),$$

due to the intersection of $\mathcal{E}_{12}^{\mathcal{U}}$ and $\mathcal{E}_{45}^{\mathcal{V}}$. \mathcal{Q}_{1234} is a hybrid point (center-like), whereas \mathcal{Q}_{1245} is a tropical saddle.

In Fig. 13(b) we show the phase portrait for $\alpha = -4$. The return map to Σ , defined by $v = 0$, $u \in (0, -\frac{3}{4} - \frac{\alpha}{4})$, is the identity in this case (so that $c = 1$, $b = 0$ in Lemma 11.1). Consequently, there is a family of (nonhyperbolic) crossing cycles. This also means that there is a structurally stable homoclinic separatrix connection, departing and arriving at the point \mathcal{P}_{245} . A simple calculation, shows that there are no additional bifurcations for $\alpha < -3$; in particular \mathcal{P}_{245} cannot connect to \mathcal{Q}_{1245} by crossing only. At $\alpha = -3$, we have $\mathcal{P}_{245} = \mathcal{P}_{234}$ and $(\mathcal{T}, \mathcal{T}^{\mathcal{U}}, \mathcal{T}^{\mathcal{V}})$ is not in general position. Interestingly, the purple cycle in Fig. 13(b) is a limit cycle, as the red orbit coincides with it beyond \mathcal{P}_{245} . (Notice that by Definition 5.1 the purple curve is a sliding cycle, not a crossing cycle).

Remark 12.6. The tropical system (54) is the $\epsilon = 0$ singular limit of the following system

$$\begin{aligned} x' &= x^3(1 - e^{-2\epsilon^{-1}}y^3), \\ y' &= y^2(-1 + x^4 - e^{\alpha\epsilon^{-1}}x^5y^3), \end{aligned} \quad (56)$$

written in the (u, v) -coordinates, see (5). A direct calculation shows that (56) has two singularities in the first quadrant for any $\alpha < -2$ and all $0 < \epsilon \ll 1$. Indeed, these are given by the equations

$$x^4 - 1 - e^{(\alpha+2)\epsilon^{-1}}x^5 = 0, \quad y = e^{\frac{2}{3}\epsilon^{-1}},$$

and the first equation has two positive solutions $x > 0$ in this case. This is in agreement with Fig. 13.

Notice also that for $\alpha < -2$ and $0 < \epsilon \ll 1$ then there is a singularity near $x \approx 1$. A direct calculation, shows that the Jacobian at this point has positive determinant and a negative trace given by

$$-3e^{\frac{3\alpha+8}{3}\epsilon^{-1}}x^5 < 0. \quad (57)$$

The singularity is therefore hyperbolic, specifically an attracting focus for (56) for $\alpha < -2$ and all $0 < \epsilon \ll 1$. The corresponding tropical singularity at $(u, v) = (0, \frac{2}{3})$ for $\alpha < -3$ (where the trace (57) is exponentially small with respect to $\epsilon \rightarrow 0$) is not attracting for the tropical dynamical system, see Fig. 13. Indeed, it is a hybrid point (of center type).

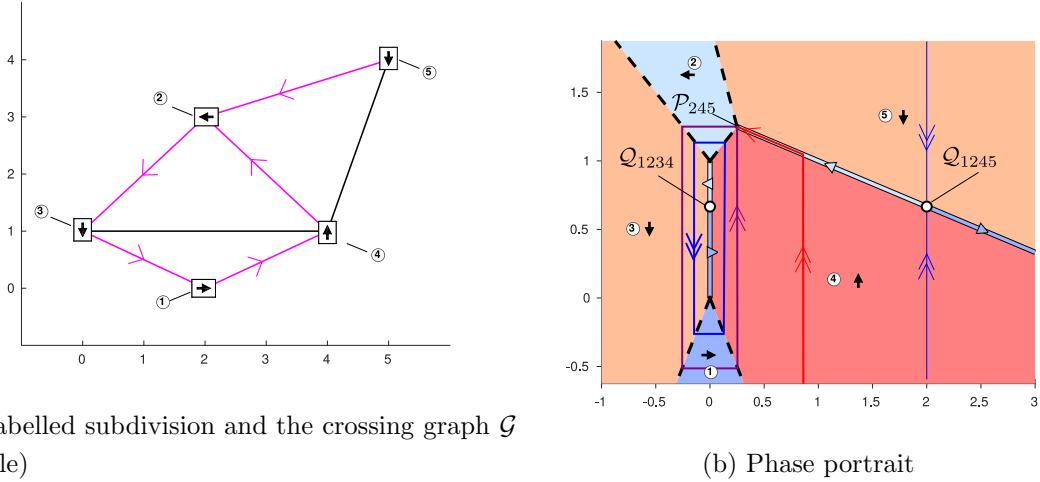


Figure 13: In (a): The labelled subdivision and the crossing graph \mathcal{G} (purple) for the tropical dynamical system defined by (54) for $\alpha < -3$. In (b): The associated phase portrait for $\alpha = -4$. There is a single cycle of the graph in (a), see (55), and a family of crossing cycles (all nonhyperbolic with $c = 1$, recall Lemma 11.1) in (b). The purple cycle is a separatrix connection the point \mathcal{P}_{245} . It is structurally stable (due to $c = 1$).

13 Main results: Structurally stable tropical dynamical systems

We are now finally in a position to state our main results.

Theorem 13.1. *Consider a tropical system*

$$TDS' \in \mathcal{TDS}(N, \{\mathbf{d}_k\}_{k \in \mathcal{I}}),$$

and assume that

1. $(\mathcal{T}', \mathcal{T}^{\mathcal{U}}, \mathcal{T}^{\mathcal{V}})$,
2. all separatrix connections,
3. and all crossing cycles,

of TDS' are in general position, cf. Definition 7.6, Definition 10.9, and Definition 11.3, respectively. Then TDS' is structurally stable.

Proof. It follows from the previous sections, that all tropical vertices, singularities, separatrix connections, and all crossing cycles are locally structurally stable.

Consider any departure (or arrival) separatrix of a point \mathcal{P}' , which is not a (structurally stable) separatrix connection. Either it is crossing only (of (28)), or it intersects a sliding manifold (Filippov or transversal nullcline) away from arrival separatrices of tropical singularities. Suppose the former. Then since the crossing flow defines a usual dynamical system, either the separatrix goes unbounded or the ω -limit (α -limit) set is a crossing limit cycle, which is hyperbolic by assumption. The same holds for the departure (arrival) orbit of the perturbed $\mathcal{P}(\alpha)$, $\alpha \in O$, since it is not a separatrix connection. Moreover, all intersections with the crossing switching manifolds of \mathcal{T} of $TDS \in \mathcal{O}$, with \mathcal{O} a neighborhood of TDS' , vary in an affine way with respect to $\alpha \in O$.

Now, we turn to stable (unstable) sliding. In forward (backward) time, orbits can only leave a sliding segment at a tropical vertex, through a departure (arrival, respectively) orbit. Otherwise, it goes unbounded (only possible if the sliding segment is unbounded) or it goes to a tropical singularity. Since $(\mathcal{T}', \mathcal{T}^{\mathcal{U}}, \mathcal{T}^{\mathcal{V}})$ is in general position, see Lemma 8.3 and Lemma 9.2, the same is true for \mathcal{T} of $TDS \in \mathcal{O}$. We can therefore conclude that TDS' and $TDS \in \mathcal{O}$ have the same orbit equivalence classes. Consequently, TDS' is structurally stable. □

Theorem 13.2. *There is an open dense subset \mathcal{D} of*

$$\mathcal{TDS}(N, \{\mathbf{d}_k\}_{k \in \mathcal{I}}),$$

with the associated subset $D \subset \mathbf{A}(2M)$ (recall the notation in Remark 3.20) consisting of a finite union of convex polytopes, upon which we have the following:

1. Any $TDS \in \mathcal{D}$ is structurally stable.

2. There is a finite number of equivalence classes of structurally stable systems on \mathcal{D} .

Proof. To prove the theorem, we focus on item 2 and show that there is a finite number of equivalence classes of structurally stable systems. This will in turn show the existence of \mathcal{D} in item 1.

By Lemma 7.5, for a structurally stable system we may assume that (or more accurately, consider a representative of the structural stable system for which) $(\mathcal{T}, \mathcal{T}^{\mathcal{U}}, \mathcal{T}^{\mathcal{V}})$ is in general position. There are finitely many (regular) triangulations of $\mathcal{S}^{\mathcal{U}}$ and $\mathcal{S}^{\mathcal{V}}$. For each fixed pair of triangulation of $\mathcal{S}^{\mathcal{U}}$ and $\mathcal{S}^{\mathcal{V}}$, there are finitely many triangulations of $\mathcal{S}^{\mathcal{I}}$. We then fix $\mathcal{S}^{\mathcal{U}}$, $\mathcal{S}^{\mathcal{V}}$ and $\mathcal{S}^{\mathcal{I}}$. This corresponds to fixing a convex polytope $O \subset \mathbf{A}(2M)$, see Theorem 2.4. Within this set, the corresponding tropical curves $\mathcal{T}^{\mathcal{U}}, \mathcal{T}^{\mathcal{V}}$ and $\mathcal{T}^{\mathcal{I}}$ are fixed up to homotopy, but their relative positions are not, [50]. However, there are finitely many ways that $\mathcal{T}^{\mathcal{U}}$ and $\mathcal{T}^{\mathcal{V}}$ can intersect transversally (up to homotopy) along their tropical edges – these are described by the Minkowski sum, see [50] – and each of these cases correspond to a convex polytope $O' \subset Y$. Within O' , all singularities and tropical vertices are in general position, see Lemma 8.3 and Lemma 9.2. Finally, the crossing graph \mathcal{G} , recall Definition 12.1, is fixed for $\alpha \in O'$.

We now subdivide O' further through separatrix connections (crossing cycles are handled in a similar way using the (finitely many) cycles of \mathcal{G}). Consider a departure separatrix from a point \mathcal{P} with $\alpha \in O'$. (The case of an arrival separatrix is handled in the same way.) Then in a neighborhood of \mathcal{P} this set varies in an affine way with respect to α . Now, following Lemma 12.4, we use the crossing graph \mathcal{G} to follow the departure separatrix. There are finitely many possible separatrix connections to consider. If a separatrix connection exists for some $\alpha \in O'$ with a splitting constant $b \neq 0$, then we divide O' into two convex polytopes (corresponding to $\Delta(\alpha) \gtrless 0$). Proceeding in this way, we obtain finitely many convex polytopes – the union of which is open and dense – and where Theorem 13.1 applies. In turn, we have finitely many equivalence classes of structurally stable systems. This completes the proof. □

14 Example: A generalized autocatalator

In this section, we consider a generalized tropical autocatalator model defined by the following tropical pairs:

$$\begin{aligned}
F_1(u, v) &:= \alpha_1 - u, & \mathbf{d}_1 &:= (1, 0), \\
F_2(u, v) &:= \alpha_2, & \mathbf{d}_2 &:= (-1, 0), \\
F_3(u, v) &:= \alpha_3 + 2v, & \mathbf{d}_3 &:= (-1, 0), \\
F_4(u, v) &:= \alpha_4, & \mathbf{d}_4 &:= (0, -1), \\
F_5(u, v) &:= \alpha_5 + u - v, & \mathbf{d}_5 &:= (0, 1), \\
F_6(u, v) &:= \alpha_6 + u + v, & \mathbf{d}_6 &:= (0, 1),
\end{aligned} \tag{58}$$

with $\mathcal{U} = \{1, 2, 3\}$, $\mathcal{V} = \{4, 5, 6\}$. In comparison with (43), all tropical coefficients $\alpha_1, \dots, \alpha_6$ are “free”, in the sense that $\alpha_1 = \alpha - 1$, $\alpha_2 = -1$, $\alpha_3 = -1$, $\alpha_4 = 0$, $\alpha_5 = 0$, $\alpha_6 = 0$ in (58) gives (43). In particular, the tropical flow vectors in (58) are the same as in (43). *We believe that this mimics the general situation in chemical reaction networks, where the signs of the terms are known, but the (magnitude of the) parameters are uncertain/unknown.*

Proposition 14.1. *There are 15 different structurally stable phase portraits of the tropical dynamical system defined by (58).*

To prove this claim, we follow the approach of the proof of Theorem 13.2 and first determine the different $(\mathcal{T}, \mathcal{T}^{\mathcal{U}}, \mathcal{T}^{\mathcal{V}})$ in general position, see Definition 7.6. For this purpose, we notice that $\mathcal{S}^{\mathcal{U}}$ and $\mathcal{S}^{\mathcal{V}}$ for $\alpha_i \in \mathbb{R}$, $i \in \{1, \dots, 6\}$, each consist of a single triangle, see Fig. 14, since there are three monomials (with $\deg F_k$ not co-linear) in each direction. Next, for $\mathcal{S}^{\mathcal{I}}$, we use a refinement poset [13] of the point configuration associated with (58), see Fig. 15. The notion of a refinement gives an ordering of the subdivision into layers according to how far a subdivision is from being a triangulation, see [13]. The upper-most subdivision is the trivial subdivision (where all points lie on the same plane in the $(\deg F, \alpha)$ -space). The second layer (row) consists of the almost-triangulations which connect exactly two triangulations in the third layer (row) by a *flip* (indicated by the lines). A flip [13, Section 2.4] is a local change that transforms one triangulation into another. (In general, the numbers of rows and columns of a refinement poset depend upon the point configuration.) We enumerate the triangulations in the final layer by 1, 2, ..., 5 as indicated in the figure. Notice that the cases 1, 4 and 5 come in different pairs according to whether $(0, 0)$ is labelled as $\mathbf{d}_2 = (-1, 0)$ (H =horizontal) or as $\mathbf{d}_4 = (0, -1)$ (V =vertical), cf. item 2 of Lemma 7.5, see Definition 7.6. We write C^H and C^V , $C = 1, 4, 5$, to separate these cases further. In the following, we consider the cases separately.

14.1 Case 1^H

We illustrate the labelled subdivision $\mathcal{S}^{\mathcal{I}}$ and the associate tropical curves $\mathcal{T}^{\mathcal{U}}$ (blue), $\mathcal{T}^{\mathcal{V}}$ (red), and $\mathcal{T}^{\mathcal{I}}$ (black) in Fig. 16. We also illustrate $\mathcal{T}^{\mathcal{U}}$ and $\mathcal{T}^{\mathcal{V}}$ and indicate that subsets of each of the tropical edges of $\mathcal{T}^{\mathcal{U}}$ belong to $\mathcal{T}^{\mathcal{I}}$. On the other hand, only one tropical edge of $\mathcal{T}^{\mathcal{V}}$ (\mathcal{E}_{56}) is a subset of $\mathcal{T}^{\mathcal{I}}$. This leads to three distinct subcases of case 1^H where $(\mathcal{T}, \mathcal{T}^{\mathcal{U}}, \mathcal{T}^{\mathcal{V}})$ in general position, cf. item 3 of Lemma 7.5, see Definition 7.6. These are indicated in the figure. Here we use that $\mathcal{T}^{\mathcal{V}}$ cannot intersect \mathcal{E}_{35} without changing the subdivision of $\mathcal{S}^{\mathcal{I}}$. This should be clear enough, see also Fig. 14. However, $1_c^H \sim 1_b^H$, since the separatrix connection in between does not generate new equivalence classes, and there are therefore only two (up to equivalence) distinct phase portraits. We provide examples of these in Fig. 17 (parameters are indicated in the caption).

14.2 Case 1^V

We illustrate the labelled subdivision $\mathcal{S}^{\mathcal{I}}$ and the associate tropical curves $\mathcal{T}^{\mathcal{U}}$ (blue), $\mathcal{T}^{\mathcal{V}}$ (red), and $\mathcal{T}^{\mathcal{I}}$ (black) in Fig. 18 (similar to Fig. 16). There are two different subcases of case

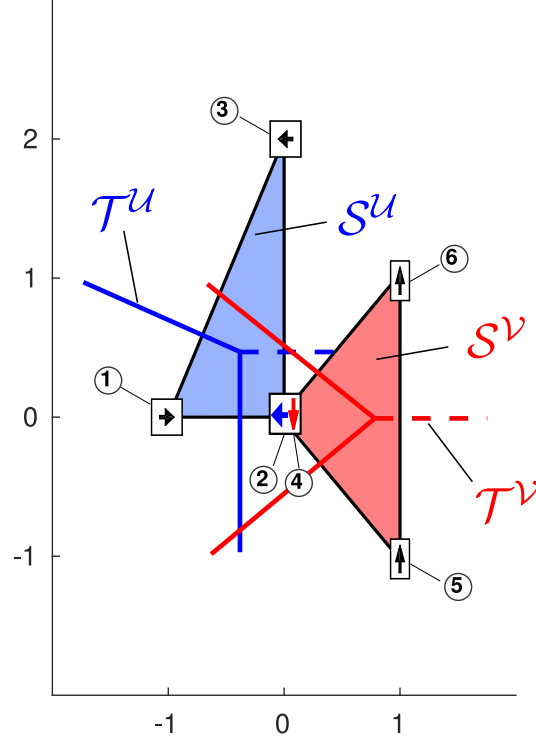


Figure 14: The subdivisions \mathcal{S}^u and \mathcal{S}^v and their dual tropical curves \mathcal{T}^u and \mathcal{T}^v , respectively. Only the full lines correspond to nullcline sliding.

1^V with $(\mathcal{T}, \mathcal{T}^u, \mathcal{T}^v)$ in general position. These corresponds to two different intersections of \mathcal{T}^u (blue) and \mathcal{T}^v (red) along \mathcal{E}_{45} , cf. item 3 of Lemma 7.5, see Definition 7.6. However, the phase portraits are clearly equivalent. We illustrate an example of the single phase portrait (up to equivalence) associated to case 1^V in Fig. 19 (see parameters in the figure caption).

14.3 Case 2

We illustrate the labelled subdivision \mathcal{S}^I and the associate tropical curves \mathcal{T}^u (blue), \mathcal{T}^v (red), and \mathcal{T}^I (black) in Fig. 20. There is only one case of $(\mathcal{T}, \mathcal{T}^u, \mathcal{T}^v)$ being in general position. Here we again use that \mathcal{T}^v cannot intersect \mathcal{E}_{35} without changing the subdivision \mathcal{S}^I . We illustrate an example of the single phase portrait (up to equivalence) associated to case 2 in Fig. 21 (see parameters in the figure caption).

14.4 Case 3

We illustrate the labelled subdivision \mathcal{S}^I and the associate tropical curves \mathcal{T}^u (blue), \mathcal{T}^v (red), and \mathcal{T}^I (black) in Fig. 22. There is only one case of $(\mathcal{T}, \mathcal{T}^u, \mathcal{T}^v)$ being in general position. Here we again use that \mathcal{T}^v cannot intersect \mathcal{E}_{35} and \mathcal{E}_{36} without changing the subdivision \mathcal{S}^I . We illustrate an example of the single phase portrait (up to equivalence) associated to case 3 in Fig. 23 (see parameters in the figure caption).

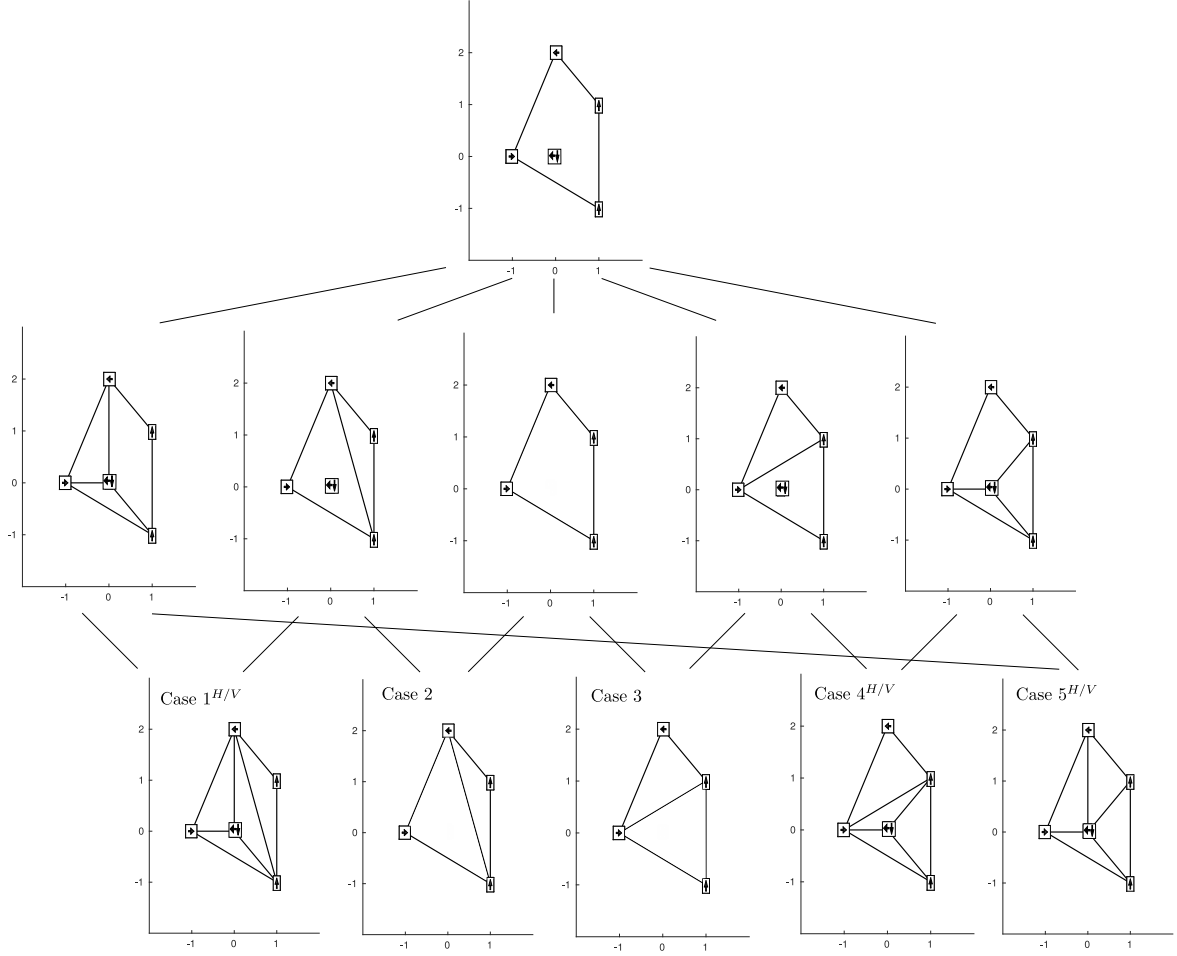


Figure 15: Refinement poset of the point configuration associated with the generalized tropical autocatalator model, see (58).

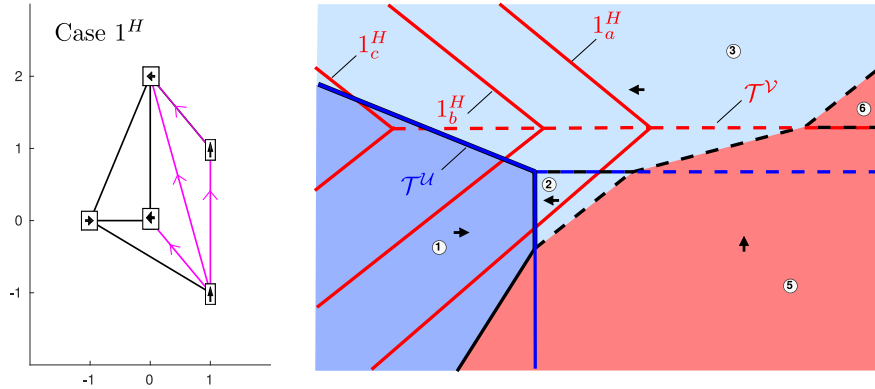


Figure 16: The subdivision associated with case 1^H and the associated tropical curves. There are three different cases of $(\mathcal{T}, \mathcal{T}^u, \mathcal{T}^v)$ in general position. Subsets of each of the tropical edges of \mathcal{T}^u (blue) belong to \mathcal{T}^I (in black) as indicated, whereas only one tropical edge of \mathcal{T}^v (\mathcal{E}_{56} in red) is a subset of \mathcal{T}^I . The separatrix connection, that occurs between 1_b^H and 1_c^H , does not generate new orbit equivalence classes.

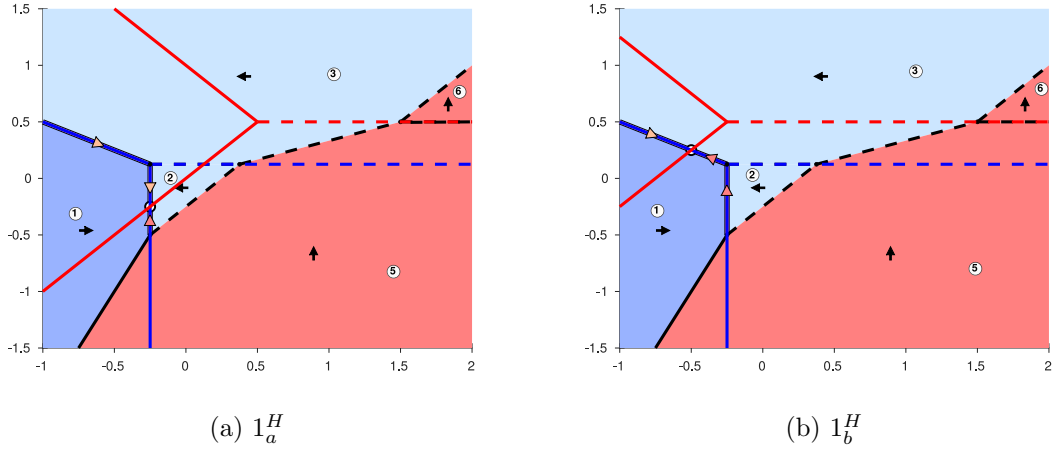


Figure 17: Two nonequivalent phase portraits 1_a^H (a) and 1_b^H (b) for the case 1^H , see Fig. 16. \mathcal{T}^U and \mathcal{T}^V are blue and red, whereas \mathcal{T}^I is in black. Full lines indicate sliding. The values of the tropical coefficients in the examples are: $\alpha_1 = 0$, $\alpha_2 = 0.25$, $\alpha_3 = 0$, $\alpha_5 = 0$, $\alpha_6 = -1$ and $\alpha_4 = 0$ in (a) and $\alpha_4 = -0.75$ in (b).

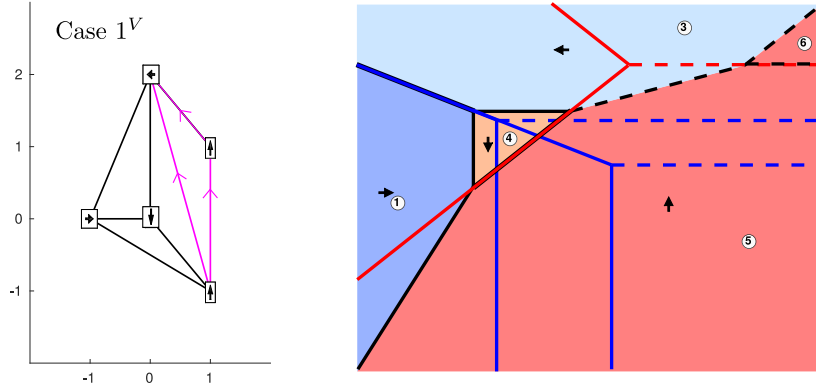


Figure 18: The subdivision associated with case 1^V and the associated tropical curves. There are two different cases of $(\mathcal{T}, \mathcal{T}^U, \mathcal{T}^V)$ in general position.

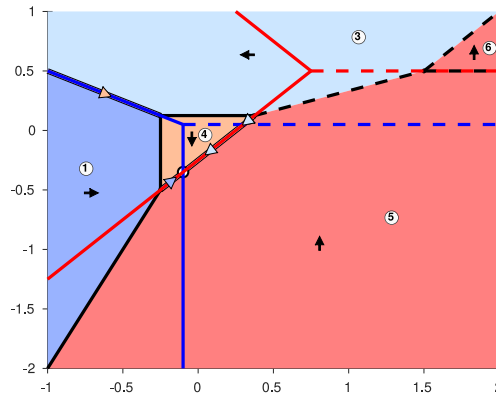


Figure 19: Phase portrait in the case 1^V , see Fig. 18. The values of the tropical coefficients are: $\alpha_1 = 0$, $\alpha_2 = 0.1$, $\alpha_3 = 0$, $\alpha_4 = 0.25$, $\alpha_5 = 0$ and $\alpha_6 = -1$.

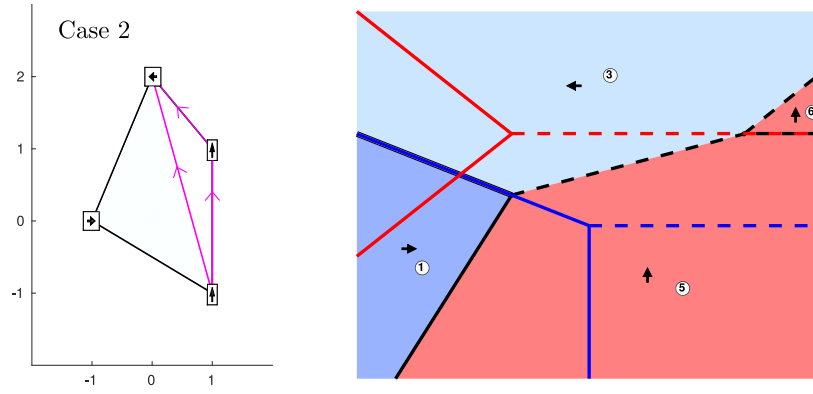


Figure 20: The subdivision associated with case 2 and the associated tropical curves.

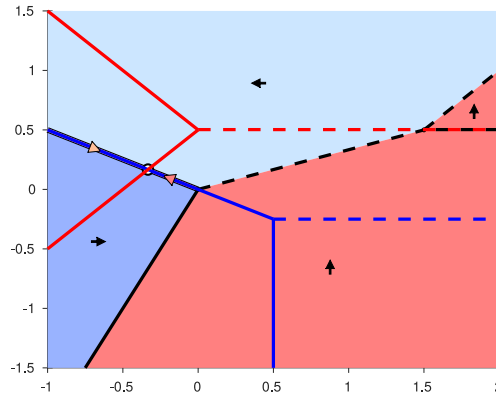


Figure 21: Phase portrait in the case 2, see Fig. 20. The values of the tropical coefficients are: $\alpha_1 = 0$, $\alpha_2 = -0.5$, $\alpha_3 = 0$, $\alpha_4 = -0.5$, $\alpha_5 = 0$ and $\alpha_6 = -1$.

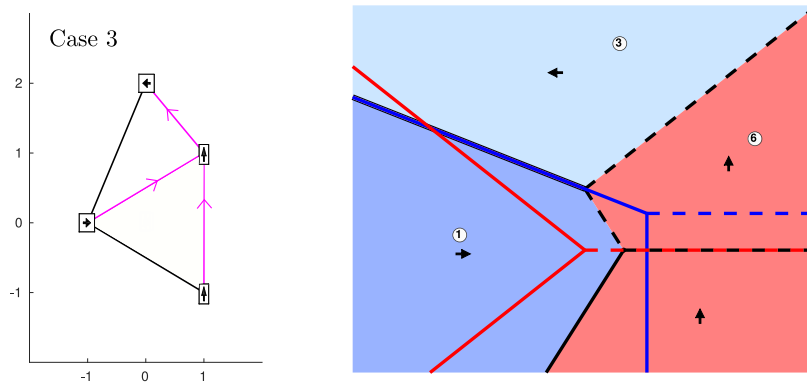


Figure 22: The subdivision associated with case 3 and the associated tropical curves.

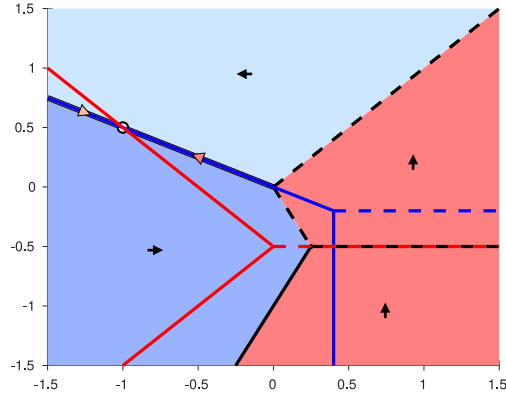


Figure 23: Phase portrait in the case 3, see Fig. 22. The values of the tropical coefficients are: $\alpha_1 = 0$, $\alpha_2 = -0.4$, $\alpha_3 = 0$, $\alpha_4 = -0.5$, $\alpha_5 = -1$ and $\alpha_6 = 0$.

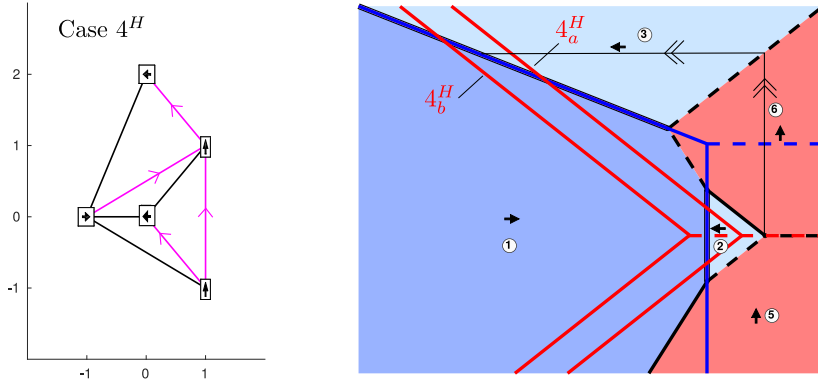


Figure 24: The subdivision associated with case 4^H and the associated tropical curves.

14.5 Case 4^H

We illustrate the labelled subdivision $\mathcal{S}^{\mathcal{I}}$ and the associate tropical curves $\mathcal{T}^{\mathcal{U}}$ (blue), $\mathcal{T}^{\mathcal{V}}$ (red), and $\mathcal{T}^{\mathcal{I}}$ (black) in Fig. 24. There are two cases of $(\mathcal{T}, \mathcal{T}^{\mathcal{U}}, \mathcal{T}^{\mathcal{V}})$ being in general position. We denote these by 4_a^H and 4_b^H . There is a bifurcation in between, where two singularities along \mathcal{E}_{12} coalesce. Interestingly, this bifurcation is also related to another global bifurcation of a separatrix connection (indicated in black). We illustrate examples of the two phase portraits (up to equivalence) associated to case 4^H in Fig. 25 (see parameters in the figure caption).

14.6 Case 4^V

We illustrate the labelled subdivision $\mathcal{S}^{\mathcal{I}}$ and the associate tropical curves $\mathcal{T}^{\mathcal{U}}$ (blue), $\mathcal{T}^{\mathcal{V}}$ (red), and $\mathcal{T}^{\mathcal{I}}$ (black) in Fig. 26. There are two cases of $(\mathcal{T}, \mathcal{T}^{\mathcal{U}}, \mathcal{T}^{\mathcal{V}})$ being in general position. We denote these by 4_a^V and 4_b^V . There is a bifurcation in between, where two singularities along $\mathcal{E}_{12}^{\mathcal{U}}$ coalesce. We illustrate examples of the two structurally stable phase portraits (up to equivalence) associated to case 4^V in Fig. 27 (see parameters in the figure caption).

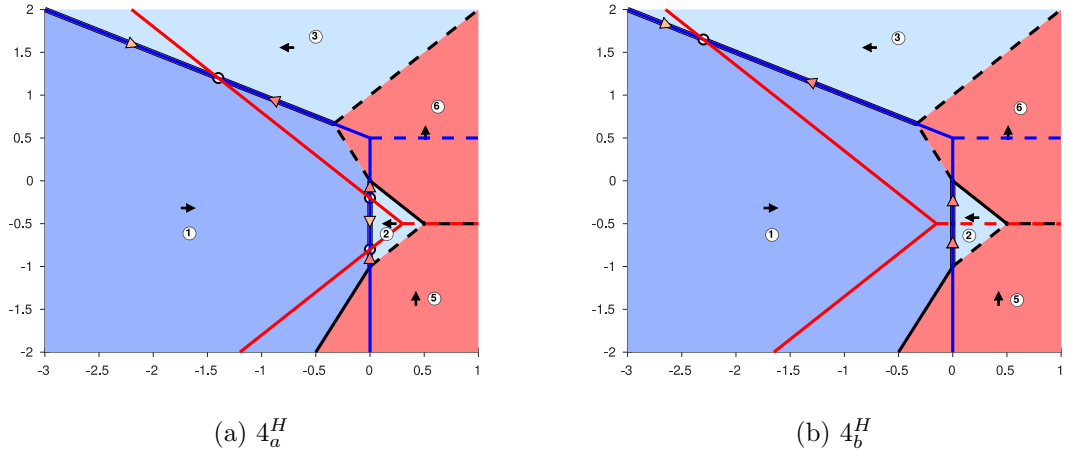


Figure 25: Phase portraits in the case 4^H , see Fig. 24. The values of the tropical coefficients are: $\alpha_1 = 0$, $\alpha_2 = 0$, $\alpha_3 = -1$, $\alpha_5 = -1$ and $\alpha_6 = 0$ and $\alpha_4 = -0.2$ in (a) and $\alpha_4 = -0.65$ in (b).

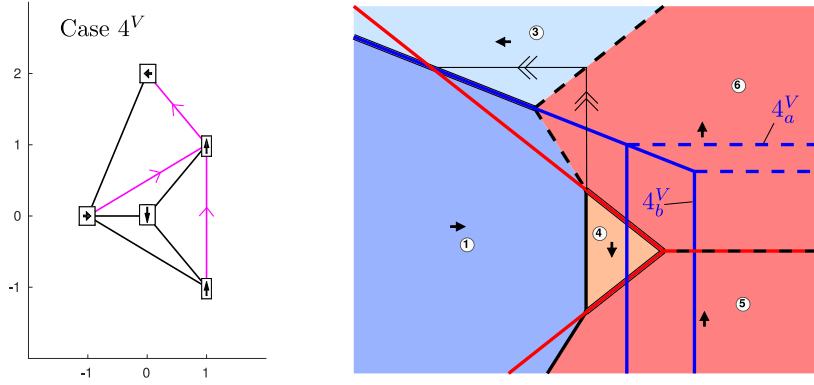


Figure 26: The subdivision associated with case 4^V and the associated tropical curves.

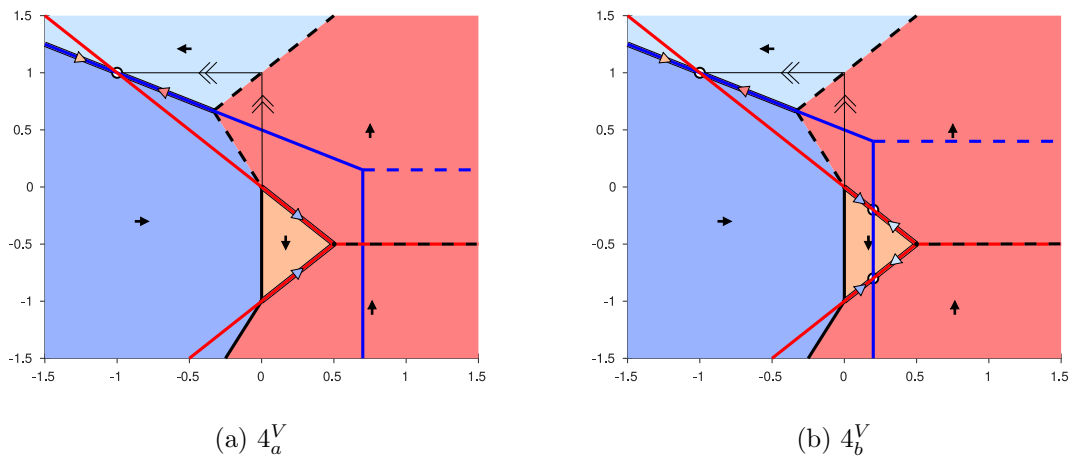


Figure 27: Phase portraits in the case 4^V , see Fig. 26. The values of the tropical coefficients are: $\alpha_1 = 0$, $\alpha_3 = -1$, $\alpha_4 = 0$, $\alpha_5 = -1$ and $\alpha_6 = 0$ and $\alpha_2 = -0.7$ in (a) and $\alpha_4 = -0.2$ in (b).

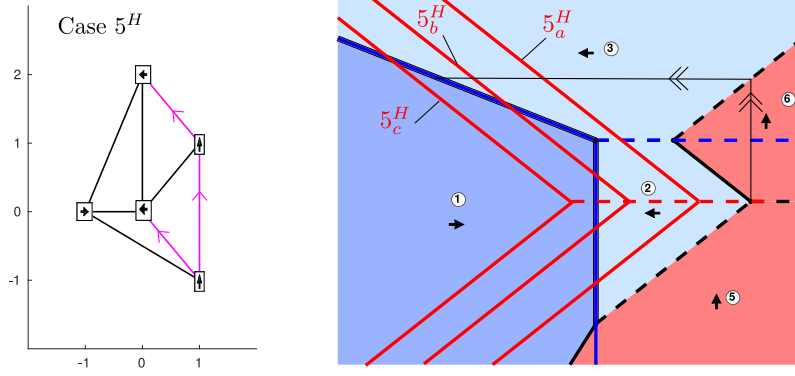


Figure 28: The subdivision associated with case 5^H and the associated tropical curves.

14.7 Case 5^H

We illustrate the labelled subdivision $\mathcal{S}^{\mathcal{I}}$ and the associate tropical curves $\mathcal{T}^{\mathcal{U}}$ (blue), $\mathcal{T}^{\mathcal{V}}$ (red), and $\mathcal{T}^{\mathcal{I}}$ (black) in Fig. 28. There are three cases of $(\mathcal{T}, \mathcal{T}^{\mathcal{U}}, \mathcal{T}^{\mathcal{V}})$ being in general position. We denote these by 5_a^H , 5_b^H and 5_c^H . There are bifurcations in between, where two singularities along $\mathcal{E}_{12}^{\mathcal{U}}$ coalesce. The structurally unstable case between 5_b^H and 5_c^H is (again) also associated with a global bifurcation due to a separatrix connection (indicated in black). We illustrate examples of the three structurally stable phase portraits (up to equivalence) associated to case 5^H in Fig. 29 (see parameters in the figure caption).

14.8 Case 5^V

We illustrate the labelled subdivision $\mathcal{S}^{\mathcal{I}}$ and the associate tropical curves $\mathcal{T}^{\mathcal{U}}$ (blue), $\mathcal{T}^{\mathcal{V}}$ (red), and $\mathcal{T}^{\mathcal{I}}$ (black) in Fig. 30. There are three cases of $(\mathcal{T}, \mathcal{T}^{\mathcal{U}}, \mathcal{T}^{\mathcal{V}})$ being in general position. We denote these by 5_a^V , 5_b^V and 5_c^V . There are bifurcations in between, where two singularities coalesce. We illustrate examples of the three structurally stable phase portraits (up to equivalence) associated to case 5^V in Fig. 31 (see parameters in the figure caption). There is a limit cycle in case 5_c^V , see Fig. 31(c).

14.9 Completing the proof of Proposition 14.1

In conclusion, we have found precisely two different phase portraits of 1^H , one single phase portrait for each of 1^V , 2, and 3, two different phase portraits for each of 4^H and 4^V , and finally, three different phase portraits for each of 5^H and 5^V . This gives 15 in total, as claimed by Proposition 14.1. Notice that there is only a limit cycle in the case 5_c^V and it is unique.

Remark 14.2. *The 15 different structurally stable phase portraits of the generalized autocatalator model are only determined by the tropical curves $\mathcal{T}^{\mathcal{I}}$, $\mathcal{T}^{\mathcal{U}}$ and $\mathcal{T}^{\mathcal{V}}$ and the different intersections of the two latter ones. In particular, there are no crossing cycles and no structurally unstable separatrix connections that divide the α -space into further equivalence classes.*

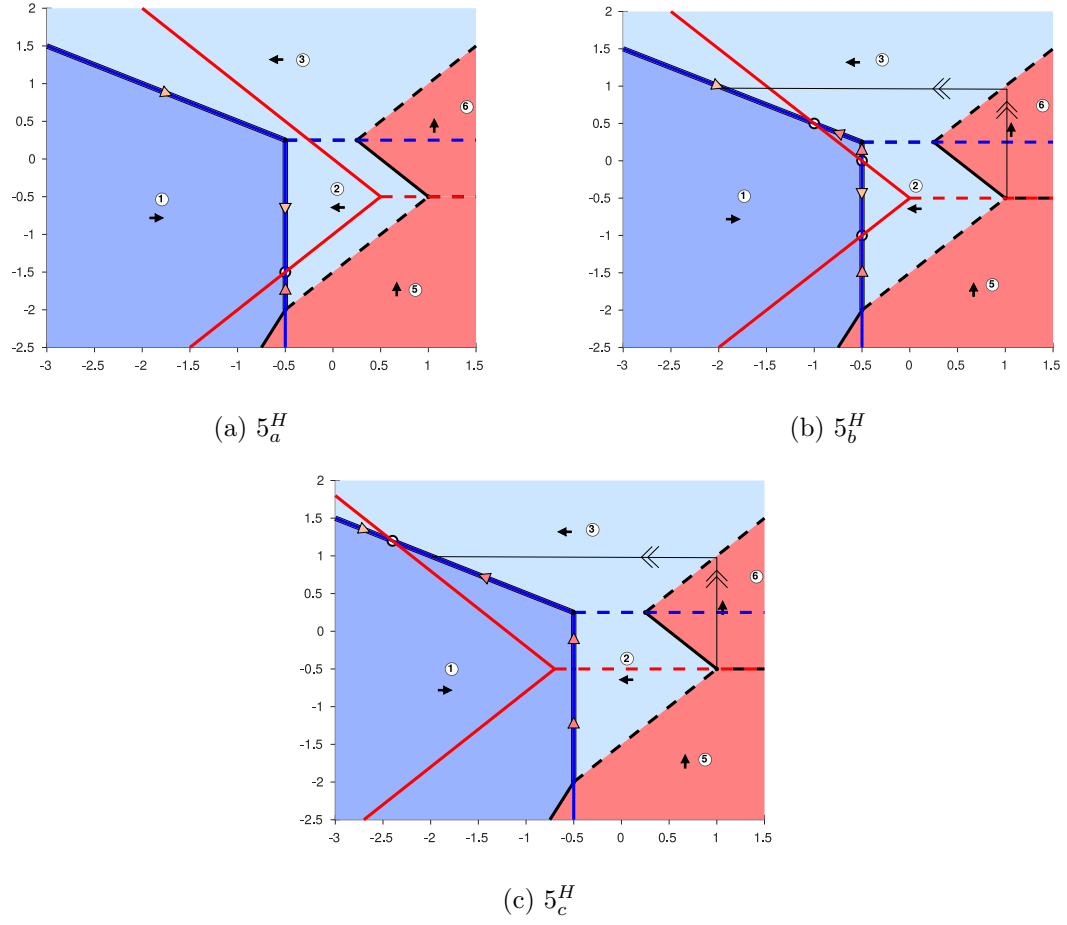


Figure 29: Phase portraits in the case 5^H , see Fig. 28. The values of the tropical coefficients are: $\alpha_1 = 0$, $\alpha_2 = 0.5$, $\alpha_3 = 0$, $\alpha_5 = -1$ and $\alpha_6 = 0$ and $\alpha_4 = 0$ in (a), $\alpha_4 = -0.5$ in (b) and $\alpha_4 = -1.2$ in (c).

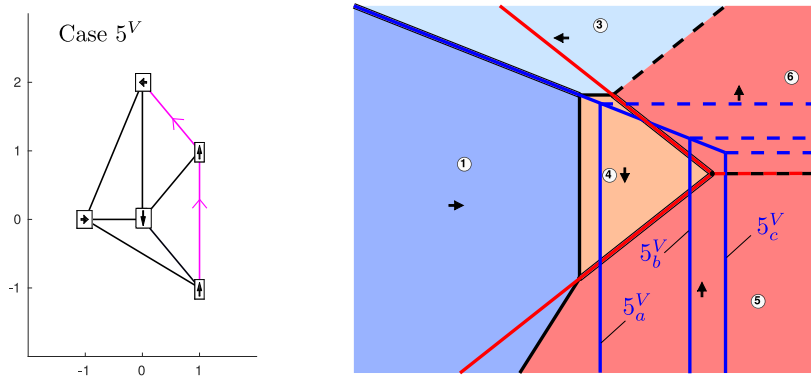
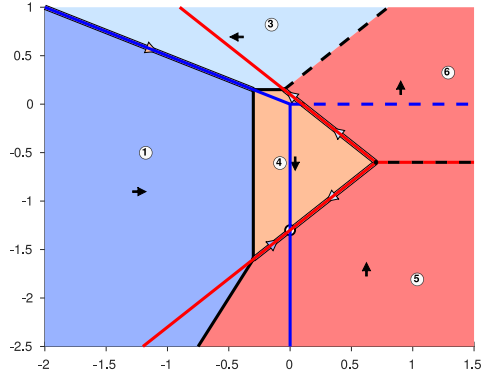
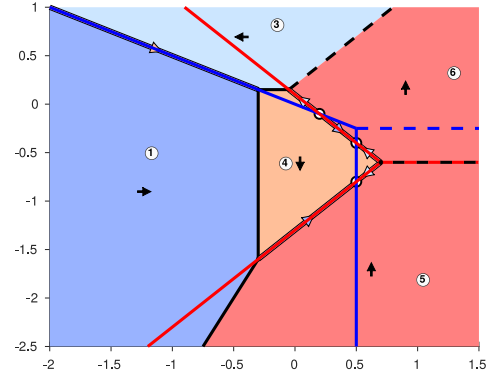


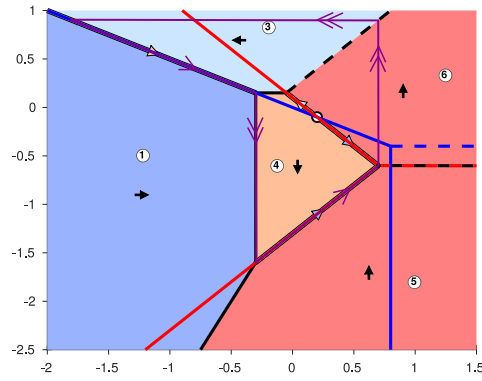
Figure 30: The subdivision associated with case 5^V and the associated tropical curves.



(a) 5_a^V



(b) 5_b^V



(c) 5_c^V

Figure 31: Phase portraits in the case 5^V , see Fig. 30. The values of the tropical coefficients are: $\alpha_1 = 0$, $\alpha_3 = 0$, $\alpha_4 = 0.3$, $\alpha_5 = -1$ and $\alpha_6 = 0.2$ and $\alpha_2 = 0$ in (a), $\alpha_2 = -0.5$ in (b) and $\alpha_4 = -0.8$ in (c). There is a limit cycle (purple) in (c).

Remark 14.3. For the “original” tropical autocatalator, defined by (43), having only the single tropical coefficient $\alpha - 1$ of F_1 as a free parameter, there are four distinct structurally stable phase portraits (up to equivalence). These correspond to cases 3 ($\alpha > 1$), 4_a^V ($\alpha \in (\frac{1}{2}, 1)$), 5_a^V ($\alpha < 0$) and 5_c^V ($\alpha \in (0, \frac{1}{2})$), compare with Section 6 and Fig. 5 and Fig. 6. (Notice that (43) is special in the sense that $\mathcal{E}_{2,3}^U \cap \mathcal{E}_{5,6}^U \subset \{v = 0\}$ is non-empty for all α . Although this does not play a role for the classification of structurally stable systems, this property is not the case in Fig. 31.)

15 Discussion

In this paper, we have introduced the notion of a tropical dynamical system by building upon the approach initiated in [56] and using a differential inclusion framework. This led to a (new) notion of equivalence of tropical dynamical systems and in our main result, Theorem 13.2, we showed that there are finitely many structurally stable phase portraits. In contrast, it is known for *quadratic* polynomial vector-fields that there are 44 different phase portraits on the Poincaré sphere, but only modulo limit cycles [3]. A similar result for general polynomial systems, would depend upon a solution to Hilbert’s 16th problem [4].

In future work, we aim to relate our notion of equivalence to the usual notion of equivalence. For example, we would like to study the other direction in Lemma 7.7. We are also interested in enumerating the structurally stable phase portraits for each N (which – following the proof of Theorem 13.2 – is essentially “computable”). In fact, we believe that there are many directions for future research. We elaborate on a few additional ones below.

15.1 Limit cycles

Firstly, since separatrix connections can be structurally stable (for zero splitting constants), we have not bounded the number of limit cycles on the finitely many structurally stable phase portraits, see Fig. 32 (and the figure caption for details) as well as Remark 9.4. It requires a more thorough description of the case of zero splitting constant for the description of canard-like phenomena as in Fig. 32; the larger cycle in Fig. 32 is reminiscent of a canard cycle of jump type, see [14]. (Notice that there are more than just two equivalence classes of limit cycles in Fig. 32. Indeed, as solutions of (38), we can (without further assumptions) have (pathological) periodic solutions of arbitrary period, e.g. going n times around the inner red limit cycles and then subsequently m times around the outer red limit cycles before repeating itself.)

Having said that, the number of *crossing limit cycles* is obviously bounded on \mathcal{TDS} since the number of cycles in the planar crossing graphs \mathcal{G} provides an upper bound, see Lemma 12.3. It would be interesting to determine the maximal number of crossing cycles in future work. This is essentially a graph theoretical problem. (The upper bound on general directed planar graphs in [1] is not appropriate in the present context; for one thing, since orbits of the crossing flow only consist of horizontal and vertical line segments, the path length of cycles of \mathcal{G} are greater than or equal to four, see Lemma 12.3). In fact, we believe

that the graph theoretical viewpoint can be expanded in such a way that \mathcal{G} also encodes sliding cycles.

On the other hand, the system (24) is a singular perturbation problem for $\epsilon \rightarrow 0$. The reference [2] realizes the asymptotic bound (4) on the number of limit cycles through canard cycles in slow-fast systems. From this perspective, we do not believe that it is reasonable to expect that a bound on the number of limit cycles on the set of structurally stable tropical dynamical systems will lead to an improvement beyond (4) (see discussion about the connection to $\epsilon > 0$ below). In fact, disregarding the possibility of canards as in Fig. 32 on the set of structurally stable systems, so that at most one tropical limit cycle passes through each tropical vertex, then *the number of sliding limit cycles is bounded by the number of triangles in \mathcal{S}^T* , which is given by

$$2 \left\lceil \frac{1}{2}(N+1)(N+4) \right\rceil - (3N+2) - 2 = N(N+2),$$

see [13, Lemma 3.1.3] and [58]. Here the square bracket is the number points in the point configuration, see (25), whereas the other bracket $(3N+2)$ is the number of points on the boundary of the Newton polygon. In his thesis [58], the second author constructed a family of tropical dynamical systems with

$$\frac{1}{2}(N-2)(N-3),$$

many sliding limit cycles for each degree $N \geq 4$. The family is constructed by duplicating (using the labelled subdivision) a certain template system for $N = 4$. For further details, we refer to the script

`lower_bound_script.m`

available through the link provided in Section 1.3, for running the program **Tropical Phase Portrait**. This script constructs the tropical phase portrait of the family for each $N \geq 4$. We expect that these limit cycles can be perturbed into limit cycles of (24) (and therefore (1)) of relaxation type for all $0 < \epsilon \ll 1$, see also Conjecture 15.1 and the discussion below.

Although these bounds are not competitive with (4), we do believe that pursuing such bounds in the context of tropical dynamical systems is meaningful nonetheless. Indeed, “optimal” lower bounds for the number of limit cycles in polynomial slow-fast systems occur in a very narrow parameter regime (due to canards). In fact, this is a general observation: When we pick a polynomial system at “random”, then we “do not tend” to see limit cycles at the order of (4). (Here “do not tend” is very imprecise but refers to something strictly less than probability one, since the limit cycles of [2] are hyperbolic.) The well-known example by Songling of a quadratic system with four limit cycles, see [60], is also very sensitive to variations of the parameters. This is of course just an observation, difficult (if not outright impossible) to make precise as a general mathematical result on (1). However, we speculate that tropical dynamical systems on the set of structurally stable systems offer a route for addressing this observation.

Moreover, as the phase portrait of a tropical dynamical system is determined by linear inequalities on the tropical coefficients, tropical dynamical systems essentially offers a framework where Coppel's problem of characterizing the phase portraits of quadratic systems by means of algebraic inequalities on the coefficients, see [12], is solvable on any degree. This is in contrast to the classical case, see [54, Section 4.14], where such a classification [18] (if possible at all) would require nonanalytic inequalities.

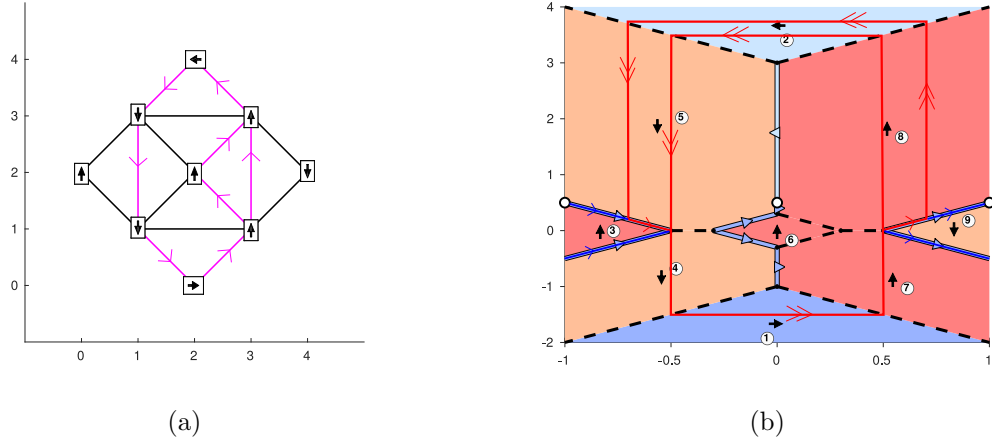


Figure 32: An example with infinitely many limit cycles. In (a): the subdivision and the associated crossing graph \mathcal{G} . In (b): The associated phase portrait. The red orbits are examples of limit cycles, whereas the blue orbits are examples of orbits having the limit cycles as their ω - or α -limit sets. The situation in (b) is structurally unstable, since the tropical vertices \mathcal{P}_{345} and \mathcal{P}_{789} can move independently. Consequently, the heteroclinic connection between \mathcal{P}_{345} and \mathcal{P}_{789} can be broken (its splitting constant b is nonzero). To bound the number of limit cycles on the set of structurally stable systems, we need to show that all cases of this type (and others) are structurally unstable.

15.2 Tropicalization of the full plane

Secondly, there is the issue of tropicalization of (1) in the full plane \mathbb{R}^2 . Our methods and results apply to each quadrant. Specifically, we can tropicalize (1) in each quadrant by setting

$$\begin{aligned} u_{\text{sign}(x)} &= \epsilon \log(\text{sign}(x)x), \\ v_{\text{sign}(y)} &= \epsilon \log(\text{sign}(y)y), \end{aligned} \tag{59}$$

for $(x, y) \neq (0, 0)$. However, the present paper does not deal with the connection problem that arises when matching across the quadrants. By (59), we have coordinates (u_+, v_+) in the first quadrant, (u_-, v_+) in the second quadrant and so on. It is clear that the matching between the first quadrant and the second has to be done along $u_{\pm} \rightarrow -\infty$. This naturally leads to a compactification of each of the four copies of $\mathbb{R}^2 \ni (u_{\pm}, v_{\pm})$ as $(\mathbb{R} \cup \{-\infty\})^2$. This is also very natural from the perspective that the tropical monomials themselves take values in $\mathbb{R} \cup \{-\infty\}$. We will explore this further in future work.

15.3 Extensions to \mathbb{R}^n

Thirdly, there is the problem of extending this theory to higher dimensions. Much of the initial development translates directly, including the definition of crossing and sliding. This is even the basis for the computational methods [43] based on tropical geometry. In this regard, it is important to highlight that there is a recursive structure to these systems, in the sense that along a higher dimensional switching manifold of transversal nullcline-type, there is a tropical system of dimension one less. In particular, in three dimensions we can (locally) reduce to a planar tropical dynamical systems, as studied in the present paper, along two-dimensional sliding switching manifolds of transversal nullcline-type.

15.4 The singular perturbation problem defined by $0 < \epsilon \ll 1$

Finally, there is the problem of addressing the connection between the tropical dynamical system and the associated smooth system (24) for all $0 < \epsilon \ll 1$. We leave this to future work, but do state the following:

Conjecture 15.1. *Suppose that a tropical dynamical system has a tropical edge \mathcal{E} that is either of transversal Filippov-, or transversal nullcline sliding type and consider a compact line segment $\mathcal{S}_0 \subset \mathcal{E}$ upon which \mathbf{d}_{FP} or \mathbf{d}_{nc} is constant. Then for all $0 < \epsilon \ll 1$, (24) has a locally invariant manifold \mathcal{S}_ϵ , diffeomorphic to \mathcal{S}_0 , of the same stability type, and with $\mathcal{S}_\epsilon \rightarrow \mathcal{S}_0$ for $\epsilon \rightarrow 0$. The one-dimensional flow on \mathcal{S}_ϵ is topologically equivalent to the flow on \mathcal{S}_0 given by \mathbf{d}_{FP} or \mathbf{d}_{nc} in the two cases.*

Conjecture 15.2. *Suppose that a tropical dynamical system has a hyperbolic crossing cycle γ_0 . Then for all $0 < \epsilon \ll 1$, (24) has a limit cycle γ_ϵ of the same stability type with $\gamma_\epsilon \rightarrow \gamma_0$ for $\epsilon \rightarrow 0$.*

Conjecture 15.3. *Suppose that a tropical dynamical system has a tropical singularity at (u_0, v_0) of either sink-, source- or saddle-type, recall Definition 9.1. Then there is a neighborhood X of (u_0, v_0) in which the associated smooth system (24) for all $0 < \epsilon \ll 1$ has a unique hyperbolic singularity at (u_ϵ, v_ϵ) , with $\lim_{\epsilon \rightarrow 0}(u_\epsilon, v_\epsilon) = (u_0, v_0)$, of the same type (stable node, unstable node or saddle).*

We feel certain that these results can be obtained using blowup and Fenichel's theory, see [22, 23, 24, 36] and [33, 40, 39] for applications of these methods in smooth systems approaching nonsmooth ones. We also refer to [56], where a version of Conjecture 15.1 is proven in the context of the Michaelis-Menten model.

It is also possible to perturb certain sliding limit cycles, like those in Fig. 5. Nonhyperbolic crossing cycles and hybrid points, on the other hand, do not persist (in general) as similar objects for (24) for $0 < \epsilon \ll 1$. It is straightforward to construct examples, see also Remark 12.6. A consequence of this last fact is that structural stability of the tropical system does not imply structural stability of (24) (in the usual sense) for all $0 < \epsilon \ll 1$, at least not without imposing additional assumptions.

Acknowledgement. The first author would like to offer genuine thanks to Peter Sz-molyan for introducing the subject of tropical geometry and for providing valuable insights into its potential applications in chemical reaction networks. The first author also thanks Sam Jelbart for helpful discussions. Finally, both authors thank the students Jonas Dammann, Thomas Haastrup, Victor Hansen (all project students at the bachelor level) and Daniel Munch Nielsen (master thesis, see [52]) for their contribution, which helped plant the seed for the development of the theory.

References

- [1] R. E. L. Aldred and C. Thomassen. On the maximum number of cycles in a planar graph. *Journal of Graph Theory*, 57(3):255–264, 2008.
- [2] M. J. Álvarez, B. Coll, P. De Maesschalck, and R. Prohens. Asymptotic lower bounds on Hilbert numbers using canard cycles. *J. Differential Equations*, 268(7):3370–3391, 2020.
- [3] J. C. Artés, R. E. Kooij, and Jaume Llibre. Structurally stable quadratic vector fields. *Memoirs of the American Mathematical Society*, 134(639):VIII–+, 1998.
- [4] J. C. Artés, M. C. Mota, and A. C. Rezende. Structurally unstable quadratic vector fields of codimension two: Families possessing a finite saddle-node and an infinite saddle-node. *Electronic Journal of Qualitative Theory of Differential Equations*, 2021(35):35, 2021.
- [5] J. P. Aubin and A. Cellina. *Differential Inclusions : Set-Valued Maps and Viability Theory*. Springer, 1984.
- [6] M. Baker, S. Payne, and J. Rabinoff. Nonarchimedean geometry, tropicalization, and metrics on curves. *Algebraic Geometry*, 3(1):63–105, 2016.
- [7] B. L. J. Braaksma. Multisummability of formal power-series solutions of nonlinear meromorphic differential-equations. *Annales De L Institut Fourier*, 42(3):517–540, 1992.
- [8] F. Brauer and C. Castillo-Chavez. *Mathematical Models in Population Biology and Epidemiology*. Springer Science+Business Media, LLC, 2012.
- [9] M. E. Broucke, C. C. Pugh, and S. N. Simic. Structural stability of piecewise smooth systems. *Computational and Applied Mathematics*, 20(1-2):51–89, 2001.
- [10] V. Carmona and F. Fernández-Sánchez. Integral characterization for poincaré half-maps in planar linear systems. *Journal of Differential Equations*, 305:319–346, 2021.
- [11] V. Carmona, F. Fernández-Sánchez, and D. D. Novaes. Uniform upper bound for the number of limit cycles of planar piecewise linear differential systems with two zones separated by a straight line. *Applied Mathematics Letters*, 137:108501, 2023.

- [12] W. A. Coppel. A survey of quadratic systems. *Journal of Differential Equations*, 2(2):293–304, 1965.
- [13] J. A. De Loera, J. Rambau, and F. Santos. *Triangulations : Structures for Algorithms and Applications*. Springer-Verlag Berlin Heidelberg, 2010.
- [14] P. De Maesschalck, F. Dumortier, and R. Roussarie. *Canard Cycles : From Birth to Transition*. Springer International Publishing, 2021.
- [15] A. Desoievres, P. Szmolyan, and O. Radulescu. Qualitative dynamics of chemical reaction networks: An investigation using partial tropical equilibrations. *Lecture Notes in Computer Science (including Subseries Lecture Notes in Artificial Intelligence and Lecture Notes in Bioinformatics)*, 13447:61–85, 2022.
- [16] M. di Bernardo, C. J. Budd, A. R. Champneys, and P. Kowalczyk. *Piecewise-smooth Dynamical Systems: Theory and Applications*. Springer Verlag, 2008.
- [17] M. di Bernardo, A.R. Chapneys, C. J. Budd, and P. Kowalczyk. *Piecewise-smooth Dynamical Systems*. Springer London, 2008.
- [18] F. Dumortier and P. Fiddelaers. Quadratic models for generic local 3-parameter bifurcations on the plane. *Transactions of the American Mathematical Society*, 326(1):101–126, 1991.
- [19] F. Dumortier, J. Llibre, and J. C. Artés. *Qualitative theory of planar differential systems*. Springer Berlin Heidelberg, 2006.
- [20] M. Esteban, J. Llibre, and C. Valls. The 16th Hilbert problem for discontinuous piecewise isochronous centers of degree one or two separated by a straight line. *Chaos*, 31(4):043112, 2021.
- [21] M. Feinberg. *Foundations of chemical reaction network theory*. Springer, 2019.
- [22] N. Fenichel. Persistence and smoothness of invariant manifolds for flows. *Indiana University Mathematics Journal*, 21:193–226, 1971.
- [23] N. Fenichel. Asymptotic stability with rate conditions. *Indiana University Mathematics Journal*, 23:1109–1137, 1974.
- [24] N. Fenichel. Geometric singular perturbation theory for ordinary differential equations. *J. Diff. Eq.*, 31:53–98, 1979.
- [25] A.F. Filippov. *Differential Equations with Discontinuous Righthand Sides*. Mathematics and its Applications. Kluwer Academic Publishers, 1988.
- [26] M. Guardia, T. M. Seara, and M. A. Teixeira. Generic bifurcations of low codimension of planar filippov systems. *Journal of Differential Equations*, 250(4):1967–2023, 2011.

- [27] R. Huzak and K. U. Kristiansen. The number of limit cycles for regularized piecewise polynomial systems is unbounded. *Journal of Differential Equations*, 342:34–62, 2023.
- [28] Y. Ilyashenko. Centennial history of Hilbert’s 16th problem. *Bulletin of the American Mathematical Society*, 39(3):301–354, 2002.
- [29] I. Itenberg, G. Mikhalkin, and E. Shustin. *Tropical algebraic geometry*, volume 35 of *Oberwolfach Seminars*. Birkhäuser Verlag, Basel, second edition, 2009.
- [30] I. Itenberg and E. Shustin. Singular points and limit cycles of planar polynomial vector fields. *Duke Mathematical Journal*, 102(1):1–37, 2000.
- [31] M. R. Jeffrey. *Hidden dynamics: The mathematics of switches, decisions and other discontinuous behaviour*. Springer International Publishing, 2018.
- [32] M. R. Jeffrey and S. J. Hogan. The geometry of generic sliding bifurcations. *SIAM Review*, 53(3):505–525, January 2011.
- [33] S. Jelbart, K. U. Kristiansen, P. Szmolyan, and M. Wechselberger. Singularly perturbed oscillators with exponential nonlinearities. *Journal of Dynamics and Differential Equations*, pages 1–53, 2021.
- [34] S. Jelbart, K. U. Kristiansen, and M. Wechselberger. Singularly perturbed boundary-equilibrium bifurcations. *Nonlinearity*, 34(11):7371–7314, 2021.
- [35] S. Jelbart, K. U. Kristiansen, and M. Wechselberger. Singularly perturbed boundary-focus bifurcations. *Journal of Differential Equations*, 296:412–492, 2021.
- [36] C. K. R. T. Jones. *Geometric Singular Perturbation Theory, Lecture Notes in Mathematics, Dynamical Systems (Montecatini Terme)*. Springer, Berlin, 1995.
- [37] I. Kosiuk and P. Szmolyan. Geometric singular perturbation analysis of an autocatalator model. *Discrete and Continuous Dynamical Systems - Series S*, 2(4):783–806, 2009.
- [38] K. U. Kristiansen. Blowup for flat slow manifolds. *Nonlinearity*, 30(5):2138–2184, 2017.
- [39] K. U. Kristiansen. The regularized visible fold revisited. *Journal of Nonlinear Science*, 30(6):2463–2511, 2020.
- [40] K. U. Kristiansen and S. J. Hogan. On the use of blowup to study regularizations of singularities of piecewise smooth dynamical systems in \mathbb{R}^3 . *SIAM Journal on Applied Dynamical Systems*, 14(1):382–422, 2015.
- [41] K. U. Kristiansen and S. J. Hogan. Resolution of the piecewise smooth visible-invisible two-fold singularity in \mathbb{R}^3 using regularization and blowup. *Journal of Nonlinear Science*, 29(2):723–787, 2018.
- [42] K. U. Kristiansen and P. Szmolyan. Relaxation oscillations in substrate-depletion oscillators close to the nonsmooth limit. *Nonlinearity*, 34(2):1030–1083, 2021.

- [43] N. Kruff, C. Lüders, O. Radulescu, T. Sturm, and S. Walcher. Algorithmic reduction of biological networks with multiple time scales. *Mathematics in Computer Science*, 15(3):499–534, 2021.
- [44] M. Krupa and P. Szmolyan. Relaxation oscillation and canard explosion. *Journal of Differential Equations*, 174(2):312–368, 2001.
- [45] J. Li. Hilbert’s 16th problem and bifurcations of planar polynomial vector fields. *International Journal of Bifurcation and Chaos in Applied Sciences and Engineering*, 13(1):47–106, 2003.
- [46] T. Li and J. Llibre. On the 16th Hilbert Problem for Discontinuous Piecewise Polynomial Hamiltonian Systems. *Journal of Dynamics and Differential Equations*, pages 1–16, 2021.
- [47] G. L. Litvinov. Maslov dequantization, idempotent and tropical mathematics: A brief introduction. *Journal of Mathematical Sciences*, 140(3):426–444, 2007.
- [48] G. L. Litvinov and V. P. Maslov. Idempotent mathematics: A correspondence principle and its applications to computing. *Russian Mathematical Surveys*, 51(6):1210–1211, 1996.
- [49] J. Llibre, M. A. Teixeira, and J. Torregrosa. Lower bounds for the maximum number of limit cycles of discontinuous piecewise linear differential systems with a straight line of separation. *International Journal of Bifurcation and Chaos*, 23(4):1350066, 2013.
- [50] D. Maclagan and B. Sturmfels. *Introduction to Tropical Geometry*. Graduate Studies in Mathematics, 161. American Mathematical Society, 2015.
- [51] R. Morrison. Tropical geometry. *A Project-based Guide To Undergraduate Research in Mathematics*, pages 63–105, 2020.
- [52] D. M. Nielsen. Tropical geometry and geometric singular perturbation theory with applications in biology, Technical University of Denmark, Master thesis (supervised by Kristiansen, K. U.), 2021.
- [53] V. Noel, D. Grigoriev, S. Vakulenko, and O. Radulescu. Tropical geometries and dynamics of biochemical networks application to hybrid cell cycle models. *Electronic Notes in Theoretical Computer Science*, 284:75–91, 2012.
- [54] L. Perko. *Differential equations and dynamical systems*, volume 7. Springer-Verlag, Berlin, 1991.
- [55] V. Petrov, S.K. Scott, and K. Showalter. Mixed-mode oscillations in chemical-systems. *Journal of Chemical Physics*, 97(9):6191–6198, 1992.
- [56] S. Portisch. A novel approach to dimension reduction in enzyme kinetics, Vienna University of Technology, Diploma thesis (supervised by Szmolyan, P.), 2017.

- [57] S. S. Samal, D. Grigoriev, H. Fröhlich, and O. Radulescu. Analysis of reaction network systems using tropical geometry. In *Computer Algebra in Scientific Computing - 17th International Workshop, CASC 2015, Aachen, Germany, September 14-18, 2015, Proceedings*, pages 424–439, 2015.
- [58] A. H. Sarantaris. Tropical dynamics: Dimension reduction and graph representation of multi-scale polynomial systems, Technical University of Denmark, Bachelor thesis (supervised by Kristiansen, K. U.), 2021.
- [59] S. Soliman, F. Fages, and O. Radulescu. A constraint solving approach to model reduction by tropical equilibration. *Algorithms for Molecular Biology*, 9(1):24, 2014.
- [60] S. Songling. A concrete example of the existence of four limit cycles for plane quadratic systems. *Sci. Scientia*, 2:153–158, 1980.
- [61] J. Sotomayor and M. A. Teixeira. Regularization of discontinuous vector fields. In *Proceedings of the International Conference on Differential Equations, Lisboa*, pages 207–223, 1996.
- [62] B. Sturmfels. *Solving systems of polynomial equations*, volume 97 of *CBMS Regional Conference Series in Mathematics*. Published for the Conference Board of the Mathematical Sciences, Washington, DC; by the American Mathematical Society, Providence, RI, 2002.
- [63] O. Viro. Dequantization of real algebraic geometry on logarithmic paper. *European Congress of Mathematics, Vol I*, 201:135–146, 2001.
- [64] O. Y. Viro. Real plane algebraic curves: constructions with controlled topology. *Algebra i Analiz*, 1(5):1–73, 1989.